國立臺灣大學生命科學院植物科學研究所
碩士論文

Institute of Plant Biology
College of Life Science
National Taiwan University
Master Thesis

鋅逆境下水稻代謝物之變化

Metabolic response of rice (*Oryza sativa* L.) under Zn stress

華雨桑

Yu-Sang Hua

指導教授： 陳賢明 博士

共同指導教授：林雅芬 博士

Advisor: Hieng-Ming Ting, Ph.D.

Co-advisor: Ya-Fen Lin, Ph.D.

中華民國110年2月

February, 2021

doi:10.6342/NTU202100671

國立臺灣大學碩士學位論文

口試委員會審定書

鋅逆境下水稻代謝物之變化

Metabolic response of rice (*Oryza sativa* L.) under Zn stress

本論文係華雨桑君（R06B46026）在國立臺灣大學植物科學研究所完成之碩士學位論文，於 2021 年 1 月 27 日承下列考試委員審查通過及口試及格，特此證明

口試委員：

國立臺灣大學 植物科學研究所
陳賢明 助理教授（指導教授） 陳賢明

國立臺灣大學 農藝學系暨研究所
林雅芬 助理教授（共同指導教授） 林雅芬

國立臺灣大學 農業化學系
盧毅 助理教授

國立臺灣大學 分子與細胞生物學研究所
蔡皇龍 助理教授 蔡皇龍

中央研究院 植物暨微生物學研究所
馬麗珊 助研究員

Acknowledgement

I would first give thanks to Yahweh for if without Him this would not have been possible; the journey was full of trials but with His guidance the trials became my victory.

I want to also express my most sincere gratitude to the most amazing advisor Hieng-Ming Ting and co-advisor Ya-Fen Lin. They have accepted me into their lab with open arms and provided a place of scientific learning and nurturing. They guided me along with their knowledge and expertise, with patience and a ton of encouragement. Even when they are so knowledgeable in their field of study, they are so humble to learn, so eager to discuss with their students, and so very down to earth. I feel like home in the lab.

I also want to express my appreciation for professor Lay-Sun Ma as she had provided us with assistance in visualizing the ultrastructures through TEM. For the preparation of these TEM samples I would like to thank the Electron Miroscope, Division, Cell Biology Core Lab in Academia Sinica under Dr. Wann-Neng Jane and his amazing assistants that were so eager to help and explain the structures. Another institution I want to thank is also the Agricultural Biotchnology Research Center Metabolomics Core Lab who have provided exemplary service for our metabolomics study. Special thanks to the Institute of Plant Biology and the wonderful faculty members and staff who are the backbone of our department; without you I would not have the support to finish my thesis. A heartfelt thanks to the Ministry of Higher Education and the Council of Science and Technology, Taiwan for the financial support.

I also want to thank our post-doctorate Dr. Boon-Huat Cheah for teaching me many of the statistical analysis, and my senior Yu-Ling Chen for guiding me during my experiments dealing with rice, zinc treatments and sample collection.

I would also like to acknowledge the labmate who have taught and guided me with so much kindness. I would mention your name but your help has definitely allowed me to grow and acquire the necessary skills to perform. I also want to thank all my amazing friends and other lab mates for the motivation, comfort, prayers, and mental support.

Lastly, I want to thank my mom and dad, who have paved my way to Taiwan with their hard work and dedication. You have always been the best example of determination for me, working from the ground up in a country not your own and in a language so unfamiliar you were able to raise three amazing children and put them all through higher education, I am forever proud to be your daughter. I want to “big up”, a word often used in Belize, my sister and brother who have supported me both financially and emotionally. Ma-leva-ken to my family in Piyuma. And of course to my boyfriend, I love you. Thank you.

doi:10.6342/NTU202100671

中文摘要

植物微量營養元素鋅對作物的生長扮演重要的角色，故其在水稻中的調控的分子機制已被廣泛研究。然而，鋅逆境如何改變轉錄體和代謝體，進而影響其生理反應之機制，仍然未知。實驗室過去轉錄體學（RNA 定序）的研究結果發現：在鋅逆境下，初級代謝物相關基因會差異性表現。為瞭解轉錄體變化對代謝物的影響，本實驗使用 10 天大的水稻（*Oryza sativa* L. cv Kitaake）幼苗進行 3、14 和 21 天的不同濃度鋅處理，包括缺鋅（0.002 μM $ZnSO_4$），正常鋅（0.2 μM $ZnSO_4$）和過量的鋅（300 μM $ZnSO_4$），觀察其性狀並進一步分析其代謝產物的變化。研究結果發現，缺鋅和過量鋅處理的水稻幼苗，其根長變短、株高變矮、和葉片白化或黃化。缺鋅處理下的葉片細胞有大量澱粉粒在葉綠體中積累，過量鋅處理則會破壞細胞膜並改變葉綠體的結構。缺鋅期間碳水化合物濃度的變化和澱粉粒的累積，可能是由於澱粉生合成速率增加及澱粉降解受抑制所致。缺鋅處理下的水稻，其氨基酸的累積亦會增加，脂肪酸含量則降低；而在過量的鋅逆境下，碳水化合物，氨基酸和脂肪酸的變化很小。因此，水稻初級代謝的調節與鋅的有效濃度有關。

關鍵字

缺鋅, 水稻, 透射電子顯微, 代謝產物, 澱粉降解, 澱粉生合成

doi:10.6342/NTU202100671

Abstract

The molecular mechanism of zinc (Zn) stress in plants have been studied extensively due to its importance to agricultural crop; however, there are still puzzles pertaining to the metabolic regulation in response to both Zn deficiency and phytotoxicity. Preliminary RNA-sequencing results showed that GO-categorized genes for the regulation of primary metabolic process were differentially expressed during Zn stress. To understand the mechanism behind these transcriptional changes, rice (*Oryza sativa* L. cv. Kitaake) seedlings were treated with different concentration of Zn for 3, 14, and 21 days, inclusive of Zn deficiency (0.002 μM), normal Zn (0.2 μM), and excess Zn (300 μM); and their metabolic profiling were further analyzed. Our results showed noticeable morphological changes such as reduced root length, decreased shoot height and increased leaf chlorosis in the Zn deficient and excess Zn-treated plant, compared to its corresponding normal plants. The Zn deficient leaf cells showed accumulation of starch granules in chloroplast, and excess Zn cells exhibited damages on cell membrane and chloroplast. Altered carbohydrate concentration and starch accumulation during Zn deficiency was likely due to increase in the rate of starch biosynthesis, and inhibition of starch degradation. Zinc deficiency also lead to the increased accumulation of amino acids and decrease fatty acid contents in rice plants, whereas alterations in carbohydrates, amino acids, and fatty acids were minimal under excess Zn stress. Consequently, regulation of primary metabolism in rice is heavily reliant on Zn availability.

Key words

Zinc deficiency, *Oryza sativa* L., Transmission Electron Microscope (TEM), Primary metabolites, Starch degradation, Starch biosynthesis

doi:10.6342/NTU202100671

Table of contents

doi:10.6342/NTU202100671

doi:10.6342/NTU202100671

List of Tables

doi:10.6342/NTU202100671

List of Figures

doi:10.6342/NTU202100671

List of Appendices

doi:10.6342/NTU202100671

Introduction

Importance of nutrient in agronomy

The concept of fertilization progressed from the discovery of nutrients required by plants, which are divided into macro- and micronutrients; the importance of this agricultural knowledge is its contribution to the advancement of civilization. For thousands of years the success of agriculture and agronomy is due to “long-term soil fertility”, an example is the “milpa” farming system devised by the ancient Mayan civilization in Central America (Nigh and Diemont, 2013). It wasn’t; however, until the time of Justus von Liebig that the knowledge of essential mineral was conceptualized and established as a scientific discipline, propelling the agricultural revolution. From his research and several others that followed, important minerals were discovered to be essential for plant’s growth; however, plant mineral composition was not an effective way to determine whether an element is essential or not, therefore the elements were considered only if in its absence it causes consequential effects on plant growth and development (Scharrer, 1949; Kirkby, 2012). These nutrients were then divided into two large groups: macronutrients, such as potassium (K), nitrogen (N), phosphorus (P), calcium (Ca), sulphur (S), and magnesium (Mg), that are present in large quantities in plants, and micronutrients which is equally important but present at much lower quantities. Micronutrients in higher plants consist of iron (Fe), manganese (Mn), boron (B), zinc (Zn), copper (Cu), molybdenum (Mo), chlorine (Cl), and nickle (Ni) (López-Arredondo et al., 2017). Most of these micronutrients consist of heavy metals that are required in small amounts but are crucial to many enzymatic functions in plants (Vallee, 1955). The study of nutrients contributed greatly to the improvement in our agricultural production; however, there are still much to investigate such as the effect of micronutrient on plant’s growth and development.

doi:10.6342/NTU202100671

One of the micronutrients causing grave impact to global crop health is Zn, this is because Zn has unique chemical and geometrical properties that play an important role in plant metalloproteins. Proteins contain a limited rage of amino acid R groups that are crucial for catalytic activity; in order to expand the biochemical capability of proteins, metals, such as Zn, are necessary due to its different chemical properties like its coordination geometry, redox potential, charge, and kinetics that consequently leads to specific and diverse chemistry (Waldron et al., 2009). Zn ion is an ideal metal co-factor for reactions that need a stable ion, because of its stability caused by the Zn atom's filled d orbital (d^{10}) making it a redox-stable ion (McCall et al., 2000). Zn is the only metal to be present in all six enzyme classes: oxidoreductases, transferases, hydrolases, lyases, isomerases, ligases (Broadley et al., 2007; Merchant, 2010). Due to its contribution to diverse chemical properties, Zn is therefore the second most abundant metal in living organism and the second most prevalent cofactor found in proteins (Waldron et al., 2009; Kirkby, 2012). Despite its importance, Zn is the most prevalent micronutrient deficiency devastating the world today. Due to its diverse chemistry, Zn is an important metallofactor in all six classes of enzyme, and changes in Zn availability in the soil will affect many processes within the plant that can lead to consequential ultrastructural damages (Barceló and Poschenrieder, 2004).

The damages caused by Zn stress, either phytotoxicity or deficiency, is manifested in the phenotype of both aerial and ground tissues (Barceló and Poschenrieder, 2004; Sharma, 2006; Mohammad, 2010). In Zn deficient plant the growth is severely inhibited with reduced and condensed shoot growth, reduced leaf size, and shortening of internodes with leaves curling and showing spatially heterogenous or interveinal chlorosis and necrosis (Sharma, 2006). Zn phytotoxicity, becoming more frequent due to increased anthropogenic waste, also exhibit similar symptoms: stunted growth, inward folding of

doi:10.6342/NTU202100671

the leaves, and iron deficiency induced chlorosis on sub-terminal leaves (Mohammad, 2010). Both Zn stress also cause significant damage to the morphological features of roots with reduced root length, root tip damage, decrease in overall biomass and decrease in vessel diameter. This change is primarily due to the disruption in both cell proliferation and elongation in the roots (Barceló and Poschenrieder, 2004). Zn phytotoxicity or deficiency can cause physiological damage to both aerial and ground organs, reducing its growth and damaging the cells.

One contributing factor to these physiological damages is the disruption of plant metabolic homeostasis: such as the regulation of primary metabolite related metabolism; namely protein synthesis, carbohydrate metabolism, indoleacetic acid (IAA) synthesis, membrane integrity, and lipid peroxidation; or accumulation of antioxidant or osmoprotectant in order to acclimate to Zn deficiency or phytotoxicity (Broadley et al., 2007; Shulaev et al., 2008). Plant metabolites, which will be later discussed in more details, are the building blocks of: cellular structures, proteins or important signaling molecules. It is thus vital for plants to maintain metabolic homeostasis to retain normal metabolic regulation.

Effect of Zn on plant metabolites

Metabolites are chemical compound found in living organisms that partake in metabolic pathways as substrates or products; currently they are divided into three widely accepted groups: primary metabolites, secondary or specialized metabolites, and plant hormones with different but overlapping functions (Erb and Kliebenstein, 2020). Metabolites that are directly involved in primary metabolism of the plant are commonly known as primary metabolites, such as: amino acid, fatty acid and carbohydrates (Fernie and Pichersky, 2015). Those that are required for environmental and ecological interactions are known as secondary metabolites and those molecules that regulate the plant growth, development

doi:10.6342/NTU202100671

or defense are termed as plant hormones; however, the function of these three groups do overlap and are complex (Hartmann, 2007; Erb and Kliebenstein, 2020). The "omics" tools such as metabolomics and transcriptomic are now used and integrated to understand these processes and better combat the Zn stress problems. All three groups of metabolite, primary metabolite, secondary metabolite, and hormones, are defined by functions that may overlap, making understanding or characterization of the metabolite and its regulation difficult, so in this study they will be termed as metabolites and we will be reviewing the current understanding on the changes of three specific metabolites: amino acids, carbohydrates, and fatty acids during Zn stress.

Effect of Zn on amino acids

Amino acids have diverse chemistry and are grouped based on these properties; due to their diversity, they play a variety of important roles in plant growth and stress response. Amino acids can also be grouped according to their chemical property, they are commonly divided into uncharged non-polar and polar, positively charged and negatively charged amino acids. Non-polar amino acid consists of glycine, alanine, valine, cysteine proline, leucine, isoleucine, tryptophan, and phenylalanine. Polar amino acid includes serine, threonine, tyrosine, asparagine, and glutamine. For the charged group, positively charged amino acids are lysine, arginine, and histidine; whereas negatively charged amino acid consists of aspartic acid and glutamic acid (Whitford, 2005). Amino acids are the building blocks of protein molecules in all living things but in plants they play a variety of roles in addition to their participation in protein synthesis such as synthesis of chlorophyll, regulation of stomas during stress, precursors for phytohormones, assistance in pollen fertility, chelation of micronutrients, and the production of vital growth related hormones Indole-3-acetic acid and cytokinin (Tsui, 1948; Cakmak et al., 1989; Sharma, 2006; Abdelhamid et al., 2014; Biancucci et al., 2015). All amino acids differ in molecular

doi:10.6342/NTU202100671

property and changes dynamically according to the current state of the plant cell as they are essential in many cellular processes; these changes can be important for stress tolerance or acclimation (Hildebrandt et al., 2015).

One of the ways in which plant respond to either Zn deficiency or phytotoxicity is by altering its amino acid composition; amino acids accumulate during both Zn deficiency and phytotoxicity as a response against disruption in protein synthesis and metal chelation respectively (Kitagishi and Obata, 1986; Sharma and Dietz, 2006). During Zn deficiency, amino acids significantly increase in accumulation and older studies attribute this massive accumulation of amino acids to the depression of protein production caused by disorder in nitrogen metabolism and protein synthesis (Kitagishi and Obata, 1986; Kitagishi et al., 1987). Another response of Zn stress, phytotoxicity, is the production of metal-binding thiol and non-thiol compounds. These compounds are important for the exclusion, compartmentalization, and complexation of heavy metals to prevent both: the presence of free metal ion in plant cytoplasm, and the metal ions from contacting sensitive cellular structure causing irreversible damage (Callahan et al., 2006; Broadley et al., 2007; Rascio and Navari-Izzo, 2011; Anjum et al., 2015). Non-thiol compounds, like organic acids and amino acids, can perform such functions. At low pH, organic acid such as citric acid or malic acid play a role in hyperaccmulation; however organic acids do not bind to metal ions strong enough to either extract them from soil or induce specificity, so while they may play a role in vacuole sequestration they might not play an important role in long-distance transporting (Callahan et al., 2006). As pH increase the amino acid-Zn complex is most likely responsible for long-distance transport; therefore, the joint work of these non-thiol compound is essential in heavy metal stress response (White, 1981). Currently proline, cysteine, glutamic acid, glycine and histidine have been widely studied to be involved in metal ion ligand binding in hyperaccumulating

doi:10.6342/NTU202100671

or metal-tolerant plants; however, the role of other amino acids that can form an amino acid-Zn complex and be involved in metal chelation and transport is still not extensively studied (Callahan et al., 2006; Sharma, 2006; Broadley et al., 2007). By altering its amino acid composition during Zn deficiency or phytotoxicity it can either be as a result of protein synthesis disruption or as a strategy for metal chelation respectively; another common building block that also participates in response is carbohydrates.

Effect of Zn on carbohydrates

The production and transport of carbohydrate from sink to source is strictly regulated as any disruption to these processes can affect starch synthesis or degradation. Carbohydrates are produced in source organs, such as fully developed leaves, where assimilation of CO_2 from the atmosphere take place; this CO_2 is converted to high energy molecule sugar, like glucose, where it will be transported to sink organs, and stored or used for organ growth. (Rodrigues et al., 2019). The transport of carbohydrate between source and sink is determined by the regulation of carbon assimilation, carbon storage and growth which must reach a balance; if this balance is disrupted starch synthesis during the light stage and degradation during the dark phase will be affected (Rodrigues et al., 2019). Starch synthesis and degradation in plant is sophisticated as it considers not only the circadian clock, but also nutrient availability and photosynthesis; therefore, posttranscriptional regulation is essential for the control of diurnal metabolism of starch (Smith et al., 2004). Post transcriptional modification regulate these biosynthetic and degradative enzymes by the means of allosteric regulation, redox modulation, protein-protein interaction and phosphorylation (Kötting et al., 2010). The transcriptional and post transcriptional regulation of carbohydrate metabolism involves several processes which affects one another the production and transportation of carbohydrate and the biosynthesis and degradation of starch, making it sophisticated

doi:10.6342/NTU202100671

The production and transport of carbohydrate from sink to source is strictly controlled via post transcriptional regulation as any disruption to these processes can affect starch synthesis or degradation

Micronutrient deficiency such as Zn, Cu, Co, Ni, or Mg, alters the carbohydrate content of the leaf as a means of abiotic stress response or disruption to carbohydrate metabolism processes (Vesk et al., 1966; Samarakoon and Rauser, 1979; Gupta and Kaur, 2005). For example, studies in tomato, spinach, maize and the common beans have reported a decrease in transitory starch in the chloroplast in which Jyung et al. (1975) relates to the reduction of starch synthetase activity (Reed, 1939; Vesk et al., 1966; Jyung et al., 1975). However, other studies had conflicting results such as the ones done in rice, where Zn deficiency caused an increase in the accumulation of transitory starch (Suzuki et al., 2012; Zeng et al., 2019). These study combined microarray data with the phenotype and proposed that accumulation of starch in rice shoot and root is due to the up-regulation of starch synthesis and transport related genes during Zn deficiency. It can then be assumed that rice plants may increase starch production to withstand the abiotic stress (Suzuki et al., 2012). It can be possible that this accumulation is due to the disruption of glycolysis the process of extracting energy from glucose, as it has been reported that the activity of Fructose-bisphosphate aldolase (FBP aldolase) decrease under Zn deficiency (Quinlan-Watson, 1951).

Effect of Zn on fatty acids

Plant fatty acids are versatile primary metabolites as it is important in membrane component, energy reserve and stress signaling. Fatty acids are components of cellular membranes and barriers composed of cutin and suberin, they also act as energy reserves in the form of triacyglycerols, and are precursors of several bioactive molecules including

doi:10.6342/NTU202100671

stress signaling regulators, jasmonates and nitroalkenes (He and Ding, 2020). In response to abiotic or biotic stress, fatty acids can react with reactive oxygen species (ROS) and partake in phytohormone signaling (Upchurch, 2008; Yuan et al., 2012).

Fatty acids react with ROS during Zn stress reducing membrane integrity but simultaneously acting as antioxidants and precursor of bioactive molecules necessary for abiotic response. During Zn phytotoxicity, an increase in ROS damages membrane bounded structures, including photosynthetic apparatus of the plant, through unsaturated fatty acid peroxidation of membrane lipids which mainly composed of linoleic and linolenic acid (Maksymiec, 2007). This disruption in membrane integrity leads to the leaking of membrane exudates, overall decrease in total lipid content, and production of oxylipins (Cakmak and Marschner, 1988; Ouariti et al., 1997; Nouairi et al., 2006; Bidar et al., 2008). These by-products, however, are exploited by plants as signaling molecules particularly in defense. While fatty acids may be vulnerable to oxidation and detrimental to cellular component like in the case of malondialdehyde (MDA), a latent reactive carbonyl species, they may also act as antioxidants, reacting with reactive oxygen species (ROS) and consuming it, giving rise to oxylipins like jasmonic acid (JA) which can activate ROS responsive genes and induce production of other ROS scavenging protein or metabolites (He and Ding, 2020). Zn deficiency in plants can also enhance peroxidation of membrane constituents and affect the fatty acid desaturation (Sharma, 2006). Even though ROS production during Zn stress can de-stabilize membrane structures in plant cell by reacting with fatty acid membrane components, the oxidized fatty acid can act as antioxidants or precursor of signaling molecules to initiate abiotic stress response.

doi:10.6342/NTU202100671

The Scope of thesis

Zn is naturally low in abundance in soils, so many agricultural land around the world suffers from Zn deficiency, causing low yields of crops (Hacisalihoglu, 2020). Zn deficiency in agricultural plant is also a contributing factor to Zn deficiency in the human food chain as 1/3 of the world's population suffer from either a mild or severe Zn deficiency (Sillanpää, 1982). Excess Zn similarly can affect the physiology of the plant, and it can also be a source of environmental and health hazard; Therefore, it is important to keep Zn at optimal concentration to avoid physiological damages (Mohammad, 2010; Wuana and Okieimen, 2011). To combat global Zn related problems, it is important to first study the responses, regulation, and effects of both Zn deficiency and phytotoxicity in plants, especially economically important crop like rice.

Our study material is rice (*Oryza sativa* L. cv Kitaake) as it is not the most important economical food crop in Asia (Jain et al., 2019). In order to understand rice response to Zn phytotoxicity or deficiency, RNA-sequencing was performed using rice seedlings under either excess Zn or Zn deficient treatments for 3 days. When comparing between excess Zn and Zn decienxy, there were 930 Differentially Expressed Genes (DEGs), 683 in shoots and 247 in roots of rice with 40 expressed in both tissues (**Figure 1A**)**.** The GO-enrichment analysis (**Figure 1B**) revealed that primary and secondary metabolite related genes were differentially expressed during Zn stress.

These metabolites related DEGs were involved in several biological process such as "cellular biogenic amine metabolism", "polysaccharide catabolic process", "hydrolase activity", and "fatty acid biosynthesis process" (**Figure 1B**). For DEGs related to cellular biogenic amine metabolism (**Figure 2, Table 1**), two of the three nicotianamine synthase genes (*OsNAS*) were upregulated in both root and shoot under Zn excess treatment and were known to facilitate iron chelation and transport (von Wirén et al., 1999). The DEGs,

doi:10.6342/NTU202100671

related to polysaccharide catabolic process (**Figure 3, Table2**), were up-regulated during Zn deficiency, but down-regulated dueing excess Zn condition. This may result in the increase breaking down of polysaccharide during Zn deficiency. This can be reflected in DEGs related to hydrolase activity (**Figure 4, Table 3**), as excess Zn treatments showed a down-regulation in the gene expression while Zn deficiency had the opposite effect. For fatty acid biosynthesis process (**Figure 5, Table 4**), an opposing effect could also be observed DEGs with down-regulation during Zn deficiency but up-regulation during excess Zn treatment. This may result in decrease of fatty acid content during Zn deficiency. In summary, the transcriptomic data implied that metal transport may play an important role to maintain the metal hoemostasis during excess Zn,; however, the catabolism or hydrolysis of carbonhudrates/sugars increased and fatty acid biosynthesis may decline during Zn deficiency.

To investigate how this can affect the primary metabolite amongst both type of Zn treatments in rice, a combination of phenotypic observation and metabolomics would be perforemd to not only compare the differences amongst the metabolites (amino acids, fatty acids and carbonhydrates) but also to propose new ideas and direction of how and why this phenotype occurred.

doi:10.6342/NTU202100671

Materials and Methods

Plant growth and Zn treatments

Rice (*Oryza sativa* L. cv. Kitaake) was used for this study due to its rapid life cycle (9 weeks seed to seed) and easy propagation (Jain et al., 2019). Seeds were first surface sterilized in 1 % commercial hypochlorite solution (commercial bleach solution diluted with distilled water) then shaken on a belly-dancer for an hour. The seeds were washed with distilled water at least five times until the strong hypochlorite odor disappeared to ensure removal of the remaining sterilization solution. In the 37^{o}C incubator, the seeds were soaked in distilled water for one day and then germinated on moistened sterilized filter paper for two days. During this time white root began to emerge, an indication that the seeds were ready for sowing. After pre-germination, seeds of similar growth rate were transplanted unto the hydroponics container (**Figure 6A**, part a) using autoclaved tweezers and cultured in 1x Kimura B nutrient hydroponic solution for one week. The nutrient solution for normal Zn treatment contained: 0.36 mM $(NH_4)_2SO_4$, 0.18 mM KNO_3, 0.55 mM $MgSO_4$, 0.18 mM KH_2PO_4, 61.20 µM Fe citrate, 0.37 mM $Ca(NO_3)_2$, 2.51 µM H_3BO_3, 0.20 µM $MnSO_4$, 0.2 µM $ZnSO_4$, 0.05 µM $CuSO_4$, and 0.05 µM H_2MoO_4 (Yoshida and Institute, 1976) (**Table 5**). After seven days the seedlings were given three different concentration of zinc sulfate ($ZnSO_4$), normal or optimal concentration of zinc ([Zn] = 0.2 µM), deficient Zn ([Zn] = 0.002 µM), excess Zn ([Zn] = 300 µM). Plants were grown in the greenhouse with temperature of 30/25^{o}C (day/night), 12/12 hours (light/dark), with relative humidity of 60 %. The kimura solution was changed three times a week. This experiment was carried out in quadruplet and samples were collected timely at 3, 14, and 21 days after treatment (DAT).

Plant growth parameters including root length, shoot height, fresh and dry weights of roots and shoots which were measured at 3, 14, 21 DAT and the shoot materials were

doi:10.6342/NTU202100671

also collected for fatty acids analysis. The leaf blade was also observed and collected at each time. The leaves from 21 DAT were fixed for further ultrastructural analysis. The shoot materials of 3, 14, 21 DAT under different Zn treatments for metabolomics analysis were kindly provided by Miss Yu-Ling Chen.

Rice leaf fine structural observation

Materials The leaf blades from 21 DAT were used for the observation of fine structure. Five different site on leaf blade were collected: the control, the albino section on the leaf base and the green region on the leaf tip of Zn-limited leaves, and the green section near the leaf base and the chlorotic region near the leaf tip of excess Zn-treated leaves.

Fixation. The specific rice section from leaf blades was fixed with a mixture of 2.5 % glutaraldehyde (in 0.1 M phosphate buffer, pH = 7.0) overnight in 4^{o}C to promote extended storage. The samples were then washed with phosphate buffer 3 times, each time for 30 minutes. After rinsing, the sample was postfixed with 1 % osmium tetroxide/O_sO_4 (in 0.1 M phosphate buffer) for 4 hours in room temperature. This was then followed by washes in phosphate buffer that was also done 3 times, each time for 30 minutes.

Dehydration. The samples were then dehydrated by a gradient series of acetone (30 minutes at each concentration): 30 %, 50 %, 70 %, 85 %, 95 %, 100 % and another 100 %; this process was done in a desiccator. For infiltration, the sample was first placed in a mixture of Spurr's resin to acetone ratio of 1:3 overnight, followed by a mixture of Spurr's resin to acetone ratio of 1:1 for 8 hours in, then overnight in a mixure of Spurr's resin to acetone ratio of 3:1 and finally 100 % Spurr's resin twice overnight under vacuum.

Embedding and sectioning. Samples were placed in capsules containing embedding medium (Spurr's resin) and heated at 70^{o}C for 16 hours. The sample sections were then stained using 5 % uranyl acetate/UA in 50 % methanol followed by post staining in 0.4

doi:10.6342/NTU202100671

% lead citrate in 0.1 N sodium hydroxide. For the optical microscope slide the section was dyed using Toluene Blue in water. In all these processes low vacuum was used when applicable.

Observation by light microscopy. For light microscope sections, the samples were embedded unto a microscope slide glass and observed using an optical microscope (Zeiss Axio Imager M1), equipped with a Axiocam 105 color.

Observationby TEM. Section was observed using TEM (FEI Tecnai G2 Spirit, 2014), equipped with a 4Kx4K CCD camera for STEM and tomography.

Metabolite extraction

Metabolites were extracted by Dr. Hieng Ming Ting using previous protocols (Lisec et al., 2006) with minor modifications. Liquid nitrogen snap-frozen shoots of 3, 14, and 21 DAT were transferred unto a 50 ml falcon tube with a 2 cm ceramic bead. The samples were then grounded at 600 rpm for 40 seconds twice in a 2010 Geno/Grinder® (SPEX SamplePrep). To begin the process of partitioning ,100 mg of the grounded samples were transferred to a 15 ml Eppendorf tube. Two milliliters of pre-chilled MeOH:H_2O (80:20) with internal standard ribitol (50 µg ribitol/ml) was added, it was placed in the ultrasonic bath for 60 minutes at around 50^oC. After sonication, the samples were cooled to room temperature before it was centrifuged for at least 10 minutes at 3,100 rpm at 4^oC. The clear supernatant was transferred to a 1.5 ml round-bottom Eppendorf tube and then dried in the SpeedVac overnight without heating. For the derivatization procedure, the dried residue is first re-dissolved in 80 µl of 20 mg/ml methoxyamine hydrochloride in pyridine and slightly vortexed to ensure it completely dissolved. The solution was incubated at 30^oC for 60 minutes. To ensure the sample fully dissolve into solvent solution it was left for 30 minutes. In the case that there is non-dissolved residue, the tube was transferred to ultrasonic bath in full power at 30^oC for 30 minutes and then placed back to the incubator

doi:10.6342/NTU202100671

for another 30 or 60 minutes (depending on the amount of precipitation). The sample was then treated with 80 µl of MSTFA (N-Methyl-N-(trimethylsilyl)trifluoroacetamide), slightly vortexed and then incubated at 37ºC for 30 minutes. It was then transferred to 1.5ml autosampler vials, with glass inserts to ensure maximal content retrival, prior to GC/MS.

Fatty acid extraction

Similar to previous metabolite extraction (Daisaku et al., 2021), the 3, 14, and 21 DAT rice shoots were grounded in a 2010 Geno/Grinder® (SPEX SamplePrep). From the grounded samples 100 mg was transferred to a 2 ml round-bottom eppendorf tube and 1 ml of pre-chilled extraction liquid solution (containing 5:2:1 methanol, chloroform and 2 % acetic acid with 10 µl 2mg/ml pentadecanoic (C15) acid) was added unto the grounded samples and vortexed for 30 seconds followed by an additional 30 seconds chilling on ice; this step was repeated for five consecutive times. The samples were then centrifuged at 12,000 xg for 10 minutes at 4ºC and the supernatant was transferred to a new 2 ml eppendorf tube. This procedure was repeated two more times to ensure a good extraction and the supernatants were combined into the same tube. The supernatant was further washed by adding a mixture containing 500 µl ultrapure water and 400 µl chloroform (pre-chilled solutions at 4ºC overnight), it was then mixed via vortex for 1 minute and then centrifuged for 2 minutes at 12,000 rpm to separate the polar and non-polar layer. The non-polar layer was transferred to a 2ml screw-top glass tube and dried under a nitrogen stream. For derivatization, 500µl methanolic hydrochloride was used for methylation of fatty acid on the dried non-polar residue. After addition of the reagent, it was then incubated at 85ºC for 150 minutes. It was then washed with a mixture of ultrapure water and hexane; the organic layer (hexane) was transferred to a autosampler vial with glass inserts prior to GC/MS.

doi:10.6342/NTU202100671

Metabolite detection

Metabolite detection in both metabolite and fatty acid extraction was done using GCxGC-TOFMS with the collaboration of the Metabolomic laboratory in Agricultural Biotechnology Research Center (ABRC) in Academia Sinica. For both metabolite and fatty acid extraction, the samples prepared were injected onto the Pegasus 4D GCxGC-TOF/MS (Leco, St. Joseph, MI, USA) equipped with Rtx 5-MS capillary column (30 m × 0.25 mm × 0.25 μm). All the samples and replicates were separately and continuously auto-injected. Each 1 μl aliquot of the derivatized sample solution was injected in splitless into the GC column at a constant flow rate of helium of 1 ml/min. Solvent delay was set to 210 second and the temperature of the injector was operated isothermally at 250 °C. The mass spectrometry (MS) transfer line temperature to the quadruple was set to 300 °C and the electron impact (EI) ion source ion temperature was 200 °C. Compound elution settings were 1 minute at 40 °C, followed by a 10 °C/min oven temperature gradient to a final 300 °C, and then hold for 8 min. The spectra were recorded with a scanning range of 50–600 m/z. Peak list was filtered and then normalized with the internal standard, ribitol (for metabolite extraction) and pentadecanoic acid (C15) (for fatty acid extratction). The peak area of the compounds identified through the GC-MS library including NIST, LECO/Fiehn and Wiley Regist 9th Ediction mass spectral libraries to identify compound ID.

Metabolite analysis

Metabolite peak list, provided by the ABRC Metabolomics core lab, included: library defined compound name, retention time, base peak mass and normalized peak area. Peak areas were normalized with known concentration of internal standard ribitol, for metabolite extraction, and pentadecanoic acid, for fatty acid extraction. It was then used for consequent metabolite analysis: Principal Component Analysis (PCA) plot, heatmap,

doi:10.6342/NTU202100671

box plot, Log_2 Fold Change, and line graph. To assess the variation between samples the normalized metabolite peak areas were used to construct a PCA plot using the prcomp command and ggbiplot packages in RStudio (Vu, 2011). Heatmap was drawn to look at the cumulative proportion of metabolites. Dendrograms of heatmap built using Pearson's correlation coefficient on the horizontal axis and Euclidean correlation coefficient on the vertical axis, using the packages: tidyverse (Hadley Wickham, 2019), cluster (Hornik, 2019), and factoextra (Alboukadel and Fabian, 2020) in R-Studio version 4.0. Box plot and Log_2 Fold Change was used to confirm significant metabolite concentration changes (Team, 2020). A line graph was drawn for observations of shoot fatty acid over time (3, 14 and 21 days), using the R packages: ggplot2 (Wickham, 2016), dplyr (Wickham et al., 2020), and viridis (Garnier, 2018).

DEGs analysis

The Gene Ontology analysis of DEGs were done by Dr. Boon Huat Cheah (Cheah et al., 2020). The set of genes related to metabolites were then selected. Heatmap of these genes were generated using Log_2 Fold Change of Fragments Per Kilobase of transcript per Million mapped reads (FPKM). Dendrograms of heatmap drawn using the Pearson's correlation coefficient on the horizontal axis and Euclidean correlation coefficient on the vertical axis, using the packages: tidyverse (Hadley Wickham, 2019), cluster (Hornik, 2019), and factoextra (Alboukadel and Fabian, 2020) in R-Studio version 4.0.

Statistics analysis

For statistical analysis two-way ANOVA was carried out followed by Tukey's post hoc test with different letters denoting statistical significance at $p<0.05$ using the packages lsmeans (Length, 2016), ggplot2 (Wickham, 2016), and multcomp (Westfall, 2008). Two sample t-test statistics was also performed to compare metabolite levels (Team, 2020).

doi:10.6342/NTU202100671

Results

1. Rice morphological changes in response to Zn stress

Zinc (Zn) is an important micronutrient needed for the growth and development of plants; however, optimal concentration is required as both deficiency and phytotoxicity can occur at reduced or excess Zn concentration respectively. To validate our Zn stress, deficiency and phytotoxicity and observe the morphological changes, 10-day-told rice seedlings grown in optimal Zn concentration (0.2 μM $ZnSO_4$) were transferred to different Zn treatments: deficient concentration (0.002 μM $ZnSO_4$) termed dZn, excess Zn concentration (300 μM $ZnSO_4$) termed eZn, and normal zinc concentration termed NZn. Phenotype observations were recorded at 3 days after treatment (DAT), 14 DAT and 21 DAT. Morphological changes including plant growth, leaf blade phenotype, and cellular structures were examined.

1.1 Plant growth under Zn stress

To validate the Zn stress phenotype, the rice plants were treated in NZn, dZn and eZn concentrations and observed phenotypes at 3, 14, and 21 DAT. The rice seedlings did not differ in their growth at 3 DAT (**Figure 7A & 8A**). At 14 DAT, the phenotypic changes began to manifest in reduced height of dZn-treated rice (**Figure 7B & 8B**); and at 21DAT, the phenotype of dZn treatment caused a multitude of symptoms such a stunted growth, and reduced leaf development **(Figure 7C & 8C**). The growth of rice plants during eZn treatment, however, did not show significant reduction in height as dZn treated rice**.** In coherence with our observations, the quantitative measurements did not show a significant changes in growth between treatments until 14 and 21 DAT (**Figure 9**). For dZn treated rice, the shoot height and fresh weight were significantly reduced compared to both NZn and eZn treatments, especially at 21 DAT (**Figure 10A, C & E**). For eZn

doi:10.6342/NTU202100671

treated rice, its shoot growth was also reduced but not as server as that of dZn. At 21 DAT, the average shoot height of NZn treated plants (42.7 cm), were almost twice as high as dZn treated one (28.4 cm). Compared to NZn treatment, the average height of eZn treated rice was also moderately reduced (37.5 cm). Apart from shoot growth, the root growth was also measured. Compared to the NZn treatment,, the root length, fresh weight, and dry weight of both dZn and eZn treated rice were significantly reduced especifically at 14 and 21 DAT (**Figure 9 B, D & F**). For the root growth, both treatments (dZn and eZn) at 21DAT had corresponding measurements with the average root length of NZn at 21.0 cm, dZn at 17.0 cm and eZn at 18.4 cm. Both Zn stress significantly reduce the growth of both shoot and root; however, Zn deficiency was observed to affect the shoot development of the rice plant more than excess Zn treatment.

1.2 Rice leaf blade phenotype under Zn stress

The growth of rice plant was affected by both eZn and dZn treatment, but the health of rice plants is also determined by observing its leaf blade phenotype. To observe the effects of dZn and eZn treatment, the rice leaf blade phenotype was observed. Plants were treated with different concentration of Zn as described in section 1.1. The newest emerging leaf of each time point (3, 14, and 21 DAT) from each treatment (NZn, dZn, and eZn) were observed and compared. At 3 DAT, the leaves did not exhibit any differences between treatments (**Figure 10A & E**); at 14 DAT, symptoms began to develop as dZn leaf blade appeared shorter compared to NZn and eZn, and eZn leaf blade exhibited interveinal chlorosis (**Figure 10B**), but the de-chlorophyll leaf did not develop necrotic regions (**Figure 10F**); at 21 DAT, the differences are more noticeable. The fourth leaf (**Figure 10C**) developed interveinal chlorosis on sub-terminal leaves, and after the leaf undergone de-chlorophyll (**Figure 10G**) it revealed necrotic regions on areas of chlorosis. Similar results are reflected on the fifth leaf of 21 DAT (**Figure 10D**) however, since chlorosis

doi:10.6342/NTU202100671

on the fifth leaf was not as prolonged as the fourth leaf it did not cause intense damage, such as necrosis, as shown in the de-chlorophyll leaf result (**Figure 10H**). For Zn deficient plant, other than impaired elongation of the leaf and narrowing of leaf width, at 21 DAT the plant lost chlorophyll at the base of the youngest leaf (fifth leaf), appearing albino (**Figure 10D**).

1.3 Fine structures of rice leaf cell under Zn stress

The leaf blade of both dZn and eZn treatment exhibited severe symptoms of deficiency and phytotoxicity respectively. The mechanism behind these symptoms must vary depending on the stress, so to further investigate the leaf phenotype under Zn stress, different sections of the rice leaf were sampled to observe ultrastructural changes in the leaf (**Figure 11A**). For NZn treated leaf blade, one section was collected as control; for eZn treated leaf blade, two sections were collected: one near the base of the leaf where it is green and the other was near the leaf apex where showed chlorotic symptoms; for dZn treated leaf blade, two sections were also collected: one near the leaf base where an albino symptom wass evident and the other was near the leaf apex where the leaf was still green.

To observe the differences between leaf sections, the comparison was made between NZn and dZn/eZn; in addition to that, green asymptomatic sections and symptomatic sections (chlorotic eZn or albino dZn leaves) of the leaf were also compared. The collected leaf sections were fixed, and embedded with Spurr's resin before staining with Toluene Blue for Optical Microscopy (OM) or lead citrate for Transmission Electron Microscope (TEM) observation. The structure of the side veins containing the large and small vascular bundles would be viewed under the Optical Microscope (OM) as shown in the diagram on **Figure 11B**.

Compared to the NZn leaf section (**Figure 12F-H)**, both albino and green leaf section leaves displayed an abundant accumulation of starch within the chloroplast of the

doi:10.6342/NTU202100671

mesophyll cells, and the cells also seem to be more rounded than the signature lobed shape of rice mesophyll (**Figure 12A-E**). There is no different between the albino (**Figure 12A-C**) and green dZn (**Figure 12D-E**) leaf sections in the OM observations.

Compare to the NZn section (**Figure 12F-H**), both the chlorotic and green eZn leaf sections appeared enlarged vacuoles or less cytoplasmic content (**Figure 12I-N**). The chlorotic eZn section showed more changes in the overall shape of the epidermal, bulliform, and mesophyll cells (**Figure 12 L-N**) in comparison to green eZn leaf section (**Figure 12I-K**). These cells appear to have damaged cell wall so they do not retain the original lobed shape of rice mesophyll cells.

To confirm the observed OM observations and to further explore the ultrastructure changes of leaves under Zn stress, the similar sections were collected and observed under TEM. By comparing the NZn section (**Figure 13E & F**) and the dZn sections (**Figure 13 G-J**), the massive increase in number and size of the starch granule within the chloroplast was observed. The usual lobed shape of the mesophyll cell also changed in dZn as the lobes is not as apparent as the NZn sections. The albino section has a greater number of starch grain than the green dZn section. Comparing the NZn section (**Figure 13E & F**) and the eZn sections (**Figure 13A-D**), the damage to the cell wall and membrane was observed from the drastic change in shape of the mesophyll cells and from the detachment of the cell membrane (**Figure 13B**); there also seem to be more cytoplasmic particulates within the vacuoles of eZn treated mesophyll cells. The starch within the chloroplast in eZn treated mesophyll cells were also absent compared to NZn. Compared to the green eZn section (**Figure 13C & D**), we noticed that the damages in the chlorotic region was much worse with vacuolation of the chloroplast, detachment of cell membrane, and the misshaped mesophyll and bulliform cells in the eZn chlorotic section (**Figure 13A & B**).

doi:10.6342/NTU202100671

2. Rice (primary) metabolites changes in response to Zn stress

From the previous transcriptomic data (**Figure 2**) there were DEGs related to primary metabolites, moreover the phenotype observed affected chloroplastic starch under dZn treatment and affected membrane of leaf cells under eZn treatment,. Transitory starch in chloroplast was related to carbohydrate metabolism in plants; and the breakdown of membrane or the mesophyll cell wall can release phospholipids. Both of which process were related to the metabolism of important (primary) metabolites such as carbohydrates and fatty acids. Therefore, the metabolomics approach was used in this study in order to distinguish any variation of the metabolite amongst the Zn treatments that can explain phenotypic changes we observed.

Rice seedlings were grown and treated with different concentrations of Zn similar to the phenotype experiments. Rice shoots at 3, 14, and 21 DAT were collected for metabolite extraction. Both polar and non-polar extraction methods was performed on the collected shoot samples. After partitioning, it was derivatized according to its polarity and was analyzed using GCxGC-TOF/MS system. From the polar metabolites extraction, small hydrophillic molecules would likely be detected, those that are often involved in primary metabolism. From non-polar metabolites extraction, hydrophobic molecules would be detected. By detecting, identifying and analyzing the metabolites, we aimed to explain the phenotypic changes previously recorded.

2.1 Rice shoot metabolite changes under Zn stress in polar extraction

To evaluate the variation amongst our treatments, we visualized the distance and relatedness in the primary metabolites from normal, Zn limited and excess Zn treatments using Principal Component Analysis (PCA) (**Figure 14**). The first principal component (PC1, explaining 28.2% of the variation), represented the greatest variance and separated

doi:10.6342/NTU202100671

NZn and eZn treatments from dZn, which indicated the shoot metabolic change is more strongly affected by dZn than eZn(**Figure 14A**). Besides, the second principal component (PC2, explaining 12.6% of variation) separated NZn from eZn, indicating that eZn samples are characterized by distinct metabolic profiles. These findings were further supported by another PCA clustering using PCA 1 and 3 (**Figure 14B**). Since most metabolite detected were primary metabolite, this gives the impression that primary metabolites of rice were strong affected especially by Zn deficiency.

The relative proportions of accumulated metabolites among the Zn treatments (NZn, dZn, eZn) at 3, 14, and 21 DAT were categorized with a phylogenetic tree and visualized using a heatmap (**Figure 15)**. In total, five main clusters were annotated as Group I, II, III, IV, V. Individual heatmap of each group was also shown to observe the accumulation of metabolites amongst the Zn treatments without interference of other metabolite not within the cluster. Cluster I consisted mainly amino acids (**Figure 16; Supplementary table 1**); cluster II included organic and fatty acids, and alkanes (**Figure 17 ;Supplementary table 2**); cluster III comprised mostly carbohydrates (**Figure 18 ;Supplementary table 3**); cluster IV included carbohydrates, and organic and fatty acids (**Figure 19; Supplementary table 4**); and cluster V made up by carbohydrates, alkanes and fatty acids (**Figure 20; Supplementary table 5**). In addition to the previous transcriptomic data and phenotypic observation, the variation of major metabolites, such as amino acids, carbohydrates/sugar, and fatty acids/lipids were also analyzed and compared amongst Zn stress.

2.2 Metabolite changes in polar extraction: Amino acid

To further analyze the variation in amino acid metabolites during Zn stress, these metabolite were extracted from the total primary metabolite list and shown as a heatmap (**Figure 21A, Table 6**). The averaged values from three biological repeats were also

doi:10.6342/NTU202100671

calculated and shown (**Figure 21B, Table 7**). It can be observed that the dZn treated rice plants (dZn) have significantly accumulated larger amount of amino acids compared to both normal and excess Zn treatments at 14 and 21 DAT (**Table 8**). The accumulated amino acids under dZn treatments can be divided into three major groups: Non-polar aliphatic amino acids consisting of L-alanine, Glycine, L-isoleucine, and L-methionine; polar uncharged amino acids consisting of L-proline, serine, L-threonine, cysteine, and asparagine; non-proteinogenic amino acid L-norleucine and L-ornithine; miscellaneous amino acid L-homosterine, citrulline, and tyramine; and other amino acid related metabolite α-ketoglutaric acid and leucine-glycine small peptide.

2.3 Metabolite changes in polar extraction: Carbohydrates

To further analyze the variation in carbohydrates or related metabolite during Zn stress, these metabolite were extracted from the total primary metabolite list and shown as a heatmap (**Figure 22A, Table 9**). The averaged values from three biological repeats were also calculated and shown (**Figure 22B, Table 10**). Although NZn and dZn (3 DAT) was clustered together, the abundance of carbohydrates under dZn was significantly reduced at both 14 and 21 DAT (**Table 11**); these crbohydrates are: α-ketoglutaric acid, glucose-6-phosphate, myo-inisitol, maltose, D-Fructose, and D-mannose.

2.4 Metabolite changes in polar extractione: Fatty acids

To further analyze the variation in fatty acids or related metabolites during Zn stress, these metabolite were extracted from the total primary metabolite list and shown as a heatmap (**Figure 23A, Table 12**). The averaged values from three biological repeats were also calculated and shown (**Figure 23B, Table 13**). Overall, it was observed that dZn and eZn decreased accumulation of fatty acids. However, only very few of fatty acids were detected and the main unsaturated or saturated 18 carbons fatty acids, octadecanoic acid ,

doi:10.6342/NTU202100671

and 16 carbons, hexadecanoic acids, were not detected (**Figure 23B**). This was due to the extraction and derivatization method was mainly for polar metabolites; therefore, in order to detect more fatty acids, non-polar extraction was performed coupled with the Fatty Acid Methyl Esters (FAMEs) derivatization method and the result will be presented on section 3. .

2.5 Summary: Comparisons of primary metabolite accumulation

To better understand the role of the altered metabolites in metabolism, the metabolites detected at 14 DAT and 21 DAT were mapped respectively unto a summary primary metabolism pathway, which included glycolysis, citric acid cycle and amino acid biosynthesis pathway adapted from Wang et al. (2015). During the dZn treatment, metabolites involved in amino acid biosynthesis were mostly increased in abundance at both 14 and 21 DAT, with the exception of α-ketoglutaric acid (**Figure 24**). Compared to NZn, metabolites L-alanine, L-valine, L-proline, L-phenylalanine, glycine were significantly increased under dZn at both 14 and 21 DAT. Under dZn treatment, the accumulation of L-serine was solely increased at 14 DAT; and L-threonine, L-isoleucine, and L-cysteine were accumulated only at 21 DAT. As for eZn condition, the accumulation of succinate was significantly increased while L-isoleucine was decreased at 14 DAT, when compared to NZn(**Figure 24**). At 21 DAT, the accumulation of L-threonine, aspartate, L-glutamine, L-proline, and glycine were significantly increased in eZn while L-isoleucine remained significantly lower than NZn.

Metabolites involved in carbohydrate related pathways during dZn treatment at 14 DAT were significantly depleted compared to NZn. Generally speaking, the carbonhydate related metabolites such as galactose, glucose-6-phosphate, inositol, maltose, D-fructose, and D-mannose D-mannose were significantly reduced under dZn at both 14 and 21 DAT

doi:10.6342/NTU202100671

(**Figure 25**). There was no significant change in the relative abundance of carbohydrates during eZn treatment except for the reduction of β-D-glucopyranose at 14 DAT; and the decreased β-D-glucopyranose, D-fructose, and D-mannose accumulation at 21 DAT.

3. Rice shoot metabolite changes under Zn stress in non-polar extraction

Some metabolites in nature are hydrophobic, and can only be extracted through non-polar extraction with FAME derivatization method, which is more favorable for GC-MS detection of non-polar metabolites. In this study, we therefore performed an additional non-polar extraction and analyzed the detected metabolites in a similar way with the polar extracted metabolites. Compared to the polar extracts, the non-polar extracts consisted mostly of fatty acids as depicted in the Total Ion Chromatogram (TIC) (**Figure 26A**). The fatty acids detected, from an order of short to long carbon chains, were: propanoic acid (C3) , butanoic acid (C4), hexanoic acid (C6), decanoic acid (C10), 10-undecenoic acid (C11:1), tetradecanoic acid (C14), hexadecanoic acid (C16), 7-hexadecenoic acid (C16:1), heptadecanoic acid (C17), octadecanoic acid (C18), 7-octadecynoic acid (C18:1), 9,12-octadecadienoic acid (C18:2), and 9,12,15-octadecatrienoic acid (C18:3); other small organic acid also included 1,2-benzenedicarboxylic acid, oxalic acid, nitric acid and hexanedioic acid (**Table 14**).

To evaluate the variation amongst our treatments, we visualized the distance and relatedness of fatty acid metabolites amongst NZn, dZn and eZn treatments at 3, 14, 21 DAT using Principal Component Analysis (PCA). The first principal component (PC1, explaining 50.8% of variation) separated 14 and 21 DAT from 3 DAT, indicating that the growth development phases were characterized by distinct fatty acid profiles (**Figure 26B**). The second principal component (PC2, explaining 19.0% of the variation) further

doi:10.6342/NTU202100671

separated control treatments (NZn) from Zn stress (dZn and eZn) for both 14 and 21 DAT.

To further analyze the variation in non-polar extracted fatty acids during Zn stress, these metabolites were shown as a heatmap (**Figure 27A, Table 15**). The averaged values from three biological repeats were also calculated and shown (**Figure 27B, Table 16**). From this heatmap, at 14 DAT both NZn and dZn clustered together whereas eZn clustered along with treatments at 21 DAT. During dZn treatment at 14 DAT, overall fatty acid contents decreased compared to control (NZn), including 9,12-octadecadienoic acid (C18:2), hexadecanoic acid (C16:0), heptadecanoic acid (C17:0) and 9,12,15-octadecatrienoic acid (C18:3). On the contrary, overall fatty acids increased in accumulation during eZn at 14 DAT, such as organic acids oxalic acid and nitric acid; fatty acids 9,12-octadienoic acid (C18:2), propanoic acid, 17-octadecynoic acid, 10-undecenoic acid, and 9,12,13-octadecatrienoic acid, most of which are unsaturated fatty acids. At 21 DAT, the fatty acids, 9,12-octadecadienoic acid (C18:2), tetradecanoic acid, 13-docosenoic acid, and hexanedioic acid, from both dZn and eZn were decreased compared to NZn treatment.

To examine how specific fatty acid changed over their growth stages (3, 14 and 21 days), a line graph was constructed by comparing the peak area (abundance) of the fatty acids under different Zn treatment. Our results showed that saturated fatty acids, such as hexadecanoic acid (C16:0), heptadecanoic acid (C17:0), octadecanoic acid (C18:0) increased over time; however, the unsaturated fatty acids, 7-hexadecanoic acid (C16:1), and 9,12-Octadecadienoic acid (C18:2), and 9,12,15-Octadecatrienoic acid (C18:3) showed a trend of increased accumulation from 3 DAT to 14 DAT, but decreased at 21 DAT (**Figure 28, 29**).

doi:10.6342/NTU202100671

Discussion

The previous transcriptome profiling showed that many primary metabolites related gene were differentially expressed and involved in the regulation of Zn stress response. In this study, we therefore, aimed to study the changes of rice (*Oryza sativa* L.) primary metabolism in response to Zn stress, both Zn deficiency and phytotoxicity condition. We validated and observed the response of rice to Zn deficiency and phytotoxicity, which included: the growth of rice plant, its leaf blade phenotype, and the fine structure of the leaf. From the physiological changes, dZn reduced the growth of the plant, caused loss of pigment on the new emerging leaf giving an albino appearance, and caused an accumulation of transitory starch within the chloroplast of mesophyll cells (**Figure 10D**). During eZn treatment the growth of the plant was not as severely reduced like that of dZn rice, but the excess Zn caused interveinal chlorosis on sub-terminal leaves (**Figure 10C**) and disrupted cell membrane of mesophyll cells (**Figure 13I-J**). From the shoot metabolite analysis, an accumulation of several metabolites were observed including carbohydrates, amino acid and fatty acid. From the metabolite profiling, it can be observed that amino acid accumulates during dZn, carbohydrates and fatty acids decrease at 14 DAT during dZn and a more complex and varying effects can be seen during eZn stress.

Morphological changes under Zn stress

The importance of Zn in plants was first studied in 1915 in Maize and since then the Zn deficient symptoms have been catalogued (Mazé, 1915). During Zn stress, specifically in dZn the disruption in the growth of rice plant may be due to several factors such as: the destruction of cellular structures, the impairment of protein synthesis and a direct interference of indole-3-acetic acid (IAA) metabolism (Sharma, 2006). The first proposal on the effect of Zn on IAA and auxin in plant growth was made by Skoog (1940) and

doi:10.6342/NTU202100671

Tsui (1948) in tomato plants, but the mechanism of this effect was proposed differently. Skoog believe that this interruption in IAA synthesis was caused by oxidation whereas Tsui believed that it was due to the reduced synthesis of the precursor tryptophan (Skoog, 1940; Tsui, 1948). Nevertheless these Zn deficiency caused growth stunts are now known to be due to disruption in IAA and auxin synthesis (Cakmak et al., 1989; Begum et al., 2016). During eZn stress the shoot growth is not as severely affected compared to dZn; however, the root appeared to be more damaged. This damage to the root may be due to the plant's mechanism to avoid translocating harmful amounts of heavy metal to areal parts of the plants and thus the metals are compartmentalized and sequestered in the roots, cause damages (Arif et al., 2016; Ghori et al., 2019).

For leaf blade phenotype, dZn plant, other than impaired elongation of the leaf and narrowing of leaf width, the 21 DAT plant will appear albino at the base of the youngest leaf (fifth leaf) (**Figure 10D**). This symptom appears much later in the plant's development because the rice plant, which was previously grown in optimal Zn concentration for one week before treatment, stored the necessary Zn. When the stored Zn depleted many biochemical processes are disrupted such as carbon assimilation and growth hormone synthesis which led to the inhibited elongation of leaf blade accompanied with the albino phenotype (Sharma, 2006; Mohammad, 2010). The chlorosis in eZn treatment have been recorded in plants and is due to disruption in iron (Fe) uptake, translocation or utilization especially in chlorophyll biosynthesis (Chaney, 1993).

These structural changes at organ level is as a result of damages at cellular level, in the disruption of plant ultrastructure. Plastids, especially chloroplast are central target in metal stress; this can be portrayed in the appearance of chlorosis or the loss of chlorophyll upon metal excess or deficiency. This is because some metals are

doi:10.6342/NTU202100671

micronutrients (such as iron, copper, and manganese) which play an important role in the photosystem, carbon fixation, and plastid transcription of plants (Mohammad, 2010). This is partly why studies pertaining to Zn or other heavy metal stress in plant will most likely have an effect on the chloroplast system (Chen et al., 2008; Mukhopadhyay et al., 2013; Subba et al., 2014). From the fine structure or ultrastructure observation, during dZn treatment, we observed starch accumulation within the mesophyll chloroplast (**Figure 13J**). This may indicate a stress response from the rice plant, impairment in the regulation of source to sink, changes to the biosynthesis or degradation of starch, or changes to the regulation of granule initiation (Roitsch, 1999; Zeeman et al., 2004; Rosa et al., 2009; Streb and Zeeman, 2012; Pfister and Zeeman, 2016). During the eZn stress, both the chlorotic (**Figure 12L-N**) and green (**Figure 12I-K**) leaf sections appear to have enlarged vacuoles or less cytoplasmic content that can be caused by plasma or cell membrane damage from lipid peroxidation, or sequestration and chelation of Zn metal into the vacuoles (Moura et al., 2012; Ghori et al., 2019). These damages may also be due to excess Zn oxidative damage; Zn ion cause oxidative damage by binding to cysteine residue of protein and enzymes or replace other essential metal within their catalytic sites (Nieboer and Richardson, 1980; Schützendübel and Polle, 2002).

Altering primary metabolism in response to Zn

Metabolomic in heavy metal studies have looked at the overall accumulations of amino acid, organic acid, lipids, carbohydrates, and phenolics just to name a few (Singh et al., 2015). Many research is now investigated the cross-talk between metabolome, ionome, and transcriptome as a whole to see which pathway is affected during heavy metal stress in plant, or linking the morphological response to the metabolic response (Wang et al., 2015; Hurtado et al., 2017; Zhang et al., 2017). In our study we also wanted to link our morphological response to the metabolite profile so after analyzing our primary

doi:10.6342/NTU202100671

metabolite data using PCA plot (**Figure 14**) and heatmap (**Figure 15**) and considering both the previous transcriptomic data and morphological observations, three groups of primary metabolite, namely amino acid, carbohydrate and fatty acid, was selected for further analysis.

Effects on amino acids

Amino acids are known as the building blocks of protein molecules and since the requirement of Zn in plant's growth, and cell division and elongation have long been studied and reported, the accumulation of amino acid during Zn deficiency in the shoots have been speculated to be due to the disruption in nitrogen metabolism and protein synthesis (Possingham, 1956; Kitagishi et al., 1987). In our study the mass accumulation of numerous fatty acid is most likely due to disruption in protein synthesis as previously described. Amino acid or short peptides have also been known to improve the heavy metal tolerance of plants acting as metal chelates to reduce its toxic effect on cellular spaces (Bottari and Festa, 1996; Sharma and Dietz, 2006). In our study, at 21 DAT, the amino acids that accumulated in rice shoots during eZn treatment were L-threonine, aspartate, L-glutamine, L-Proline, and glycine. All these amino acids have been found to play a role in either drought stress in the case of glycine and proline, or heavy metal stress (Zn, Cu and Ni) in the case of aspartate, threonine and glutamine (Sharma and Dietz, 2006). To avoid toxicity in areal tissues the plant would tolerate the excess Zn metal by storage in the ground tissue before transportation and chelation in the shoots; therefore, root amino acid concentration for eZn stress treatment should be done to observe amino acid accumulations.

Effects on carbohydrates

In our study, the accumulation of chloroplast transitory starch (**Figure 13A-B**) was observed during dZn treatment and a decrease in carbohydrates content, such as: glucose-

doi:10.6342/NTU202100671

6-phosphate and maltose when compared to both normal and excess Zn treatment (**Figure 24**). The decrease in starch biosynthesis-related carbohydrate, glucose-6-phosphate, may be due to the up-regulation of biosynthesis related genes. Glucose-6-phosphate, an intermediate of the Calvin Cycle, is converted to Glucose-1-phosphate which is the substrate for ADP-Glc pyrophosphorylase (AGPase); this enzyme is critical for the production of ADP-glucose which act as the building block for starch synthases (SS) during biosynthesis of starch (**Figure 30**). The decrease in glucose-6-phosphate during dZn treatment may be due the increase in the rate of starch biosynthesis, more so than the rate glucose-6-phosphate production in Calvin Cycle, resulting in limited reaction and the built-up of starch. Studies done by Suzuki et al. (2012) and Zeng et al. (2019) found that starch biosynthesis related genes were significantly up-regulated, pushing glucose-6-phosphate towards the production of starch grain.

The decrease in starch degradation-related carbohydrate, maltose, is likely due to the disruption of starch degradation through post-translational regulation. The sugar maltose is an important product of hydrolytic starch degradation and the main sugar exported from the chloroplast, it is also correlated with circadian signals, temperature and day length; any inhibition to its transport or metabolism can greatly influence starch degradation (Lu and Sharkey, 2006; Weise et al., 2006) (**Figure 30**). The significant decrease in maltose during dZn treatment may be due to disruption in starch degradation pathway; a study direction not yet proposed. Even if the sample collected may not be according to day length or circadian rhythm, the maltose content is still significantly less than both the control and the excess during the time point collected. In the results of studies done by Suzuki et al. (2012) and Zeng et al. (2019) there was no down regulation of genes related to starch degradation at 28 days and 13 days respectively; these genes also did not show any differential expression during our dZn treatment at 3 DAT. Perhaps the regulation of

doi:10.6342/NTU202100671

starch degradation during dZn in rice is due to the activation of the degradative enzymes through post-translational modification such as phosphorylation or redox activation (Markwell et al., 1984; Tetlow et al., 2004). Many enzymes that participate in the degradation of starch is redox modified such as: dikinase (GWD), phosphoglucan water dikinase (PWD), β-amylases (BAM1 and BAM3), α-Amylase (AMY3), isoamylase 3(ISA3), and limit dextrinase 1 (LDA) (Santelia et al., 2015). dZn is known to disrupt redox homeostasis, and this obstruction may affect the activation of degradative enzymes (Höller et al., 2014).

Carbohydrates play a diversity of role within the plant; apart from energy production they have also been studied to cope with heavy metal stress and help with osmoregulation (Rosa et al., 2009); in our study the disruption in starch degradation in combination with the increase in starch biosynthesis most likely lead to the observed starch accumulation in the chloroplast and the decrease in metabolites related to both pathways. In our results both the substrate metabolite of starch synthesis and the main product of hydrolytic starch degradation decreased in accumulation. In combination with our ultrastructural observations, perhaps dZn hampered the starch degradation process as well. The starch degradation process; however, is a complicated system that is controlled by several factors other than transcriptional regulation including physiological problem like disruption of a plant's growth, metabolite signaling , and environmental cues that may change: the redox potential of the enzyme, or the sink and source balance of the plant (Roitsch, 1999; Sharma, 2006; Rosa et al., 2009; Santelia et al., 2015). Due to the complexity of starch degradation and biosynthesis there are still uncertainties; however, according to the results in this study it can be proposed that the excessive build-up of starch within the chloroplast is due to the effect on both pathways as a response to limited Zn stress.

doi:10.6342/NTU202100671

Effects on fatty acids/lipids

Fatty acids are important component of plants, contributing to resistance against both abiotic and biotic stresses including low and elevated temperatures, salt and drought stress, heavy metal stress, and pathogens; this inducible stress resistance can come from the remodeling of the membrane fluidity and the regulation of fatty acid desaturase or lipase activity (Upchurch, 2008). Heavy metal stress causes an increase in reactive oxygen species (ROS) which damages membrane bounded structures including photosynthetic apparatus of the plants and, inhibition of the growth process in aerial- and underground parts that eventually leads to senescence (Maksymiec, 2007).

From the non-polar extract, most of which are fatty acids, PCA plot was drawn (**Figure 27B**) and revealed that fatty acid content is mostly affected by developmental changes (3, 14, and 21DAT) and amongst the treatments (NZn, dZn, and eZn) the 14 DAT time point had the most variation. To analyze the trends of the fatty acid over time depending on the different Zn treatments (NZn, dZn, and eZn) a line graph was drawn consisting of the major fatty acids: hexadecanoic acid, 7-hexadecanoic acid, heptadecanoic acid (**Figure 28**), octadecanoic acid, 9,12-octadecadienoic acid, and 9,12,15-octadecatrienoic acid (**Figure 29**). From the line graph most fatty acid increase in concentration overtime with the exception of 7-hexadecanoic acid and 9,12-octadecadienoic acid in rice shoots. Overtime these fatty acid may be used as structural component, energy, or even signaling molecules in rice. During dZn treatment, the fatty acid octadecanoic acid and 9,12,15-octadecatrienoic acid was significantly higher at 21 DAT compared to NZn and eZn treatment. In a study done in rice plant during drought stress, different treatments triggered coping mechanism of rice plant, and 18 carbons fatty acid trend changed over a short period of time in which the author correlate to the production of important signaling molecule like Jasmonic acid (Sánchez-Martín et al.,

doi:10.6342/NTU202100671

2018). Perhaps by increasing time points, pro-longing treatment, and decreasing sample variation a more perceptible trend can be observed.

From the PCA and line graph it seemed that between 14 and 21DAT the distribution and quantity of fatty acid changed during both eZn and dZn treatments. Using a heatmap (**Figure 27B**) it was observed that during dZn there is a decrease in fatty acid and since fatty acids are important component of cellular membrane and barriers, dZn may have affected the structure of the membrane or disrupted the saturated fatty acid synthesis (He and Ding, 2020); however in our ultrastructural section we could not see any membrane damage. Perhaps an earlier collection of leaf sample at 14 DAT needs to be done to observe the changes corresponding to this decrease in fatty acid. In our early transcriptomic analysis at 3 DAT (**Figure 6**) fatty acid elongation and desaturase related gene was down-regulated. Perhaps dZn affected the early fatty acid synthesis processes as described previously (He and Ding, 2020). However, after the depletion of fatty acid content at 14 DAT, it was followed by a surge in fatty acids content that lead to a recovery at 21 DAT. It can be inferred that this recovery is due to rice plant response to Zn deficiency stress and this mechanism need to be further investigated.

doi:10.6342/NTU202100671

Conclusion

From the previous transcriptomic data, we explored the possibility of metabolic regulation during both types of Zn stress, Zn deficiency and excess Zn. The current study revealed the alterations in primary metabolite amino acids, fatty acids and carbohydrates under Zn deficiency was greater than that under excess Zn.

Under Zn deficiency, the accumulated amino acids, decreased in carbohydrate content, and reduced fatty acid contents at 14DAT were observed. In addition, a large amount of starch granules were accumulated within the chloroplast; we proposed, is due to the effect of Zn deficiency on starch degradation and biosynthesis (**Figure 30**). Under Zn deficient condition, a reduced amount of glucose-6-phosephate (G6P) may explained by increasing starch synthesis; on the other hands, the hydrolytic degradation of starch was somehow to be blocked, which lead to the reduced maltose. Combined both effects, the starch granules were therefore accumulated on Zn-deficient leaves. Enzymes involved in this pathway were

Under excess Zn condition, a few amino acids known to be related to stress responses were significantly accumulated and a decrease in overall carbohydrates were detected, although not significant. The membrane damage observed did not respond to a decrease in amino acid content at 21 DAT during eZn treatments; therefore, damaged region of rice shoot is not primarily due to reduction in fatty acid content or effects on lipid membrane. It can also be due to fatty acid content of healthy tissue overwriting the alterations in content of damaged ones. In our fatty acid profiling, the change is also more evident during Zn deficiency than excess Zn such as the decrease in overall fatty acid content at 14 DAT and the significant increase in accumulation of C18 fatty acid during 21 DAT; however, to fully understand the fatty acid profiling, increasing time points,

doi:10.6342/NTU202100671

coinciding TEM sampling at 14 DAT, and decreasing sample variation is required to observe a more perceptible trend and make a more conclusive rationale.

Overall, the study revealed interesting findings and new proposal for the effect of dZn on starch degradation, the likely participation of amino acids during Zn phytotoxicity, and propose the likelihood of rice plant response and recovery of during Zn deficiency by observing fatty acid profile overtime.

doi:10.6342/NTU202100671

References

Abdelhamid M, Sadak M, Schmidhalter U (2014) Effect of foliar application of aminoacids on plant yield and some physiological parameters in bean plants irrigated with seawater. Acta Biol Colomb **20:** 140-152

Alboukadel K, Fabian M (2020) factoextra: extract and visualize the results of multivariate data analyses.

Anjum NA, Hasanuzzaman M, Hossain MA, Thangavel P, Roychoudhury A, Gill SS, Rodrigo MAM, Adam V, Fujita M, Kizek R, Duarte AC, Pereira E, Ahmad I (2015) Jacks of metal/metalloid chelation trade in plants—an overview. Front Plant Sci **6**

Arif N, Yadav V, Singh S, Singh S, Ahmad P, Mishra RK, Sharma S, Tripathi DK, Dubey NK, Chauhan DK (2016) Influence of high and low levels of plant-beneficial heavy metal ions on plant growth and development. Front Environ Sci **4**

Barceló J, Poschenrieder C (2004) Structural and ultrastructural changes in heavy metal exposed plants. *In* MNV Prasad, ed, Heavy metal stress in plants: from biomolecules to ecosystems. Springer Berlin Heidelberg, Berlin, Heidelberg, pp 223-248

Begum MC, Islam M, Sarkar MR, Azad MAS, Huda AKMN, Kabir AH (2016) Auxin signaling is closely associated with Zn-efficiency in rice (Oryza sativa L.). J Plant Interact **11:** 124-129

Biancucci M, Mattioli R, Forlani G, Funck D, Costantino P, Trovato M (2015) Role of proline and GABA in sexual reproduction of angiosperms. Front Plant Sci **6:** 680-680

Bidar G, Verdin A, Garçon G, Pruvot C, Laruelle F, Grandmougin-Ferjani A, Douay F, Shirali P (2008) Changes in fatty acid composition and content of two plants (Lolium perenne and Trifolium repens) grown during 6 and 18 months in a metal (Pb, Cd, Zn) contaminated field. Water Air Soil Pollut **192:** 281-291

Bottari E, Festa MR (1996) Asparagine as a ligand for cadmium(II), lead(II) and zinc(II). Chem Speciat Bioavailab **8:** 75-83

Broadley MR, White PJ, Hammond JP, Zelko I, Lux A (2007) Zinc in plants. New Phytol **173:** 677-702

Cakmak I, Marschner H (1988) Increase in membrane permeability and exudation in roots of zinc deficient plants. J Plant Physiol **132:** 356-361

Cakmak I, Marschner H, Bangerth F (1989) Effect of zinc nutritional status on growth, protein metabolism and levels of indole-3-acetic acid and other phytohormones in bean (Phaseolus vulgaris L.). J Exp Bot **40:** 405-412

Callahan DL, Baker AJ, Kolev SD, Wedd AG (2006) Metal ion ligands in hyperaccumulating plants. J Biol Inorg Chem **11:** 2-12

Chaney RL (1993) Zinc Phytotoxicity. *In* AD Robson, ed, Zinc in Soils and Plants, Vol 55. Springer, Dordrecht

Cheah BH, Chen Y-L, Lo J-C, Tang I-C, Yeh K-C, Lin Y-F (2020) Divalent nutrient cations: friend and foe during zinc stress in rice. Authorea

Chen W, Yang X, He Z, Feng Y, Hu F (2008) Differential changes in photosynthetic capacity, 77 K chlorophyll fluorescence and chloroplast ultrastructure between Zn-efficient and Zn-inefficient rice genotypes (Oryza sativa) under low zinc stress. Physiol Plant **132:** 89-101

Daisaku O, Takumi O, Atsushi O (2021) Research Square

Erb M, Kliebenstein DJ (2020) Plant secondary metabolites as defenses, regulators, and

doi:10.6342/NTU202100671

primary metabolites: the blurred functional trichotomy. Plant Physiol **184:** 39-52
Fernie AR, Pichersky E (2015) Focus issue on metabolism: metabolites, metabolites everywhere. Plant Physiol **169:** 1421-1423
Garnier S (2018) viridis: Default Color Maps from 'matplotlib'.
Geigenberger P (2011) Regulation of starch biosynthesis in response to a fluctuating environment. Plant Physiol **155:** 1566-1577
Ghori NH, Ghori T, Hayat MQ, Imadi SR, Gul A, Altay V, Ozturk M (2019) Heavy metal stress and responses in plants. Int J Environ Sci Technol **16:** 1807-1828
Gupta AK, Kaur N (2005) Sugar signalling and gene expression in relation to carbohydrate metabolism under abiotic stresses in plants. J Biosci **30:** 761-776
Hacisalihoglu G (2020) Zinc (Zn): The Last Nutrient in the Alphabet and Shedding Light on Zn Efficiency for the Future of Crop Production under Suboptimal Zn. Plants (Basel) **9**
Hadley Wickham MA, Jennifer Bryan, Winston Chang, Lucy D'Agostino McGowan, Romain François, Garrett Grolemund, Alex Hayes, Lionel Henry, Jim Hester, Max Kuhn, Thomas Lin Pedersen, Evan Miller, Stephan Milton Bache, Kirill Müller, Jeroen Ooms, David Robinson, Dana Paige Seidel, Vitalie Spinu, Kohske Takahashi, Davis Vaughan, Claus Wilke, Kara Woo, Hiroaki Yutani (2019) Welcome to the {tidyverse}. Journal of Open Source Software **4:** 1686
Hartmann T (2007) From waste products to ecochemicals: Fifty years research of plant secondary metabolism. Phytochemistry **68:** 2831-2846
He M, Ding N-Z (2020) Plant unsaturated fatty acids: multiple roles in stress response. Front Plant Sci **11**
Hildebrandt TM, Nunes Nesi A, Araújo WL, Braun HP (2015) Amino Acid Catabolism in Plants. Mol Plant **8:** 1563-1579
Höller S, Meyer A, Frei M (2014) Zinc deficiency differentially affects redox homeostasis of rice genotypes contrasting in ascorbate level. J Plant Physiol **171:** 1748-1756
Hornik MMaPRaASaMHaK (2019) cluster: Cluster Analysis Basics and Extensions.
Hurtado C, Parastar H, Matamoros V, Piña B, Tauler R, Bayona JM (2017) Linking the morphological and metabolomic response of Lactuca sativa L exposed to emerging contaminants using GC × GC-MS and chemometric tools. Sci Rep **7:** 6546
Jain R, Jenkins J, Shu S, Chern M, Martin JA, Copetti D, Duong PQ, Pham NT, Kudrna DA, Talag J, Schackwitz WS, Lipzen AM, Dilworth D, Bauer D, Grimwood J, Nelson CR, Xing F, Xie W, Barry KW, Wing RA, Schmutz J, Li G, Ronald PC (2019) Genome sequence of the model rice variety KitaakeX. BMC Genom **20:** 905
Jyung WH, Ehmann A, Schlender KK, Scala J (1975) Zinc Nutrition and Starch Metabolism in Phaseolus vulgaris. Plant Physiol **55:** 414-420
Kirkby E (2012) Chapter 1 - Introduction, definition and classification of nutrients. *In* P Marschner, ed, Marschner's mineral nutrition of higher plants, Ed 3. Academic Press, San Diego, pp 3-5
Kitagishi K, Obata H (1986) Effects of zinc deficiency on the nitrogen metabolism of meristematic tissues of rice plants with reference to protein synthesis. J Soil Sci **32:** 397-405
Kitagishi K, Obata H, Kondo T (1987) Effect of zinc deficiency on 80S ribosome content of meristematic tissues of rice plant. J Soil Sci **33:** 423-429
Kötting O, Kossmann J, Zeeman SC, Lloyd JR (2010) Regulation of starch metabolism:

doi:10.6342/NTU202100671

the age of enlightenment? Curr Opin Plant Biol **13:** 320-328
Length R (2016) Least-squares means: the {R} package {lsmeans}. J Stat Softw **69:** 1-33
Lisec J, Schauer N, Kopka J, Willmitzer L, Fernie AR (2006) Gas chromatography mass spectrometry–based metabolite profiling in plants. Nat Protoc **1:** 387-396
López-Arredondo DL, Sánchez-Calderón L, Yong-Villalobos L (2017) Chapter 1 - Molecular and genetic basis of plant macronutrient use efficiency: concepts, opportunities, and challenges. *In* MA Hossain, T Kamiya, DJ Burritt, L-SP Tran, T Fujiwara, eds, Plant Macronutrient Use Efficiency. Academic Press, pp 1-29
Lu Y, Sharkey TD (2006) The importance of maltose in transitory starch breakdown. Plant Cell Environ **29:** 353-366
Maksymiec W (2007) Signaling responses in plants to heavy metal stress. Acta Physiol Plant **29:** 177
Markwell JP, Baker NR, Bradbury M, Thornber JP (1984) Use of zinc ions to study thylakoid protein phosphorylation and the state 1-state 2 transition in vitro. Plant Physiol **74:** 348-354
Mazé P (1915) Détermination des éléments minéraux rares nécessaires au développement du maïs. Comptes Rendus Hebdomadaires des Séances de L'académie des Sciences **160:** 211-214
McCall KA, Huang C-c, Fierke CA (2000) Function and Mechanism of Zinc Metalloenzymes. J Nutr **130:** 1437S-1446S
Merchant SS (2010) The elements of plant micronutrients. Plant physiol **154:** 512-515
Mohammad P (2010) Heavy metals and plastid metabolism. *In* Handbook of plant and crop Stress. CRC Press
Moura DJ, Péres VF, Jacques RA, Saffi J (2012) Heavy Metal Toxicity: Oxidative Stress Parameters and DNA Repair. *In* DK Gupta, LM Sandalio, eds, Metal Toxicity in Plants: Perception, Signaling and Remediation. Springer Berlin Heidelberg, Berlin, Heidelberg, pp 187-205
Mukhopadhyay M, Das A, Subba P, Bantawa P, Sarkar B, Ghosh P, Mondal TK (2013) Structural, physiological, and biochemical profiling of tea plantlets under zinc stress. Biol Plant **57:** 474-480
Nieboer E, Richardson DHS (1980) The replacement of the nondescript term 'heavy metals' by a biologically and chemically significant classification of metal ions. Environ Pollut B **1:** 3-26
Nigh R, Diemont SA (2013) The Maya milpa: fire and the legacy of living soil. Front Ecol Environ **11:** e45-e54
Nouairi I, Ammar WB, Youssef NB, Daoud DBM, Ghorbal MH, Zarrouk M (2006) Comparative study of cadmium effects on membrane lipid composition of Brassica juncea and Brassica napus leaves. Plant Sci J **170:** 511-519
Ouariti O, Boussama N, Zarrouk M, Cherif A, Habib Ghorbal M (1997) Cadmium- and copper-induced changes in tomato membrane lipids. Phytochemistry **45:** 1343-1350
Pfister B, Zeeman SC (2016) Formation of starch in plant cells. Cellular and Molecular Life Sciences **73:** 2781-2807
Possingham J (1956) The effect of mineral nutrition on the content of free amino acids and amides in tomato plants and a comparison of the effects of deficiencies of copper, zinc, manganese, iron, and molybdenum. Cell Mol Life Sci **9:** 539-551
Quinlan-Watson TAF (1951) Aldolase activity in zinc-deficient plants. Nature **167:** 1033-1034
Rascio N, Navari-Izzo F (2011) Heavy metal hyperaccumulating plants: How and why

doi:10.6342/NTU202100671

do they do it? And what makes them so interesting? Plant Sci J **180:** 169-181
Reed HS (1939) The relation of copper and zinc salts to leaf structure. Am J Bot **26:** 29-33
Rodrigues J, Inzé D, Nelissen H, Saibo NJM (2019) Source–sink regulation in crops under water deficit. Trends in Plant Sci **24:** 652-663
Roitsch T (1999) Source-sink regulation by sugar and stress. Curr Opin Plant Biol **2:** 198-206
Rosa M, Prado C, Podazza G, Interdonato R, González JA, Hilal M, Prado FE (2009) Soluble sugars metabolism, sensing and abiotic stress: a complex network in the life of plants. Plant Signal Behav **4:** 388-393
Samarakoon AB, Rauser WE (1979) Carbohydrate levels and photoassimilate export from leaves of phaseolus vulgaris exposed to excess cobalt, nickel, and zinc. Plant physiol **63:** 1165-1169
Sánchez-Martín J, Canales FJ, Tweed JKS, Lee MRF, Rubiales D, Gómez-Cadenas A, Arbona V, Mur LAJ, Prats E (2018) Fatty acid profile changes during gradual soil water depletion in oats suggests a role for jasmonates in coping with drought. Front Plant Sci **9**
Santelia D, Trost P, Sparla F (2015) New insights into redox control of starch degradation. Curr Opin Plant Biol **25:** 1-9
Santelia D, Trost P, Sparla F (2015) New insights into redox control of starch degradation. Current Opinion in Plant Biology **25:** 1-9
Scharrer K (1949) Justus von Liebig and today's agricultural chemistry. J Chem Educ **26:** 515
Schützendübel A, Polle A (2002) Plant responses to abiotic stresses: heavy metal-induced oxidative stress and protection by mycorrhization. J Exp Bot **53:** 1351-1365
Sharma CP (2006) Zinc. *In* Plant Micronutrients. Science Publishers, Enfield, NH
Sharma SS, Dietz KJ (2006) The significance of amino acids and amino acid-derived molecules in plant responses and adaptation to heavy metal stress. J Exp Bot **57:** 711-726
Shulaev V, Cortes D, Miller G, Mittler R (2008) Metabolomics for plant stress response. Physiol Plant **132:** 199-208
Sillanpää M (1982) Micronutrients and the nutrient status of soils: a global study, Vol 48. Food & Agriculture Org.
Singh S, Parihar P, Singh R, Singh VP, Prasad SM (2015) Heavy Metal Tolerance in Plants: Role of Transcriptomics, Proteomics, Metabolomics, and Ionomics. Front Plant Sci **6:** 1143
Skoog F (1940) Relationships between zinc and auxin in the growth of higher plants. Am J Bot **27:** 939-951
Smith SM, Fulton DC, Chia T, Thorneycroft D, Chapple A, Dunstan H, Hylton C, Zeeman SC, Smith AM (2004) Diurnal changes in the transcriptome encoding enzymes of starch metabolism provide evidence for both transcriptional and posttranscriptional regulation of starch metabolism in Arabidopsis leaves. Plant Physiol **136:** 2687-2699
Streb S, Zeeman SC (2012) Starch metabolism in Arabidopsis. The arabidopsis book **10**
Subba P, Mukhopadhyay M, Mahato SK, Bhutia KD, Mondal TK, Ghosh SK (2014) Zinc stress induces physiological, ultra-structural and biochemical changes in mandarin orange (Citrus reticulata Blanco) seedlings. Physiol Mol Biol Plants **20:** 461-473
Suzuki M, Bashir K, Inoue H, Takahashi M, Nakanishi H, Nishizawa NK (2012)

doi:10.6342/NTU202100671

Accumulation of starch in Zn-deficient rice. Rice **5:** 9
Team RC (2020) R: A Language and Environment for Statistical Computing
Tetlow IJ, Morell MK, Emes MJ (2004) Recent developments in understanding the regulation of starch metabolism in higher plants. J Exp Bot **55:** 2131-2145
Tsui C (1948) The role of zinc in auxin synthesis in the tomato plant. J Bot **35:** 172-179
Upchurch RG (2008) Fatty acid unsaturation, mobilization, and regulation in the response of plants to stress. Biotechnol Lett **30:** 967-977
Vallee BL (1955) Zinc and Metalloenzymes. *In* ML Anson, K Bailey, JT Edsall, eds, Advances in Protein Chemistry, Vol 10. Academic Press, pp 317-384
Vesk M, Possingham J, Mercer F (1966) The effect of mineral nutrient deficiencies on the structure of the leaf cells of tomato, spinach, and maize. Aust J Bot **14:** 1-18
von Wirén N, Klair S, Bansal S, Briat J-F, Khodr H, Shioiri T, Leigh RA, Hider RC (1999) Nicotianamine Chelates Both FeIII and FeII: implications for metal transport in plants. Plant Physiology **119:** 1107-1114
Vu VQ (2011) ggbiplot: A ggplot2 based biplot.
Waldron KJ, Rutherford JC, Ford D, Robinson NJ (2009) Metalloproteins and metal sensing. Nature **460:** 823-830
Wang Y, Xu L, Shen H, Wang J, Liu W, Zhu X, Wang R, Sun X, Liu L (2015) Metabolomic analysis with GC-MS to reveal potential metabolites and biological pathways involved in Pb &Cd stress response of radish roots. Sci Rep **5:** 18296-18296
Weise SE, Schrader SM, Kleinbeck KR, Sharkey TD (2006) Carbon balance and circadian regulation of hydrolytic and phosphorolytic breakdown of transitory starch. Plant Physiol **141:** 879-886
Westfall THaFBaP (2008) Simultaneous Inference in General Parametric Models. **50:** 346-363
White MC (1981) Metal complexation in xylem fluid: theoretical equillibrium model and computational computer program. Plant Physiol **67:** 301-310
Whitford D (2005) Proteins: Structure and Function. Wiley
Wickham H (2016) ggplot2: Elegant Graphics for Data Analysis.
Wickham H, François R, Henry L, Müller K (2020) dplyr: A Grammar of Data Manipulation.
Wuana RA, Okieimen FE (2011) Heavy metals in contaminated soils: a review of sources, chemistry, risks and best available strategies for remediation. ISRN Ecol **2011:** 402647
Yoshida S, Institute IRR (1976) Laboratory Manual for Physiological Studies of Rice. International Rice Research Institute
Yuan S-w, Wu X-l, Liu Z-h, Luo H-b, Huang R-z (2012) Abiotic stresses and phytohormones regulate expression of FAD2 gene in arabidopsis thaliana. J Integr Agric **11:** 62-72
Zeeman SC, Smith SM, Smith AM (2004) The breakdown of starch in leaves. New Phytol **163:** 247-261
Zeng H, Zhang X, Ding M, Zhang X, Zhu Y (2019) Transcriptome profiles of soybean leaves and roots in response to zinc deficiency. Physiol Plant **167:** 330-351
Zhang YF, Wang Y, Ding ZT, Wang H, Song LB, Jia SS, Ma DX (2017) Zinc stress affects ionome and metabolome in tea plants. Plant Physiol Biochem **111:** 318 328

doi:10.6342/NTU202100671

Tables

Table 1. List of cellular biogenic amine metabolism related DEGs (Differentially Expressed Genes).

Ten-day-old rice plants were exposed to three different Zn concentrations: dZn, representing Zn deficiency, with 0.002 μM $ZnSO_4$; NZn, representing normal Zn condition, with 0.2 μM $ZnSO_4$; and eZn, representing Zn excess, with 300 μM $ZnSO_4$ for 3 days. List of gene was obtained from GO-enrichment analysis and the Log_2 Fold Change was calculated from FPKM of three repeats.

Gene ID	Description	log2 fold change					
		dZn vs. NZn_shoot	eZn vs. NZn_shoot	eZn vs. dZn_shoot	eZn vs. dZn_root	dZn vs. NZn_root	eZn vs. NZn_root
Os03g0119100	Similar to Phospholipase D beta 2	-0.66151	0.626658	1.288168	-2.552	2.791862	0.239867
Os08g0401800	Similar to Phospholipase D	-0.0448	-0.02588	0.018922	-1.52014	-0.13216	-1.6523
Os03g0307200	Nicotianamine synthase 2 (*OsNAS2*)	0	0.684913	0	2.373444	-0.76809	1.605357
Os06g0604300	Chloroplast-localized phospholipase D, Herbivore defense	0.029474	-0.11251	-0.14198	-0.96314	0.126501	-0.83664
Os07g0689600	Nicotianamine synthase 3 (*OsNAS3*)	0.487627	-0.1028	-0.59042	-1.5401	0.359181	-1.18092
Os03g0307300	Nicotianamine synthase 1 (*OsNAS1*)	0.619568	-1.914	-2.53357	2.290051	-0.72991	1.560143

doi:10.6342/NTU202100671

Table 2. List of polysaccharide catabolic process related DEGs.

Ten-day-old rice plants were exposed to three different Zn concentrations: dZn, representing Zn deficiency, with 0.002 μM $ZnSO_4$; NZn, representing normal Zn condition, with 0.2 μM $ZnSO_4$; and eZn, representing Zn excess, with 300 μM $ZnSO_4$ for 3 days. List of gene was obtained from GO-enrichment analysis and the Log_2 Fold Change was calculated from FPKM of three repeats.

Gene ID	Description	log_2 fold change					
		dZn vs. NZn_shoot	eZn vs. NZn_shoot	eZn vs. dZn_shoot	eZn vs. dZn_root	dZn vs. NZn_root	eZn vs. NZn_root
Os06g0726100	Similar to Seed chitinase-c	1.92	0.84	-1.08	-0.20	-0.04	-0.25
Os11g0592000	Similar to Barwin	1.77	0.52	-1.26	-1.76	-0.72	-2.48
Os05g0399300	Similar to Chitinase	1.37	-0.92	-2.28	-0.92	0.05	-0.87
Os07g0543300	Similar to Beta-amylase	0.59	-0.74	-1.33	-0.05	-0.12	-0.17
Os05g0399400	*Chitinase 9*	0.43	-0.05	-0.48	-4.10	1.72	-2.37
Os01g0937000	Peptidase aspartic, catalytic domain containing protein	0.00	0.00	0.00	0.00	0.86	0.00

doi:10.6342/NTU202100671

Table 3. List of hydrolase activity related DEGs.

Ten-day-old rice plants were exposed to three different Zn concentrations: dZn, representing Zn deficiency, with 0.002 μM $ZnSO_4$; NZn, representing normal Zn condition, with 0.2 μM $ZnSO_4$; and eZn, representing Zn excess, with 300 μM $ZnSO_4$ for 3 days. List of gene was obtained from GO-enrichment analysis and the Log_2 Fold Change was calculated from FPKM of three repeats.

Gene ID	Description	log_2 fold change					
		dZn vs. NZn_shoot	eZn vs. NZn_shoot	eZn vs. dZn_shoot	eZn vs. dZn_root	dZn vs. NZn_root	eZn vs. NZn_root
Os01g0946600	glycosyl hydrolases family 17	-0.47	0.24	0.71	-1.12	-0.25	-1.37
Os07g0452100	galA, rafA; alpha-galactosidase	-1.64	-0.33	1.31	0.00	0.00	0.00
Os01g0303100	chitinase	-1.66	0.26	1.92	-0.83	-0.32	-1.15
Os01g0713200	glycosyl hydrolases family 17	0.29	-0.19	-0.48	-1.14	-0.68	-1.83
Os06g0335900	xyloglucan:xyloglucosyl transferase	-0.81	0.77	1.58	1.33	-0.56	0.77
Os11g0592000	WIP3 - Wound-induced protein precursor	1.77	0.52	-1.26	-1.76	-0.72	-2.48
Os08g0518900	chitinase	-0.20	-0.21	-0.01	-1.45	0.02	-1.43
Os06g0726100	CHIB; basic endochitinase B	1.92	0.84	-1.08	-0.20	-0.04	-0.25
Os08g0237800	TCH4; xyloglucan:xyloglucosyl transferase	0.00	0.00	0.00	1.54	-0.54	1.00
Os01g0947000	glycosyl hydrolases family 17	1.19	0.32	-0.88	-1.43	-0.10	-1.53
Os07g0543300	beta-amylase	0.59	-0.74	-1.33	-0.05	-0.12	-0.17
Os05g0399300	CHIB; basic endochitinase B	1.37	-0.92	-2.28	-0.92	0.05	-0.87
Os05g0247100	chitinase	0.53	-0.19	-0.72	-1.31	0.02	-1.29
Os05g0399400	CHIB; basic endochitinase B	0.43	-0.05	-0.48	-4.10	1.72	-2.37
Os05g0366000	Os5bglu21 - beta-glucosidase homologue	0.37	0.52	0.16	-1.29	-0.16	-1.44
Os04g0513400	bglB; beta-glucosidase	0.01	-0.27	-0.27	-2.71	-0.61	-3.32
Os04g0604300	TCH4; xyloglucan:xyloglucosyl transferase	-0.59	0.15	0.74	1.09	-0.10	0.99
Os10g0416500	glycosyl hydrolase	1.63	-0.02	-1.65	-1.27	-1.03	-2.31
Os01g0691000	unknown	0.10	0.88	0.78	-1.13	0.31	-0.81
Os07g0539100	glucan endo-1,3-beta-glucosidase precursor	0.53	0.03	-0.50	-1.10	-0.24	-1.35
Os04g0513700	glB; beta-glucosidase	0.74	-0.82	-1.56	-2.74	0.14	-2.60

doi:10.6342/NTU202100671

Table 4. List of fatty acid biosynthetic process related DEGs.

Ten-day-old rice plants were exposed to three different Zn concentrations: dZn, representing Zn deficiency, with 0.002 μM $ZnSO_4$; NZn, representing normal Zn condition, with 0.2 μM $ZnSO_4$; and eZn, representing Zn excess, with 300 μM $ZnSO_4$ for 3 days. List of gene was obtained from GO-enrichment analysis and the Log_2 Fold Change was calculated from FPKM of three repeats.

Gene ID	Description	log_2 fold change					
		dZn vs. NZn_shoot	eZn vs. NZn_shoot	eZn vs. dZn_shoot	eZn vs. dZn_root	dZn vs. NZn_root	eZn vs. NZn_root
Os01g0529800	Similar to Very-long-chain fatty acid condensing enzyme CUT1	-0.88	0.25	1.13	-0.49	-0.10	-0.59
Os08g0508800	Lipoxygenase, chloroplast precursor	-0.43	0.22	0.65	-2.51	-0.30	-2.82
Os03g0220100	beta-ketoacyl-CoA synthase, Very-long-chain fatty acid (VLCFA) elongation	-0.42	0.20	0.62	2.18	-1.37	0.81
Os11g0591200	Similar to 3-ketoacyl-CoA synthase	-0.40	0.01	0.41	1.48	-0.92	0.57
Os01g0880800	Similar to Acyl-[acyl-carrier-protein] desaturase, (Stearoyl-ACP desaturase)	-0.27	0.21	0.49	1.62	-0.09	1.52
Os02g0731900	Similar to 3-ketoacyl-CoA synthase	-0.14	-0.11	0.03	2.28	-0.28	2.01
Os08g0509100	Similar to Lipoxygenase, chloroplast precursor	-0.11	0.46	0.57	-1.64	-0.08	-1.72
Os01g0921500	Similar to SNF1-related protein kinase regulatory gamma subunit 1 (AKIN gamma1) (AKING1)	0.49	-0.10	-0.59	2.69	-1.01	1.69

doi:10.6342/NTU202100671

Table 5. Full strength Kimura solutions.

(**A**) 1L full-strength kimura solution contain a 2:2:1 ml of A, B and C stock solution. The pH was adjusted to 5.0 ± 0.02 with 1M HCl and 1M KOH. Zn stock concentration made separate from solution C. (**B**) Zn working solution is added to kimura solution according to Zn treatments.

A

Solution A (500x, 1 L) stock		
$(NH_4)_2SO_4$		24.1 g
KNO_3		9.25 g
$MgSO_4.7H_2O$		67.5 g
KH_2PO_4		12.4 g
Solution B (500x, 1L) stock		
Fe-Citrate		7.5 g
$Ca(NO_2)_2.4H_2O$		43.1 g
12N HCl		41.67 mL
Solution C without Zn (500x, 1L) stock		
H_3BO_3		0.155 g
$MnSO_4.7H_2O$		0.034 g
$CuSO_4.5H_2O$		0.013 g
H_2MoO_4		0.008 g
$ZnSO_4$ stock solutions (500 ml)		
dZn	100 µM	0.008g
NZn	10 mM	0.807g
eZn	100 mM	8.074g

B

$ZnSO_4$ working solution (1L)		
NZn	10 mM	20 µl
dZn	100 µM	20 µl
eZn	100 mM	3 ml

doi:10.6342/NTU202100671

Table 6. Amino acids peak area from the general metabolomics profile.

Amino acids from polar shoot extraction detected through GCxGC-TOFMS were ordered in the table according to the heatmap generated (**Figure 21**). Peak areas of 3 repeats at 3, 14 and 21 days after treatment (DAT) were shown. Zn concentration used in this study was dZn = 0.002 μM $ZnSO_4$, NZn = 0.2 μM $ZnSO_4$, eZn = 300 μM $ZnSO_4$.

	Optimal Zn treatment (NZn)									Zn deficient treatment (dZn)									Zn excess treatment (eZn)								
Metabolite	**3 DAT**			**14 DAT**			**21 DAT**			**3 DAT**			**14 DAT**			**21 DAT**			**3 DAT**			**14 DAT**			**21 DAT**		
Leu-Gly	48987.58	68402.81	54663.64	163910	20994.8	163149.6	248797.2	220710.2	219488.5	127300.2	144466.7	142316.5	1184426	8853752	1282816	4833334	3965069	3389959	681829.91	544368.68	456241.36	775443.92	434222.27	817743.89	650802.03	518105.88	390822.72
Alpha-ketoglutaric acid	1792435	1222734	1593999	1651484	1469627	1521737	1349443	1490230	1444483	1574455	1693482	1560339	1040602	8451025	1132289	3965239	3097314	3714669	1320923	1315970	1819394	2127297	1206735	1547613	1181105	1094729	1937813
Colchifoleine	9703752	1214476	1118751	9940917	1093599	1030777	1064771	992486	834657	1252893	1210515	1224745	1505184	1346485	1989684	1837377	1408709	1242179	1261361	1244048	1397027	1047471	1308048	1295357	1444027	1177969	1240821
L-Aspartic acid	1371932	1384802	1669307	1105434	548294.5	1155097	237566.4	285288.6	138016	109312	180926	221503	1716608	2098022	2388428	3098902	5416819	4870449	120783	161836	119364	125302	126443	126254	158846	146138	148252
L-Homoserine	0	0	0	0	0	0	0	0	0	0	0	0	7002402	3467977	84303	2498757	2296788	2974956	0	0	0	0	0	0	0	0	0
l-Proline	2456569	2569319	2878348	2041243	1103024	1767421	820892.5	965212.8	617173.5	310109	285438	413554	2665615	2460419	3903181	2821459	2416858	1818947	267647	315815	271285	171303	239988	179391	235617	222872	194751
Serine	2001192	2006600	1794235	1534957	1110834	1401456	859306.3	727290.2	552380.6	203728	262165	317748	1063747	1102910	1554390	1521632	1014812	1082355	181656	250937	168479	168378	316335	199706	287397	279377	386537.3
L-Threonine	1182114	1261739	1341804	1321981	8776001.6	1213900	623647.2	587204.9	391983.7	135123	134956	177102	9420883	1144771	1326072	1266098	1144147	1305770	122221	143361	116866	104421	165612	547993.2	208679	148720	130772
l-Alanine	3894291	3628833	2288940	2435247	1494253	2319840	629483.9	443411.5	217033.1	207066	401859	158907	1013038	1019796	1132293	9561237	8212890	9918797	151594	270899	341559	212930	212313	144621	236007	184210	202700
asparagine 4	1219901	1424302	1593474	1814157	1254798	1162054	122271.1	181051.9	129732.7	268844.6	139186.1	389408.1	1427428	2623846	5930764	2635706	1493255	1110130	172730.7	135942.8	223590.6	188827.3	203045.6	204671.1	220603	165542.2	176066.8
Tryptophan	6773834	7424778	4937545	0	0	4474057	612306.07	159401.94	606805.84	0	134206.4	689644.45	1454644.6	2756227.7	4817747	6985699.9	9558455.6	2766979	530244.13	690359.3	804332.32	0	517799.41	404000.32	169004.4	134951.7	802133.33

doi:10.6342/NTU202100671

	Optimal Zn treatment (NZn)									Zn deficient treatment (dZn)									Zn excess treatment (eZn)								
Metabolite	**3 DAT**			**14 DAT**			**21 DAT**			**3 DAT**			**14 DAT**			**21 DAT**			**3 DAT**			**14 DAT**			**21 DAT**		
Tyramine	34481.4	26797.58	26825.51	119238.1	20053.18	50999.19	39159.19	19885.73	0	16002.36	49496.52	30346.81	65992.33	249896.8	64920.44	906011.6	4088790	1981412	31429.46	40461.32	28226.84	0	56841.77	25634.23	265434	192802.5	64253.39
L-Ornithine	0	0	36012.03	0	0	0	0	0	0	0	0	0	465592.1	1404687	601885.9	1350349	1532768	945226.7	0	0	0	0	0	0	0	0	0
L-Methionine	0	0	0	0	39778.37	0	0	0	0	0	160212.5	0	421746.7	996727.6	673320.9	1335736	1412679	960427.2	139736.4	0	0	101025.8	86117.95	0	0	121648.8	163278.3
L-Norleucine	70875.94	80229.01	34723.74	25572.1	46233.64	49852.06	13841.36	0	0	0	139784.6	43790.73	436913.1	485018.8	507428.8	695780.9	886657.5	534510.8	51061.27	80688.15	13778.74	27548.08	0	0	0	26818.12	0
l-Isoleucine	64306.47	81422.77	47730.6	81496.61	104790.5	77243.44	125363.5	110000.3	138583.9	78982.76	159118.5	98307.36	211918.5	140424.6	271107	514999	576705.7	403525.6	76296.48	69002.64	57177.22	34506.43	19248.12	40967.08	68244.66	38767.88	23738.49
Glycine	241231.9	270707.9	238174.7	197974.9	111823.8	173492.1	94629.81	87450.58	72524.51	206795.4	250038.4	275093	1837687	1442064	1604855	2744193	2528864	3072191	243713.6	275389.4	241432.5	142289.1	210132.7	150242.7	332904	234462.1	234276.8
l-Valine	339919	389140.6	313986.6	330910.1	360624.3	310685.4	383252.4	353569.4	398017.6	438208.6	563843.6	495320.1	1359733	1356324	1640456	1850794	2381122	2209122	377784.5	377193.8	324846.5	286919.1	260266.1	290776	436007.1	310986.2	282890.2
Cysteine	8974.249	0	0	0	0	0	0	0	0	0	8179.475	0	0	39061.37	0	53457.21	90189.04	69320.28	0	0	9009.702	0	0	0	0	0	0
Citrulline	24420.4	19811.33	20509.93	0	0	17803.69	15331.45	18573.2	0	30506.51	40173.44	30049.37	43931.1	152953.4	0	161451.2	198542.6	203388.3	20031.15	21967.76	0	0	21613.39	0	30542.04	29968.94	29060.1

doi:10.6342/NTU202100671

Table 7. Averaged peak area of amino acid.

Amino acids peak areas of 3 replicates at 3, 14 and 21 days after treatment (DAT) were averaged from **Table 11**. Zn concentration used in this study was dZn = 0.002 μM $ZnSO_4$, NZn = 0.2 μM $ZnSO_4$, eZn = 300 μM $ZnSO_4$.

	NZn treatment			dZn treatment			eZn treatment		
Metabolite	**3 DAT**	**14 DAT**	**21 DAT**	**3 DAT**	**14 DAT**	**21 DAT**	**3 DAT**	**14 DAT**	**21 DAT**
Alpha-ketoglutaric acid	1536389	1547616	1428052	1609425	1005998	359240.8	1485429	1627215	1404549
Leucine-Glycine	57351.34	179000.2	229665.3	138027.8	111753.9	40627.87	56080.32	67580.03	51993.55
Cysteine	2991.416	0	0	2726.492	13020.46	70988.84	3003.234	0	0
Asparagine	141255.9	141033.6	144351.9	265812.9	332734.6	1746364	177421.4	198848	187404
Tyramine	29368.16	63430.16	19681.64	31948.57	126936.5	2325405	33372.54	27492	174163.3
l-Isoleucine	64486.61	87843.52	124649.2	112136.2	207816.7	498410.1	67492.12	31573.88	43583.67
Citrulline	21580.55	5934.564	11301.55	33576.44	65628.17	187794	13999.64	7204.464	29857.03
Glycine	250038.2	161096.9	84868.3	243975.6	1628202	2781749	253511.8	167554.8	267214.3
L-Methionine	0	13259.46	0	53404.18	697265.1	1236281	46578.81	62381.24	94975.71
l-Valine	347682.1	334073.3	378279.8	499124.1	1452171	2147013	359941.6	279320.4	343294.5
L-Norleucine	61942.9	40552.6	4613.787	61191.79	476453.6	705649.7	48509.39	9182.694	8939.372
L-Ornithine	12004.01	0	0	0	824055.1	1276114	0	0	0
L-Homoserine	0	0	0	0	63002.26	25901.67	0	0	0
Serine	1934009	1349082	712992.4	2611547	12403349	12060933	2000357	2281473	2017870
L-Threonine	1261886	1137827	534278.6	1490327	11377908	12391672	1273149	1084675	1624190
l-Proline	2634746	1637229	801092.9	3362700	30097389	23524141	2849190	1969161	2177080
L-Aspartic acid	1475347	936275.1	220290.3	1704963	20676864	13758765	1339949	1259973	1510602
l-Alanine	3270688	2083113	429976.2	2560844	10550409	9230975	2545884	1899888	2077372
Threonine	296512.6	259189	275288.7	325623.2	965551.9	856659.2	392957.5	787967.2	518666.8
Colchifoleine	110120.1	103948.9	96394.5	122938.4	161378.4	149608.6	130081.2	121710.3	128768.7

doi:10.6342/NTU202100671

Table 8. The Log_2 fold change of amino acid abundance at 14 and 21 days

Peak areas of amino acid contents during both zinc deficient (dZn) and zinc excess (eZn) treatment at 14 and 21 days were used to calculate Log_2 Fold Change. Asterisk represents significance on two sided t-test analysis (p-value less than 0.05 at 0.95 confidence interval). Zn concentration used in the study was dZn = 0.00 2μM and NZn = 0.2 μM.

Metabolite	Log_2 Fold Change			
	14DAT		21DAT	
	dZn	eZn	dZn	eZn
Asparagine	1.24	0.50	3.60	0.38
L-Methionine	5.72	2.23	4.41	0.98
L-Ornithine	0.00	0.00	6.15*	0.00
L-Norleucine	3.55*	-2.14	6.26	0.56
Glycine	3.34*	0.06	5.03*	1.65*
l-Valine	2.12*	-0.26*	2.50*	-0.14
l-Isoleucine	1.24	-1.48*	2.00*	-1.52*
Cysteine	0.00	0.00	4.12*	0.00
Citrulline	3.47	0.28	3.76*	1.11
Threonine	1.90	1.60	1.64	0.91
Colchifoleine	0.63	0.23	0.63	0.42
L-Homoserine	0.00	0.00	1.17*	0.00
L-Aspartic acid	4.46*	0.43	5.96	2.78*
l-Alanine	2.34*	-0.13	4.42*	2.27*
L-Threonine	3.32	-0.07	4.54*	1.60*
Serine	3.20*	0.76	4.08*	1.50
l-Proline	4.20*	0.27	4.88*	1.44*
Leucine-Glycine	-0.68*	-1.41*	-2.50	-2.14
Tyramine	1.00	-1.21	6.70	2.96
Alpha-ketoglutaric acid	-0.62*	0.07	-1.99*	-0.02
Succinic acid	2.30	1.76*	-1.46	-0.04
L-Glutamine	3.81	0.29	5.11	1.44*
Phenylalanine	2.44*	-1.10*	3.40*	0.07

doi:10.6342/NTU202100671

Table 9. Carbohydrates peak area from general metabolite profile.

Carbohydrates from polar shoot extraction detected through GCxGC-TOFMS were ordered in the table according to the heatmap generated (**Figure 22**). Peak areas of 3 repeats at 3, 14 and 21 days after treatment (DAT) were shown. Zn concentration used in this study was dZn = 0.002 µM $ZnSO_4$, NZn = 0.2 µM $ZnSO_4$, eZn = 300 µM $ZnSO_4$).

	Optimal Zn treatment (NZn)								
Metabolite	**3 DAT**			**14 DAT**			**21 DAT**		
Sucrose	325572.7	399112.2	632793.1	725907.6	624915.6	213141.2	869822.7	263108.6	789477.1
d-Ribose	93755.78	49365.85	42625.54	60880.33	54893.52	66521.94	82279.64	44474.32	60929.65
Glucose-6-phosphate	780686.8	678348.3	734103.6	916562.4	594569.7	531228.1	581087	657150.8	488528.3
4-Ketoglucose	75272.43	60049.96	62062.36	63430.62	59070.39	56749.43	49808.93	52762.23	35084.4
alpha-D-Galactofuranoside	250381.3	321572.9	338893.1	323181	334508.8	366693	264330.1	394971.8	304035.6
Alpha-ketoglutaric acid	1409388	907339.2	1228090	1118262	1229871	1052032	1228406	1168653	1681826
Maltose	87963.51	68345.4	73521.21	84115.84	58689.79	52054.29	49266.77	66945.25	48436.65
Myo-inositol	13002439	11542983	12684065	11650384	12091825	10425990	11910695	12199679	11985052
N-Acetylglucosamine methoxime	17413.52	12022.03	13868.64	0	7822.663	0	5459.852	0	0
alpha-D-Galactoside	543511.7	336975.7	442613.2	590219.9	261282.6	294931.4	100985.3	188165.3	80527.85
Erythrose	783884.2	881351.7	1094062	623171.1	1649958	842095.9	6040040	842601	1798651

	Zn deficient treatment (dZn)								
Metabolite	**3 DAT**			**14 DAT**			**21 DAT**		
Sucrose	710607.3	648571.8	444238.7	599646.7	252806.9	1203071	675926.8	456151.2	387451.5
d-Ribose	88547.89	55463.02	40429.85	63784.65	19579.59	6790.734	10793.64	19198.81	15154.6
Glucose-6-phosphate	1069507	799716.6	504671.5	214552.1	190457.2	44404.6	63357.39	33469.55	39334.16
4-Ketoglucose	52711.35	84108.86	78089.45	33634.59	55941.59	40468.76	13806.17	0	20013.89
alpha-D-Galactofuranoside	429486.8	372875.6	316765.6	318434.1	0	468042.1	0	0	0
Alpha-ketoglutaric acid	1174066	1144557	1163623	645739.1	507903.4	710558.8	280506.1	241436.5	254601.7
Maltose	91048.23	87163.92	82958.26	24219.48	11302.75	0	13429.43	26022.4	22948.56
Myo-inositol	12478226	17639511	16361546	6742276	5892755	8748223	3941712	3306748	4345088
N-Acetylglucosamine methoxime	18485.83	21227.11	19231.28	0	0	0	0	0	0
alpha-D-Galactoside	328541.6	468334.3	496911.4	63549.26	233392	201471.4	71671.02	37069.48	48879.62
Erythrose	201992.6	836003.8	1199121	1862991	1488627	1919221	901462	822195.6	970417.9

	Zn excess treatment (eZn)								
Metabolite	**3 DAT**			**14 DAT**			**21 DAT**		
Sucrose	281426.4	215174.5	194863.4	234702.6	207910.2	697038.8	545295.9	525898.5	172768.2
d-Ribose	57246.56	47038.97	69023.56	62455.89	63961.73	69445.05	50111.94	31689.89	73071.95
Glucose-6-phosphate	731143	795299.7	1092370	749941.1	518980.2	591603.1	372783.7	511798	608295.4
4-Ketoglucose	62757.85	0	53407.26	55474.35	62513.4	63453.03	76409.32	39727.85	86607.58
alpha-D-Galactofuranoside	359447.2	358719	433680.8	412266.3	396213.4	449625.1	473624.1	410664.4	606375
Alpha-ketoglutaric acid	972548.1	1279918	1336569	1606247	933332.5	1401317	840822.9	961483.9	1564960
Maltose	53272.11	67118	67133.72	36405.85	34352.45	38728.53	29097.08	54157.78	26957.64
Myo-inositol	13164908	14115901	13280674	10441582	10099641	10726860	10142906	10331710	12658137
N-Acetylglucosamine methoxime	11443.96	13532.76	11317.37	7647.604	0	10969.81	0	0	5555.604
alpha-D-Galactoside	326102.6	556744.7	647234.5	378002.5	174256.8	379641.8	166204.6	458031.2	535850.9
Erythrose	553989.9	1233525	505551.6	565938.1	404074.8	323731.2	536979.7	850095.6	485107.6

doi:10.6342/NTU202100671

Metabolite	Optimal Zn treatment (NZn)									Zn deficient treatment (dZn)									Zn excess treatment (eZn)								
	3 DAT			14 DAT			21 DAT			3 DAT			14 DAT			21 DAT			3 DAT			14 DAT			21 DAT		
Xylitol	503335.8	970044.2	0	0	1284450	955483.6	2553988	1545735	2040049	0	1056714	1789018	1130146	820913.9	984282.7	960415.9	1016222	1080238	8711.591	0	260274.3	7157.072	293026	0	11718.62	665005.9	280374.2
Glucopyranose	466746.4	1881584	1870487	946428.9	2256703	1915536	6100603	3025919	3626224	34273.65	2118606	4340949	563513.2	118401.4	302589.5	404426.7	862327.8	265565.6	293836.5	819806.5	257647.7	114808.5	101688	42701.8	537808.4	1036365	44201.4
Galactose	189103.3	181941.7	179851.9	173210.8	134175.9	172374.4	213045.1	177977.7	344273.2	38786.32	226948.1	197491.4	48061.88	88863.82	66335.85	164813.7	157421.7	99418.2	61091.17	109370.2	248721.2	65974.49	128131.1	163965.9	275200	167397.7	116264
D-Fructose	14110259	12241723	14448153	11926550	13916740	12592375	30603502	23266897	30294293	21451924	16309890	22358383	5641395	2861542	990855	17590583	19550427	8165469	4616974	9993243	11171565	8567577	6382807	8059484	10155778	9229392	8434671
d-Mannose	8972479	7952712	9151121	8618858	9681451	8822967	18264170	14135684	19200277	13899851	10286684	13131890	3614165	2620163	961740.6	10128034	11037990	5325065	3017433	6607507	7953992	5974252	4110490	5866862	7142080	6475985	7011080
D-Xylopyranose	184860.7	930841.9	916245.5	319247.3	827610.5	719432.7	1325869	697163.6	934695.7	25843.52	1037950	2205398	420844.8	218752.3	132770.2	843582.8	1023163	503242	141188.9	406932.8	94171.99	29714.87	40578.61	5848.872	224623.8	356186.1	26670.88
Trehalose	194671	140822.9	155977.6	163829.8	143993.2	106497.4	197116.6	216223.4	267803.1	246002.6	303376.1	360783.5	177409.3	178425.7	251154.2	127065	129750.4	116406.1	140013.8	174407	203741.6	67307.82	52784.51	64801.12	62375.59	81595.72	59141.72
Gluconic acid	300427	226989.6	0	138794.2	0	0	37448.91	38721.27	0	9799340	11915192	67280.11	63587.71	90955.39	28727.91	24295.37	108646.2	193493.7	1003540	0	320397.1	64568.81	80703.58	54578.15	168102.4	71068.93	51494.53
alpha-D-Mannopyranose	7267837	7789390	3244628	5525916	1908923	2579347	1164415	1095099	489092.4	1215431	1498748	1709298	1226507	2226812	1563889	1000972	3371140	3344326	2332114	597110.8	3204623	1462057	1613432	1779714	3655583	1382235	1583903
alpha-D-Glucopyranoside	186122.7	92069.72	149487.8	266677.7	131580	104670.7	94986.47	108329.7	37214.25	111550.2	146371.3	143014.2	47404.88	100557.9	103108.9	54567.46	25402.29	38235.02	87291.83	176590.2	225591	138462.9	57715.28	122990.7	75954.44	195671.4	163087.1

doi:10.6342/NTU202100671

Table 10. Averaged peak area of carbohydrates.

Carbohydrate peak areas of 3 replicates at 3, 14 and 21 days after treatment (DAT) were averaged from **Table 14**. Zn concentration used in this study was dZn = 0.002 μM $ZnSO_4$, NZn = 0.2 μM $ZnSO_4$, eZn = 300 μM $ZnSO_4$.

	NZn treatment			dZn treatment			eZn treatment		
Metabolite	**3 DAT**	**14 DAT**	**21 DAT**	**3 DAT**	**14 DAT**	**21 DAT**	**3 DAT**	**14 DAT**	**21 DAT**
Galactose	183632.3	159920.3	245098.7	154408.6	67753.85	140551.2	139727.5	119357.2	186287.2
Glucopyranose	1406272	1706222	4250915	2164610	328168	510773.4	457096.9	86399.43	539458.1
D-Fructose	13600045	12811888	28054897	20040066	3164597	15102160	8593927	7669956	9273280
d-Mannose	8692104	9041092	17200044	12439475	2398690	8830363	5859644	5317201	6876382
Gluconic acid	175805.5	46264.74	25390.06	7260604	61090.34	108811.7	441312.5	66616.85	96888.63
D-Xylopyranose	677316	622096.8	985909.6	1089730	257455.7	789995.9	214097.9	25380.78	202493.6
Trehalose	163823.8	138106.8	227047.7	303387.4	202329.7	124407.2	172720.8	61631.15	67704.34
alpha-D-Mannopyranose	6100619	3338062	916201.9	1474492	1672403	2572146	2044616	1618401	2207240
alpha-D-Galactoside	441033.5	382144.6	123226.2	431262.4	166137.6	52540.04	510027.3	310633.7	386695.6
Glucose-6-phosphate	731046.2	680786.7	575588.7	791298.3	149804.6	45387.04	872937.7	620174.8	497625.7
Myo-inositol	12409829	11389400	12031809	15493094	7127752	3864516	13520494	10422694	11044251
Maltose	76610.04	64953.31	54882.89	87056.8	11840.74	20800.13	62507.94	36495.61	36737.5
N-Acetyl glucosamine methoxime	14434.73	2607.554	1819.951	19648.08	0	0	12098.03	6205.804	1851.868
Alpha-ketoglutaric acid	1181606	1133389	1359628	1160748	621400.4	258848.1	1196345	1313632	1122422
D-Ribose	61915.72	60765.27	62561.2	61480.25	30051.66	15049.02	57769.7	65287.56	51624.59
4-Ketoglucose	65794.91	59750.14	45885.19	71636.55	43348.31	11273.35	38721.7	60480.26	67581.58
alpha-D-Galactofuranoside	303615.8	341460.9	321112.5	373042.7	262158.7	0	383949	419368.3	496887.9
alpha-D-Glucopyranoside	0	0	0	0	8582.328	0	0	0	0
Sucrose	452492.7	521321.5	640802.8	601139.3	685174.8	506509.8	230488.1	379883.9	414654.2
Erythrose	919765.9	1038408	2893764	745705.6	1756946	898025.2	764355.6	431248	624061
Xylitol	491126.7	746644.6	2046591	948577.2	978447.4	1018959	89661.97	100061	319032.9

doi:10.6342/NTU202100671

Table 11. The Log_2 fold change of carbohydrate at 14 and 21 days.

Peak areas of carbohydrate contents were obtained from 10-day-old rice plants given both zinc deficient (dZn) and zinc excess (eZn) treatments for 14 and 21 days. The value of peak area was used to calculate Log_2 Fold Change. Asterisk represents significance on two sided t-test analysis (p-value less than 0.05 at 0.95 confidence interval_. Zn concentration used in the study was dZn = 0.002 µM and NZn = 0.2 µM. The value was calculated from 3 replicates

Metabolite	Log_2 Fold Change			
	14 DAT		21 DAT	
	dZn	eZn	dZn	eZn
Sucrose	0.39	-0.46	-0.34	-0.63
d-Ribose	-1.02	0.10	-2.06*	-0.28
Glucose-6-Phosphate	-2.18*	-0.13	-3.66*	-0.21
4-Ketoglucose	-0.46	0.02	-2.03*	0.56
alpha-D-Galactofuranoside	-0.38	0.30*	0.00	0.63
Alpha-ketoglutaric acid	-0.87*	0.21	-2.39*	-0.28
Maltose	-2.46*	-0.83	-1.40*	-0.58
Myo-inositol	-0.68*	-0.13	-1.64*	-0.12
alpha-D-Galactoside	-1.20	-0.30	-1.23	1.65
Erythrose	0.76	-1.27	-1.69	-2.21
Xylitol	0.39	-2.90	-1.01	-2.68*
Glucopyranose	-2.38	-4.30	-3.06	-2.98*
Galactose	-1.24*	-0.42	-0.80	-0.40
D-Fructose	-2.02*	-0.74*	-0.89*	-1.60*
D-Mannose	-1.91*	-0.77*	-0.96*	-1.32
D-Xylopyranose	-1.27	-4.62	-0.32	-2.28*
Trehalose	0.55	-1.16*	-0.87*	-1.75
Gluconic acid	0.40	0.53	2.10	1.93
alpha-D-Mannopyranose	-1.00	-1.04	1.49	1.27

doi:10.6342/NTU202100671

Table 12. Fatty acid peak area from the general metabolite profile.

Fatty acid from polar shoot extraction detected through GCxGC-TOFMS were ordered in the table according to the heatmap generated (**Figure 25**). Peak areas of 3 repeats at 3, 14 and 21 days after treatment (DAT) were shown. Zn concentration used in this study was dZn = 0.002 μM $ZnSO_4$, NZn = 0.2 μM $ZnSO_4$, eZn = 300 μM $ZnSO_4$).

	Optimal Zn treatment (NZn)									Zn deficient treatment (dZn)									Zn excess treatment (eZn)								
Metabolite	**3 DAT**			**14 DAT**			**21 DAT**			**3 DAT**			**14 DAT**			**21 DAT**			**3 DAT**			**14 DAT**			**21 DAT**		
2-Monopalmitin	108404.6	80866.32	66424.85	92481.71	65818.26	58091.66	0	95456.33	78840.45	92373.53	90258.07	64761.45	72431.62	69904.53	98475.93	12904.4	63675.01	48079.5	78133.7	75915.58	85372.6	72834.59	106685.7	100878.1	75293.46	109622.4	68439.97
2-Propenoic acid	369834.48	366252.54	433664.72	438319.92	372958.87	368391.11	365136.66	582511.11	287490.64	413080.41	441790.34	529260.62	0	0	0	0	0	0	608310.23	571701.18	789370.71	373772.22	476534.34	492506.66	573400.37	527860.72	625980.09
2-Butenedioic acid	115357	875102.53	875899.95	484950.08	458602.01	496403.1	384540.61	542830.85	239940.6	609660.75	818260.05	841970.24	455880.56	687360.49	549210.58	420880.46	567710.51	615460.72	103510.7	124438	115697.3	434790.22	391100.85	401170.54	449300.81	509480.91	513450.92
Propanedioic acid	187011.1	182095.6	180857.5	115183.1	116440.9	127504.6	142657.7	176608.9	122765.6	210109.6	140882.7	176231	601100.96	502950.14	515310.08	454680.65	929680.98	541960.16	620010.19	531680.48	794410.41	646040.15	657870.92	670590.74	297610.95	163780.44	127180.85
Butanoic acid	419745858	425956161	394926868	506240505	643852527	555047272	749199696	663886161	413673333	467849797	460449191	546892222	524193333	281261831	405283131	194346363	153071616	318424343	357708080	410358080	396288181	454823131	312282222	411397070	364375959	402385050	421199393
Propanoic acid	419278.6	443392	411707.8	500490.4	592264.4	533471.2	730204	608204.5	599056.4	401903.8	419482.9	406623.8	243582.8	219134.8	252311.7	136498.4	908305.51	157266.3	408299	353215.8	394272.2	326306.2	334612.4	343982.7	344981.8	292478.2	471805.2
Pentenoic acid	773051	905117.8	1031782	1242964	1401391	1257498	1324988	1402719	1843554	1227225	1599201	1167949	925748.9	826673.4	1176450	689065.4	645040.6	944634.3	1099843	959093.4	1008607	843771.1	737146.1	810753.3	920389.6	778438.4	920196.8
alpha-Linolenic acid	467661.61	938906.1	1167065.1	663338.46	821200.77	997209.7	3300489	748099.96	865692	998058.82	1148311	1238009.2	1064208.6	1041933.2	1746804.9	683650.75	828060.63	744299.96	572040.96	1215861.6	398710.82	556420.53	238610.79	344950.67	480570.55	232190.18	276330.66
monostearin	826380808	774521212	708772726	1144828281	758001017	675974742	6741715	7992248	7481237	8445934	8236943	7829116	8148295	7247265	1216545 6	1182345 8	7880359	5807247	8240906	8430171	8689642	8294415	7821856	8402820	8182572	9850023	7355808
Hexadecanoic acid	459464 1	496538 2	435804 3	530394 4	503340 1	477116 5	5091599	4967359	5818062	5071247	5218057	5385091	5470564	5148590	7281529	7777103	5269997	4427661	4980947	5264122	5306957	4743140	4961465	5007963	4977332	5129828	5156816
Octadecanoic acid	462133 8	523511 2	429153 7	586522 9	515785 1	472786 5	4661312	4923176	5670296	5397027	5410735	5422881	5617670	4998758	7620695	7523306	5079850	3973684	5273588	5475515	5774234	4714563	5179089	5230159	5028076	5415316	5306158

doi:10.6342/NTU202100671

Table 13. Averaged peak area of fatty acids.

Fatty acid peak areas of 3 replicates at 3, 14 and 21 days after treatment (DAT) were averaged from **Table 17**. Zn concentration used in this study was dZn = 0.002 μM $ZnSO_4$, NZn = 0.2 μM $ZnSO_4$, eZn = 300 μM $ZnSO_4$.

	NZn treatment			dZn treatment			eZn treatment		
Metabolite	**3 DAT**	**14 DAT**	**21 DAT**	**3 DAT**	14 DAT	**21 DAT**	**3 DAT**	**14 DAT**	**21 DAT**
Hexadecanoic acid	4639355	5036170	5292340	5224798	5966894	5824920	5184009	4904189	5087992
Octadecanoic acid	4715996	5250315	5084928	5410214	6079041	5525613	5507779	5041270	5249850
monostearin	7698916	8596013	7405066	8170664	9187005	8503688	8453573	8173030	8462801
2-Monopalmitin	85231.91	72130.54	58098.93	82464.35	80270.69	80265.64	79807.29	93466.15	84451.95
2-Propenoic acid	38990.25	39322.3	41171.47	46138.12	0	0	65646.37	44760.41	57575.06
2-Butenedioic acid	96819.83	48000.06	38911.02	75663.34	56415.54	53468.9	114548.7	40902.54	49075.22
Propanoic acid	424792.8	542075.3	645821.7	409336.8	238343.1	128198.4	385262.3	334967.1	369755
Butanoic acid	4135429	5683801	6089196	4917303	4035798	2219474	3881181	3928341	3959867
Pentenoic acid	903316.9	1300618	1523754	1331458	976290.9	759580.1	1022515	797223.5	873008.3
alpha-Linolenic acid	85807.6	82727.98	64794.68	112815.3	128435.6	75200.78	72886.12	38000	32970.13
Propanedioic acid	183321.4	119709.5	147344.1	175741.1	53979.06	64211.26	64870.36	65817.27	19619.75
Heneicosanoic acid	247053.5	185113.4	251760.5	237023.4	170835.3	255025.4	204416.1	189427.6	187068.6

doi:10.6342/NTU202100671

Table 14. Fatty acids and organic acids identified from non-polar extraction through GC-MS.

Fatty acid	
Propanoic acid	C3
Butanoic acid	C4
Hexanoic acid	C6
Decanoic acid	C10
10-Undecenoic acid	C11:1
Tetradecanoic acid	C14
Hexadecanoic acid	C16
7-Hexadecenoic acid	C16:1
Heptadecanoic acid	C17
Octadecanoic acid	C18
17-Octadecynoic acid	C18:1
9,12-Octadecadienoic acid	C18:2
9,12,15-Octadecatrienoic acid	C18:3
Organic acids	
1,2-Benzenedicarboxylic acid	
Oxalic acid	
Nitric acid	
Hexanedioic acid	

doi:10.6342/NTU202100671

Table 15. Fatty acids peak area from non-polar extraction.

Fatty acid detected from non-polar shoot extraction through GCxGC-TOFMS. Peak areas for 4 repeats at 3, 14 and 21 days after treatment (DAT) were shown. Zn concentration used in this study was dZn = 0.002 μM $ZnSO_4$, NZn = 0.2 μM $ZnSO_4$, eZn = 300 μM $ZnSO_4$).

	Optimal Zn treatment (NZn)												Zn deficient treatment (dZn)												Zn excess treatment (eZn)							
Metabolite	**3 DAT**				**14 DAT**				**21 DAT**				**3 DAT**				**14 DAT**				**21 DAT**				**3 DAT**				**14 DAT**			
Butanoic acid	3699 1.327	4048 3.51	3665 3.16	3755 9.8	4251 7.03	5133 2.36	4877 1.39	4644 6.3	4624 8.15	8777 1.7	7673 9.22	8299 1.15	3042 6.81	3284 5.85	2810 0.55	3358 7	3725 8.72	3941 2.99	3136 8.1	3425 6.47	6870 5.57	7059 2.38	7037 5.76	6756 2.64	3245 4.67	3498 9.08	3867 0.23	3668 8.58	4830 1.9	7670 6.32	5154 0.06	5538 5.08	7528 5.14	7921 2.6	9114 9.64	5744 5.165
Octadecanoic acid	4074 105.76	3876 721	5225 003	4396 441	1641 6882	1470 0888	1528 5080	1368 1916	2229 8156	1871 6555	2136 8501	1908 4272	4338 529	2059 195	2808 452	3270 188	1368 3148	1464 9504	1320 5560	1366 3830	2863 1423	2934 4010	2717 0271	2255 5809	3286 033	4255 709	5302 350	1434 317	1215 0854	1669 1405	1534 7974	1236 3665	1675 5107	2042 0131	1641 0431	1828 2716
Nitric acid	0	0	0	0	7425 0.51	7402 6.3	6645 1	6046 6.79	1297 03.7	9464 0.87	1445 20.8	1153 04.3	0	0	0	0	5170 9.53	5898 9.31	6032 2.33	6639 0.1	1163 74.9	1221 07.8	1494 28.9	8218 3.84	0	0	0	0	8408 2.86	7870 3.5	8486 1.5	7591 0.23	1258 27.9	1444 94.6	1428 21.1	1323 25.541
10-Undecenoic acid	3721. 849	1521 .155	3539 .025	5356 .201	3951 5.18	4195 8.21	3670 3.23	3504 9.99	8997 3.32	6404 7.58	7580 5.87	6245 3.3	1455 .201	1746 .026	4483 .915	2615 .321	3602 4.76	4551 2.07	4377 1.36	3558 9.97	7372 4.71	8519 8.68	9541 6.29	5961 1.34	8655 22.3	2129 .054	5171 .712	2248 .507	4261 6.75	4751 4.46	5229 0.63	4534 6.72	8159 3.33	1038 .6	7941 7.66	8194 2.53
Oxalic acid	0	0	0	0	1195 95	1250 63	1072 00	1052 99	3109 16	2145 67	2494 05	2086 07	0	0	0	0	1166 37	1581 04	1446 18	1154 51	2794 18	3220 45	3394 18	2333 06	0	0	0	0	1462 16	1690 95	1723 89	1579 18	2755 41	3575 20	2912 41	3151 97.038
17-Octadecynoic acid	3319. 37	0	4289 .594	0	6409 6.17	6403 7.29	5022 9.68	5111 7.12	1194 55.8	7850 2.19	9593 2.03	1032 64.5	9240 6.18	0	5372 5.23	0	5461 7.2	6334 7.52	6142 8.72	5524 2.33	1168 72	1011 71.9	1322 74.7	7004 1.66	6051 9.51	4625 .52	9740 0.34	0	6197 0.83	6132 3.87	6621 4.7	6340 2.84	8513 5.58	1016 .6	9059 0.99	1061 19.08

doi:10.6342/NTU202100671

Metabolite	Optimal Zn treatment (NZn)														Zn deficient treatment (dZn)												Zn excess treatment (eZn)									
	3 DAT				14 DAT				21 DAT						3 DAT				14 DAT				21 DAT				3 DAT				14 DAT				21 DAT			
Hexanoic acid	1516 58.224	1464 80	1859 86	1939 32	2613 91	2179 04	2393 55	2248 80	2689 47	1958 69	2285 23	2029 26	1425 01		9055 7.2	1050 97	1476 35		2693 86	2766 97	2173 50	1912 84		3631 81	3417 62	3424 56	3702 68	1184 74	1827 34	2211 33	6752 2.9	2035 84	3712 99	2593 21	2064 21	2385 97	2521 85	2050 35	2422 86.837
Heptadecanoic acid	5063 81.405	4520 48.1	5847 21	5608 27.7	1091 607	1066 490	1114 290	9410 72.8	1229 524	1131 790	1239 949	1154 774	5117 06.7		2813 57.8	3917 94.6	4169 73.7		7270 42.3	7571 63.6	6725 87.4	7234 11.1		1098 407	1130 685	1007 919	1049 690	4127 53.1	5179 54.2	6541 35.8	2084 06	6981 35.2	1171 122	9673 63.9	6932 06.3	8952 84.6	1049 190	8345 82.2	7949 274.429
Hexadecanoic acid	8168 1725.4	7452 1912	8949 1556	9135 3701	1.27E+08	1.27E+08	1.36E+08	1.23E+08	1.62E+08	1.47E+08	1.62E+08	1.48E+08	7795 6750		4296 6230	5519 9566	6855 4854		1.05E+08	1.07E+08	9358 0222	9717 1398		1.44E+08	1.59E+08	1.4E+08	1.33E+08	6705 4585	9270 8304	1.07E+08	3097 9624	1.01E+08	1.53E+08	1.38E+08	9517 6567	1.25E+08	1.55E+08	1.26E+08	1412 5782.5
Decanoic acid	3584 24.874	3311 60.7	4291 64.1	4321 94.9	7773 82.9	7410 15.7	7865 58.9	6662 619	8028 56.6	6891 54.9	7458 73.4	7111 19.1	3521 65.9		2185 11.2	2724 26.7	3240 14.6		5408 52.2	4924 31.9	4325 50.3	4726 86.4		6128 59.1	5930 62.9	5771 95.7	6099 12.4	2954 03.1	3816 61.5	4732 21.2	1542 74.4	5586 36.5	8335 41	7024 00.7	5110 12	6479 24.9	7950 03.3	6203 77.1	7233 05.404
9,12,15-Octadecatrienoic acid	1134 8883 6	1.12E+08	1.28E+08	1.41E+08	1.37E+08	1.45E+08	1.48E+08	1.27E+08	1.52E+08	1.64E+08	1.57E+08	1.59E+08	1.03E+08		6639 6128	8395 5511	1.03E+08		1.09E+08	1.33E+08	1.11E+08	1.07E+08		1.62E+08	1.84E+08	1.61E+08	1.45E+08	1.06E+08	1.14E+08	1.44E+08	5070 8166	1.05E+08	2.02E+08	1.68E+08	1.23E+08	1.3E+08	1.6E+08	1.36E+08	1412 1199 1
Hexanedioic acid	1315 2.613	1699 6.9	1402 7.2	0	1679 14	3552 89	3029 53	2365 69	5891 3.8	1173 42	7720 9.4	9124 4.3	1064 3		0	0	0		1556 15	1277 83	1059 86	7683 6.1		4577 5.3	4884 8.6	3269 3.6	3599 3.8	0	4804 .46	0	0	9931 1.8	1474 38	9503 1.1	7817 8.9	3303 6.9	2811 0.9	3766 3	2779 7.035
1,2-Benzenedicarboxylic acid	0	0	0	0	1149 391	2170 458	1394 161	8486 55	1834 0.08	4417 7.61	0	0	0		0	0	0		4503 51	2672 08.5	1677 21	9247 7.69		0	0	0	0	0	0	0	0	9037 6.6	1055 73	6374 6.84	4205 3.63	0	0	0	0
Propanoic acid	4805 8.237	4638 1.63	6007 9.78	5415 7.03	3750 524	8922 320	6270 541	4131 562	3914 19.8	8554 76.7	4332 11.4	4192 84.7	3201 8.29		4154 3.01	5609 8.27	3144 8.48		2449 480	1753 380	1287 367	8874 76.1		2480 91.9	2469 37.6	1954 04.5	2191 44.4	3951 6.82	0	4893 5.63	0	9512 52.7	1342 473	7720 71.8	5612 80.2	1766 30.6	1850 00.1	1472 09.1	1595 11.244
7-Hexadecenoic acid	1051 39.98	1039 19.2	2462 37.9	1187 96.3	3507 15.7	2331 89.2	2105 33.3	2004 35.5	3978	1650 45	1406 70.8	1491 97.2	1137 19.2		4773 3.18	7068 8.74	9520 2.47		2885 68.4	3646 43.7	2865 36.9	2946 39.4		1277 61.2	1523 93.1	1319 21.7	1181 54.6	9491 3.37	9994 4.54	1772 71.6	4075 0.14	1080 87.1	2455 02.6	2001 85.8	1372 28.6	1278 39	1554 51.9	1243 73.2	1312 78.469

doi:10.6342/NTU202100671

	Optimal Zn treatment (NZn)												Zn deficient treatment (dZn)												Zn excess treatment (eZn)											
Metabolite	**3 DAT**				**14 DAT**				**21 DAT**				**3 DAT**				**14 DAT**				**21 DAT**				**3 DAT**				**14 DAT**				**21 DAT**			
Tetradecanoic acid	0	0	0	0	4881759	3901138	4736519	3740347	3955538	2444361	3055561	0	0	0	0	0	2492242	2360082	2036314	2309534	1639114	1642709	0	0	0	2050211	0	0	3026027	5193643	3960233	2243025	0	2810366	0	2380578344
9,12-Octadecadienoic acid	432777.099	3628786	4845602	4524613	7624713	5532774	6284327	5286493	7001141	4253808	5236941	3850822	4395473	1671856	2278903	3400265	4515151	4248924	3353963	4599896	3642646	4079725	3177774	3380573	2890748	5868903	6491628	9688606.	4261035	5133272	5447479	2640037	3219443	4405178	3192199	4430 27.465
13-Docosenoic acid	854314.069	8049383	9655999	1040193	9418003	3727761	3404811	3535867	3820663	4740196	8764633	1452523	1264113	7017261	9150312	8834313	5905525	4172998	6822823	3700936	5155594	9746006	5547927	2768847	1018865	1302904	9144916	7261876	3951052	8420655	4292513	3908668	7453483	5759802	1059715	4183 95.868
Tetradecanoic acid	0	0	0	0	4881759	3901138	4736519	3740347	3955538	2444361	3055561	0	0	0	0	0	2492242	2360082	2036314	2309534	1639114	1642709	0	0	0	2050211	0	0	3026027	5193643	3960233	2243025	0	2810366	0	2380578344
Heneicosanoic acid	2238 19.949	1965647	2873 65	2804643	2586857	2214065	2613284	2066673	2241041	1738733	2272378	1924493	2640966	1175463	1697832	1890276	1640076	1710176	1728348	1754814	2007301	2011554	1781404	1776844	2213702	2945804	3815 51	1095402	2036 68	3398271	2948 69	1817375	1740065	2265741	1682616	1794 31.948

doi:10.6342/NTU202100671

Table 16. Averaged peak area of fatty acids.

Fatty acid peak areas of 4 replicates at 3, 14 and 21 days after treatment (DAT) were averaged from **Table 20**. Zn concentration used in this study was dZn = 0.002 μM $ZnSO_4$, NZn = 0.2 μM $ZnSO_4$, eZn = 300 μM $ZnSO_4$.

	NZn treatment			dZn treatment			eZn treatment		
Metabolite	**3 DAT**	**14 DAT**	**21 DAT**	**3 DAT**	**14 DAT**	**21 DAT**	**3 DAT**	**14 DAT**	**21 DAT**
Hexanoic acid	169514	121447.5	147466	235882.5	238679.4	260156.3	224066.3	354416.8	234526
Octadecanoic acid	4393068	3119091	3569602	15021191	13800510	14070974	20366871	26924166	17868014
9,12,15-Octadecatrienoic acid	1.24E+08	89243158	1.04E+08	1.39E+08	1.15E+08	1.5E+08	1.58E+08	1.63E+08	1.42E+08
Hexadecanoic acid	84262224	61169350	74410025	1.28E+08	1.01E+08	1.22E+08	1.55E+08	1.44E+08	1.37E+08
Heptadecanoic acid	525994.5	400458.2	448312.3	1053365	720051.1	882457	1189009	1071675	932082.8
Decanoic acid	387736.1	291779.6	326140.1	742794.1	484630.2	651397.6	737251	598257.5	696652.7
17-Octadecynoic acid	1902.241	36532.85	40636.34	57370.06	58658.94	63228.06	99288.63	105090.1	95864.07
Oxalic acid	0	0	0	114289.4	133702.5	161404.6	245873.6	293546.9	309874.8
10-Undecenoic acid	3534.558	2575.116	2603.624	38306.65	40224.54	46942.14	73070.02	78487.76	86701.27
Nitric acid	0	0	0	68798.65	59352.82	80889.52	121042.4	117523.8	136367.3
Butanoic acid	37921.95	31240.05	35700.64	47266.77	35574.07	57983.34	73437.55	69309.09	75773.14
Tetradecanoic acid	0	0	51255.28	431494.1	229958.7	360573.2	236382.5	82045.57	129773.6
Hexanedioic acid	11044.17	2660.738	1201.116	265681.4	116555.1	104990	86147.31	40827.82	31651.97
1,2-Benzenedicarboxylic acid	0	0	0	1390666	244439.5	75437.53	15629.42	0	0
Propanoic acid	52169.17	40277.01	22113.11	5768737	1594426	906769.4	524848.1	227394.6	167087.8
9,12-Octadecadienoic acid	433169.3	293662.4	405503.5	618207.7	417957.3	437061.7	508567.8	357017.3	381177.4
7-Hexadecenoic acid	143523.3	81835.91	103219.9	248718.4	308597.1	172751	114722.8	132557.7	134735.6

doi:10.6342/NTU202100671

Table 17. The Log_2 fold change of fatty acids at 14 DAT.

Peak areas of fatty acid contents were obtained from 10-day-old rice plants given both zinc deficient (dZn) and zinc excess (eZn) treatments for 14 days. The value of peak areas was used to calculate the Log_2 Fold Change. Asterisk represents significance on two sided t-test analysis (p-value less than 0.05 at 0.95 confidence interval). Concentration used in the study: dZn = 0.002 μM and NZn = 0.2 μM. The value was averaged form 3.

Metabolite	Fold(Zn-treatment/Control)	
	dZn	eZn
Butanoic acid	-0.40*	0.31
Propanoic acid	-1.79	-2.63
1,2-Benzenedicarboxylic acid	-2.41*	-4.18*
Decanoic acid	-0.65*	-0.14
Oxalic acid	0.25	0.47*
10-Undecenoic acid	0.08	0.27
7-Hexadecenoic acid	0.24	-0.52
Hexadecanoic acid	-0.35*	0.01
Heptadecanoic	-0.60*	-0.21
9,12-Octadecadienoic acid	-0.68*	-0.39
9,12,15-Octadecatrienoic acid	-0.29	0.14
Octadecanoic acid	-0.16	-0.07
Nitric acid	-0.33*	0.21*
17-Octadecynoic acid	0.01	0.09
Hexanedioic acid	-1.09	-1.27*
Tetracosanoic acid	-0.59*	0.24
Butanoic acid	-0.40*	0.31

doi:10.6342/NTU202100671

Table 18. Fatty acids peak area from non-polar extraction.

Fatty acids peak area were obtained from 10-day-old rice plants after 3, 14 and 21 days Zn treatment (DAT) through non-polar shoot extraction followed by GCxGC-TOFMS analysis. Zn concentration used in this study was dZn = 0.002 μM $ZnSO_4$, NZn = 0.2 μM $ZnSO_4$, eZn = 300 μM $ZnSO_4$). The value was averaged form 3 replicates.

Metabolite	NZn									dZn										eZn								
	3DAT			14DAT			21DAT			3DAT			14DAT			21DAT			3DAT			14DAT			21DAT		
Butanoic acid	36991	40484	36653	42517	51332	48771	46248	87772	76739	30427	32846	28101	37259	39413	31368	68706	70592	70376	32455	34989	38670	48302	76706	51540	75285	79213	91150
Hexanoic acid	151658	146480	185986	261391	217904	239355	268947	195869	228523	142501	90557	105097	269386	276697	217350	363181	341762	342456	118474	182734	221133	203584	371299	259321	238597	252185	205035
Propanoic acid	48058	46382	60080	4E+06	9E+06	6E+06	391420	855477	433211	32018	41543	56098	2E+06	2E+06	1E+06	248092	246938	195404	39517	0	48936	951253	1E+06	772072	176631	185000	147209
1,2-Benzenedicarboxylic acid	0	0	0	1E+06	2E+06	1E+06	18340	44178	0	0	0	0	450351	267208	167721	0	0	0	0	0	0	90377	105573	63747	0	0	0
Decanoic acid	358425	331161	429164	777383	741016	786559	802857	689155	745873	352166	218511	272427	540852	492432	432550	612859	593063	577196	295403	381662	473221	558637	833541	702401	647925	795003	620377
Oxalic acid	0	0	0	119595	125063	107200	310916	214567	249405	0	0	0	116637	158104	144618	279418	322045	339418	0	0	0	146216	169095	172389	275541	357520	291241
10-Undecenoic acid	3721.8	1521.2	3539	39515	41958	36703	89973	64048	75806	1455.2	1746	4483.9	36025	45512	43771	73725	85199	95416	865.22	2129.1	5171.7	42617	47514	52291	81593	103852	79418
7-Hexadecenoic acid	105140	103919	246238	350716	233189	210533	3978	165045	140671	113719	47733	70689	288568	364644	286537	127761	152393	131922	94913	99945	177272	108087	245503	200186	127839	155452	124373
Hexadecanoic acid	8E+07	7E+07	9E+07	1E+08	1E+08	1E+08	2E+08	1E+08	2E+08	8E+07	4E+07	6E+07	1E+08	1E+08	9E+07	1E+08	2E+08	1E+08	7E+07	9E+07	1E+08	1E+08	2E+08	1E+08	1E+08	2E+08	1E+08
Hexadecanoic acid	506381	452048	584721	1E+06	1E+06	1E+06	1E+06	1E+06	1E+06	511707	281358	391795	727042	757164	672587	1E+06	1E+06	1E+06	412753	517954	654136	698135	1E+06	967364	895285	1E+06	834582
9,12-Octadecadienoic acid	432777	362879	484560	762471	553277	628433	700114	425381	523694	439547	167186	227890	451551	424892	335396	364265	407973	317774	289075	586890	649163	426104	513327	544779	321944	440518	319220
9,12,15-Octadecatrienoic acid	1E+08	1E+08	1E+08	1E+08	1E+08	1E+08	2E+08	2E+08	2E+08	1E+08	7E+07	8E+07	1E+08	1E+08	1E+08	2E+08	2E+08	2E+08	1E+08	1E+08	1E+08	1E+08	2E+08	2E+08	1E+08	2E+08	1E+08
Octadecanoic acid	4E+06	4E+06	5E+06	2E+07	1E+07	2E+07	2E+07	2E+07	2E+07	4E+06	2E+06	3E+06	1E+07	1E+07	1E+07	3E+07	3E+07	3E+07	3E+06	4E+06	5E+06	1E+07	2E+07	2E+07	2E+07	2E+07	2E+07
Nitric acid	0	0	0	74251	74026	66451	129704	94641	144521	0	0	0	51710	58989	60322	116375	122108	149429	0	0	0	84083	78703	84862	125828	144495	142821
17-Octadecynoic acid	3319.4	0	4289.6	64096	64037	50230	119456	78502	95932	92406	0	53725	54617	63348	61429	116872	101172	132275	60520	4625.5	97400	61971	61324	66215	85136	101611	90591
13-Docosenoic acid	0	0	0	72470	0	63426	0	30187	54322	0	0	19065	0	0	32217	0	0	34637	0	0	0	0	51221	0	12435	0	37213
Hexanedioic acid	13153	16997	14027	167914	355289	302953	58914	117342	77209	10643	0	0	155615	127783	105986	45775	48849	32694	0	4804.5	0	99312	147438	95031	33037	28111	37663
Tetradecanoic acid	0	0	0	488176	390114	473652	395538	244436	305556	0	0	0	249242	236008	203631	163911	164271	0	0	205021	0	302603	519364	396023	0	281037	0
13-Docosenoic acid	854314	804939	965600	941800	372776	340481	382066	474020	876463	1E+06	701727	915031	590552	417308	682282	515594	974600	554793	1E+06	1E+06	914492	395105	842066	429251	745348	575980	1E+06
Heneicosanoic acid	223820	196565	287365	258686	221407	261328	224104	173873	227238	264097	117546	169783	164008	171018	172835	200730	201155	178140	221370	294580	381551	203668	339827	294869	174007	226574	168262
Tetracosanoic acid	562589	504532	703356	327481	277527	362348	237518	184152	213928	586016	283264	393346	184585	222662	236590	157989	152014	141854	567870	738536	958866	254665	466517	417983	169046	249919	177674

doi:10.6342/NTU202100671

Table 19. The average peak area of Fatty acids.

Fatty acid peak areas of 3 replicates at 3, 14 and 21 days after treatment (DAT) were averaged from **Table 23**. Zn concentration used in this study was dZn = 0.002 μM $ZnSO_4$, NZn = 0.2 μM $ZnSO_4$, eZn = 300 μM $ZnSO_4$. The value was averaged form 3 replicates.

	NZn			dZn			eZn		
Metabolite	**3DAT**	**14DAT**	**21DAT**	**3DAT**	**14DAT**	**21DAT**	**3DAT**	**14DAT**	**21DAT**
Butanoic acid	38042.7	47540.3	70253	30457.7	36013.3	69891.2	35371.3	58849.4	81882.5
Hexanoic acid	161375	239550	231113	112718	254478	349133	174114	278068	231939
Propanoic acid	51506.5	6314462	560036	43219.9	1830076	230145	29484.2	1021932	169613
1,2-Benzenedicarboxylic acid	0	1571337	20839.2	0	295093	0	0	86565.5	0
Decanoic acid	372917	768319	745962	281035	488611	594373	383429	698193	687768
Oxalic acid	0	117286	258296	0	139786	313627	0	162567	308101
10-Undecenoic acid	2927.34	39392.2	76608.9	2561.71	41769.4	84779.9	2722	47473.9	88287.5
7-Hexadecenoic acid	151766	264813	103231	77380.4	313250	137359	124043	184592	135888
Hexadecanoic acid	8.2E+07	1.3E+08	1.6E+08	5.9E+07	1E+08	1.5E+08	8.9E+07	1.3E+08	1.4E+08
Hexadecanoic acid	514383	1090796	1200421	394953	718931	1079004	528281	945541	926352
9,12-Octadecadienoic acid	426739	648060	549730	278208	403947	363337	508376	494737	360561
9,12,15-Octadecatrienoic acid	1.2E+08	1.4E+08	1.6E+08	8.5E+07	1.2E+08	1.7E+08	1.2E+08	1.6E+08	1.4E+08
Octadecanoic acid	4391943	1.5E+07	2.1E+07	3068725	1.4E+07	2.8E+07	4281364	1.5E+07	1.8E+07
Nitric acid	0	71575.9	122955	0	57007.1	129304	0	82549.3	137715
17-Octadecynoic acid	2536.32	59454.4	97963.3	48710.5	59797.8	116773	54181.8	63169.8	92445.7
13-Docosenoic acid	0	45298.5	28169.5	6355.02	10739	11545.6	0	17073.7	16549.3
Hexanedioic acid	14725.6	275386	84488.3	3547.65	129795	42439.2	1601.49	113927	32936.9
Tetradecanoic acid	0	450647	315177	0	229627	109394	68340.4	405997	93678.9
13-Docosenoic acid	874951	551686	577516	960290	563378	681662	1078754	555474	793681
Heneicosanoic acid	235917	247140	208405	183809	169287	193342	299167	279455	189614
Tetracosanoic acid	590159	322452	211866	420875	214612	150619	755090	379722	198880

doi:10.6342/NTU202100671

Figures

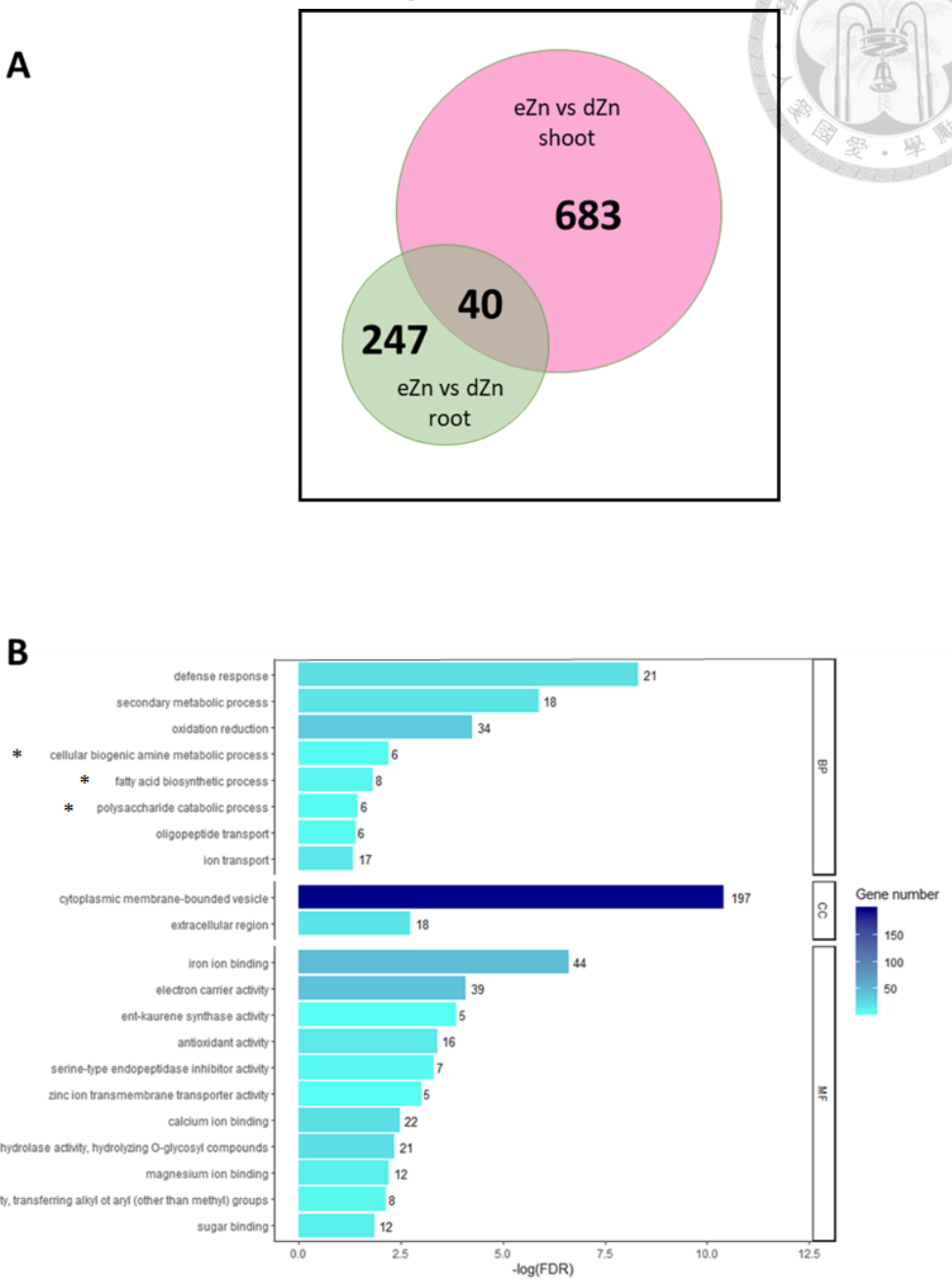

Figure 1. GO-enrichment analysis of DEGs during Zn treatments.

Rice plants were exposed to three different Zn concentrations: dZn, representing Zn deficiency, with 0.002 µM $ZnSO_4$; NZn, representing normal Zn condition, with 0.2 µM $ZnSO_4$; and eZn, representing Zn excess, with 300 µM $ZnSO_4$. Samples were collected after 3 days of treatment and sent for RNA-sequencing. (**A**) A comparison of the number of Differentially Expressed Genes (DEG) between dZn and eZn in the root (green circle) and shoot (pink circle) of rice plant using a Venn diagram (by Dr. Boon Huat Cheah). (**B**) GO-enrichment analysis of DEGs includes three categories: Biological Process (BP), Molecular Component (MC) and Cellular Component (CC). Group of genes related to metabolic regulation is marked with an asterisk, they are: cellular biogenic amine metabolic process, fatty acid biosynthesis process, and polysaccharide catabolic process.

doi:10.6342/NTU202100671

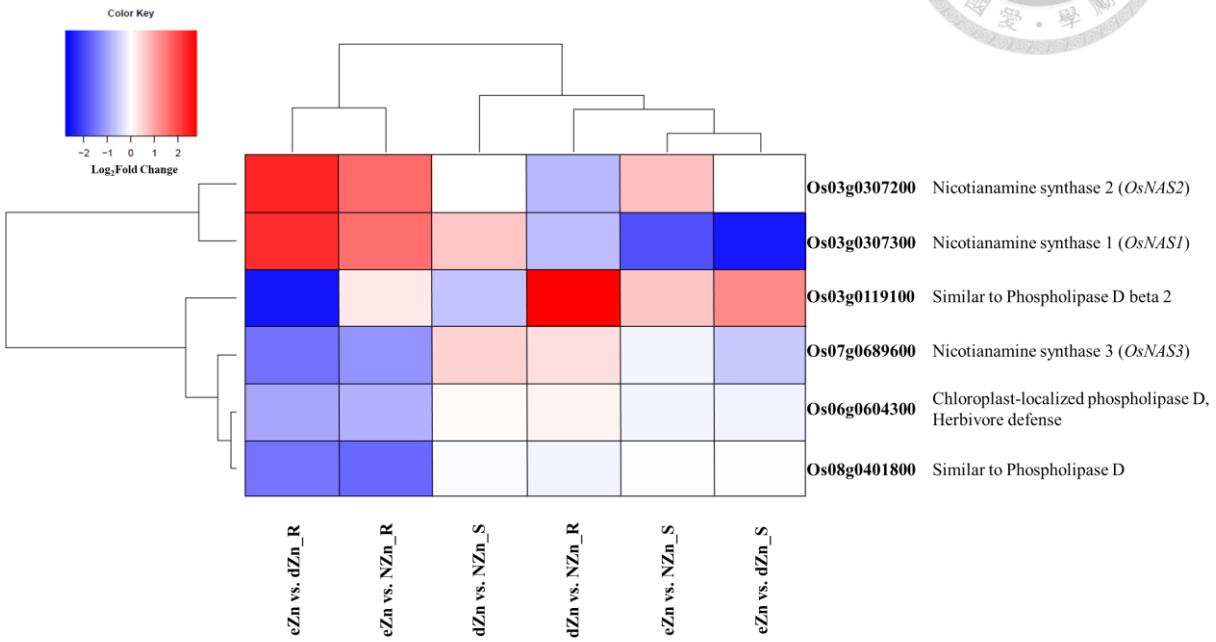

Figure 2. The cellular biogenic amine metabolism related genes from GO-enrichment analysis.

Rice plants were exposed to three different Zn concentrations: dZn, representing Zn deficiency, with 0.002 μM $ZnSO_4$; NZn, representing normal Zn condition, with 0.2 μM $ZnSO_4$; and eZn, representing Zn excess, with 300 μM $ZnSO_4$. Samples were collected after 3 days of treatment and sent for RNA-sequencing. In the color key, the up-regulated or down-regulated genes were represented by red and blue respectively. Gene expression was compared in roots (R) or shoots (S) of different Zn treatments. Zn deficiency (dZn), normal Zn (NZn) and excess Zn (eZn) and shown as Log_2 Fold Change, which was calculated from FPKM. The n (number of replicates) is 3.

doi:10.6342/NTU202100671

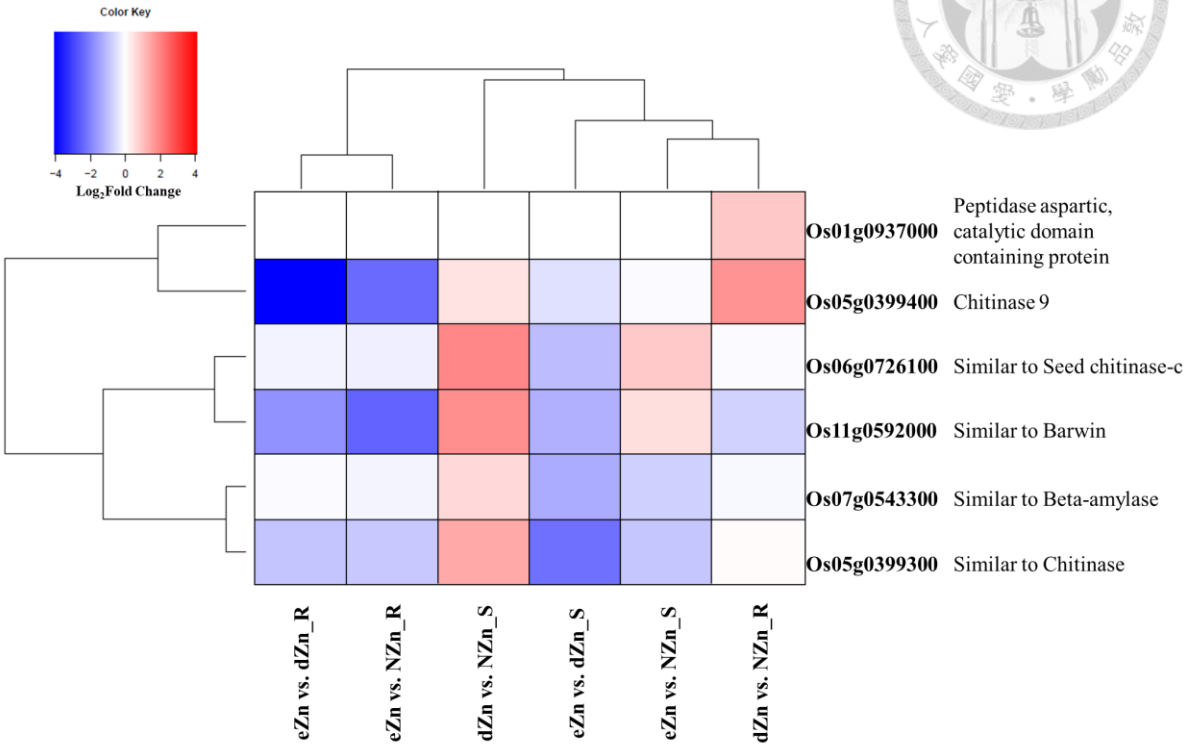

Figure 3. The polysaccharide catabolic process related genes from GO-enrichment analysis.

Rice plants were exposed to three different Zn concentrations: dZn, representing Zn deficiency, with 0.002 μM $ZnSO_4$; NZn, representing normal Zn condition, with 0.2 μM $ZnSO_4$; and eZn, representing Zn excess, with 300 μM $ZnSO_4$. Samples were collected after 3 days of treatment and sent for RNA-sequencing. In the color key, the up-regulated or down-regulated genes were represented by red and blue respectively. Gene expression was compared in roots (R) or shoots (S) of different Zn treatments. Zn deficiency (dZn), normal Zn (NZn) and excess Zn (eZn) and shown as Log_2 Fold Change, which was calculated from FPKM. The n (number of replicates) is 3.

doi:10.6342/NTU202100671

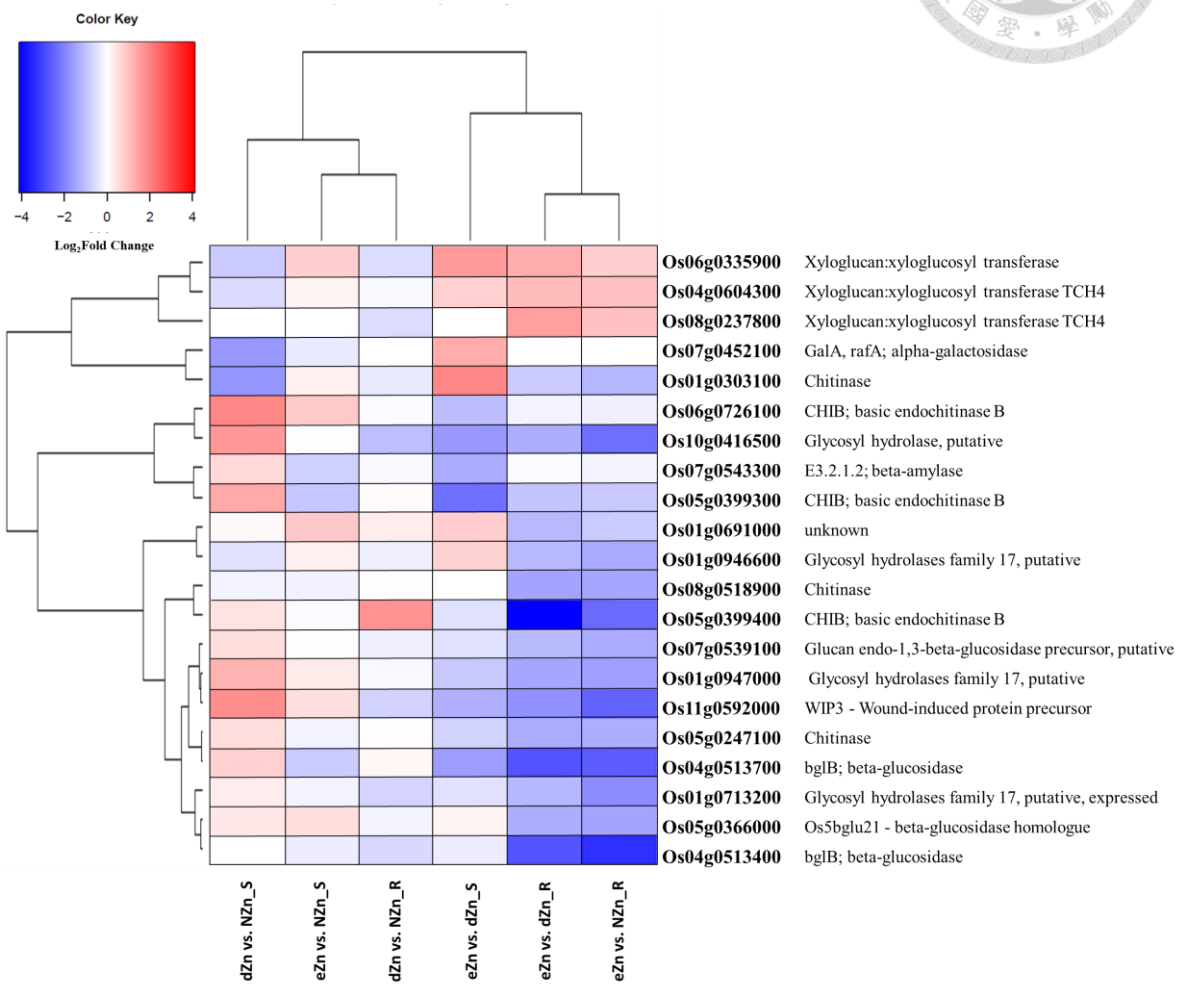

Figure 4. The hydrolase related genes from GO-enrichment analysis.

Rice plants were exposed to three different Zn concentrations: dZn, representing Zn deficiency, with 0.002 μM $ZnSO_4$; NZn, representing normal Zn condition, with 0.2 μM $ZnSO_4$; and eZn, representing Zn excess, with 300 μM $ZnSO_4$. Samples were collected after 3 days of treatment and sent for RNA-sequencing. In the color key, the up-regulated or down-regulated genes were represented by red and blue respectively. Gene expression was compared in roots (R) or shoots (S) of different Zn treatments. Zn deficiency (dZn), normal Zn (NZn) and excess Zn (eZn) and shown as Log_2 Fold Change, which was calculated from FPKM. n (number of replicates) is 3.

doi:10.6342/NTU202100671

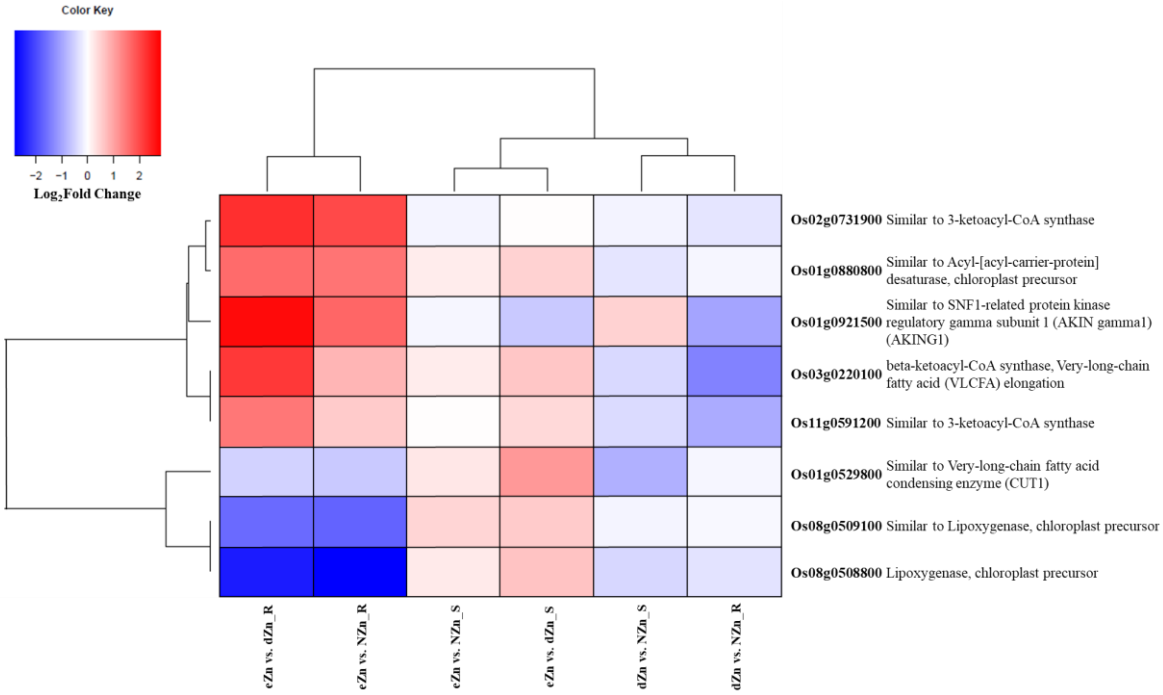

Figure 5. The fatty acid biosynthesis process related genes from GO-enrichment analysis.

Rice plants were exposed to three different Zn concentrations: dZn, representing Zn deficiency, with 0.002 μM $ZnSO_4$; NZn, representing normal Zn condition, with 0.2 μM $ZnSO_4$; and eZn, representing Zn excess, with 300 μM $ZnSO_4$. Samples were collected after 3 days of treatment and sent for RNA-sequencing. In the color key, the up-regulated or down-regulated genes were represented by red and blue respectively. Gene expression was compared in roots (R) or shoots (S) of different Zn treatments. Zn deficiency (dZn), normal Zn (NZn) and excess Zn (eZn) and shown as Log_2 Fold Change, which was calculated from FPKM. n = 3.

doi:10.6342/NTU202100671

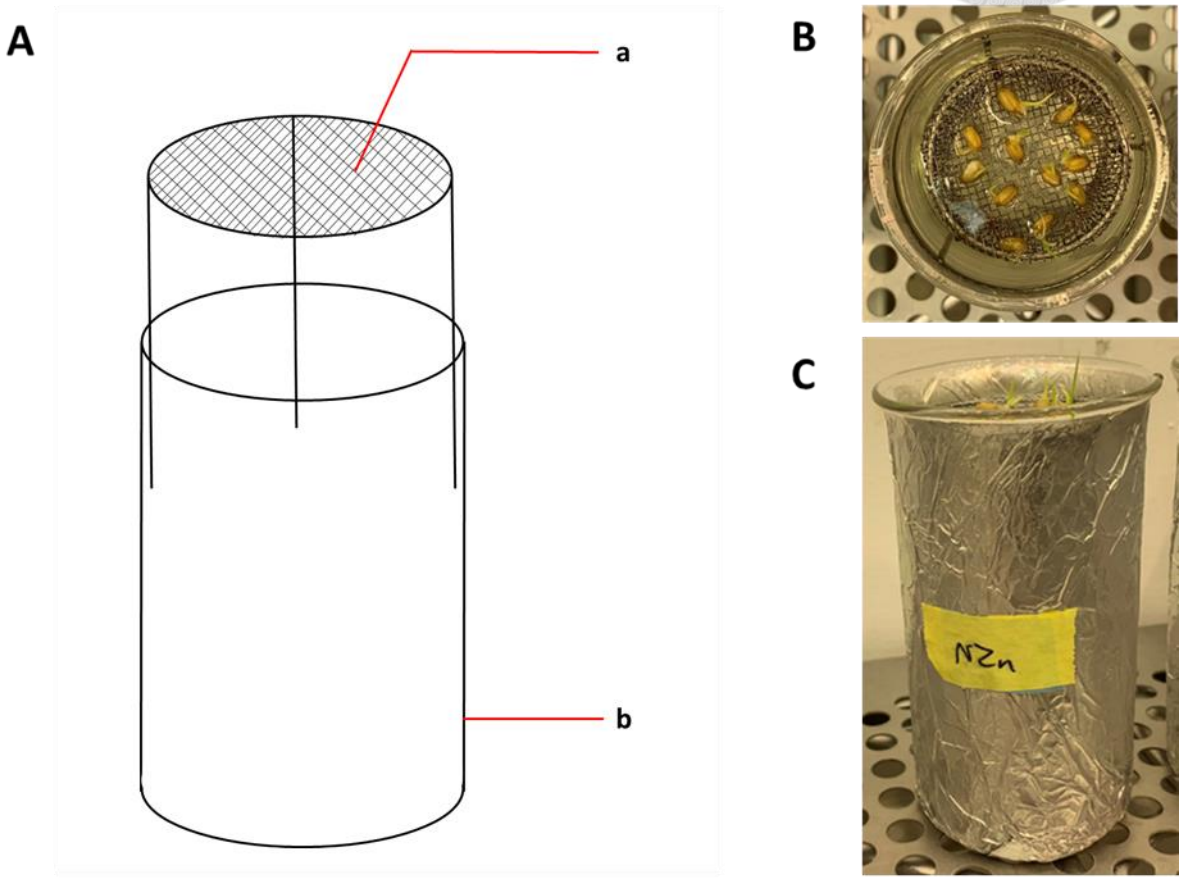

Figure 6. Hydroponic systems used in this study.

(**A**) Diagram of the (**a**) seed holding mesh and (**b**) beaker containing hydroponic solution. The beaker was covered with aluminum foil to avoid light exposure. (**B**) Top view of the mesh use to hold the seeds in place. (**C**) Side view of the hydroponic container.

doi:10.6342/NTU202100671

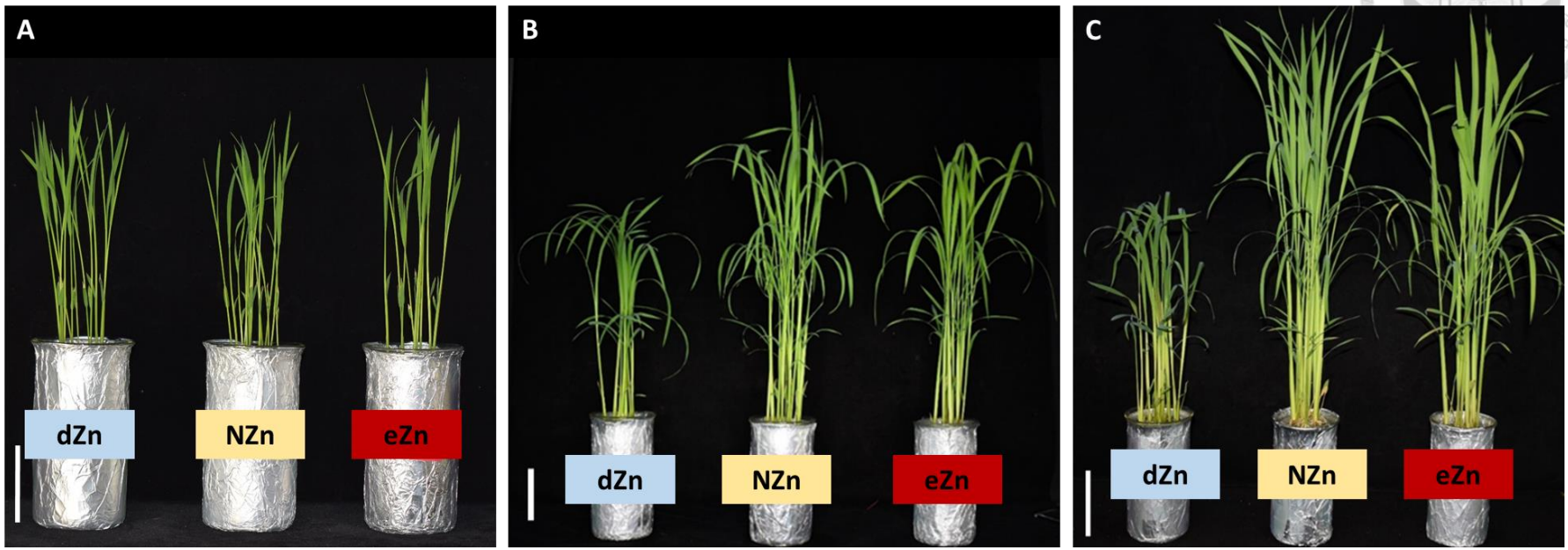

Figure 7. Morphological changes of rice plant over time under Zn treatments.

The 10-day-old rice seedlings were exposed to three different Zn concentrations: dZn, representing Zn deficiency, with 0.002 μM $ZnSO_4$; NZn, representing normal Zn condition, with 0.2 μM $ZnSO_4$; and eZn, representing Zn excess, with 300 μM $ZnSO_4$. for (**A**) 3 days, (**B**) 14 days, and (**C**) 21 days. Scale bar = 5cm and n is 3.

doi:10.6342/NTU202100671

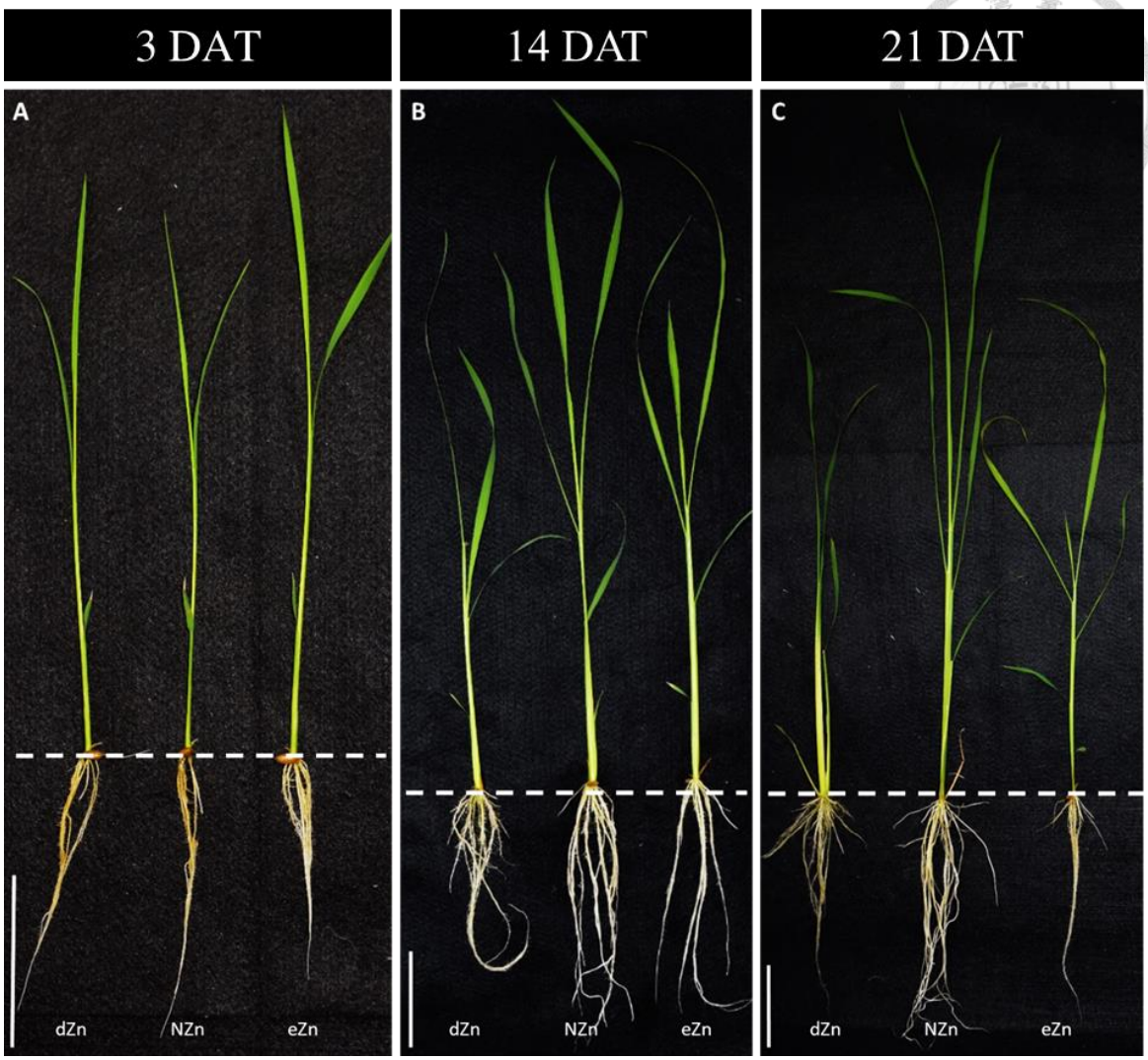

Figure 8. Morphological changes of rice plants overtime under Zn treatments.

The 10-day-old rice seedlings were exposed to three different Zn concentrations: dZn, representing Zn deficiency, with 0.002 μM $ZnSO_4$; NZn, representing normal Zn condition, with 0.2 μM $ZnSO_4$; and eZn, representing Zn excess, with 300 μM $ZnSO_4$. for (**A**) 3 days, (**B**) 14 days, and (**C**) 21 days. n = 3.

doi:10.6342/NTU202100671

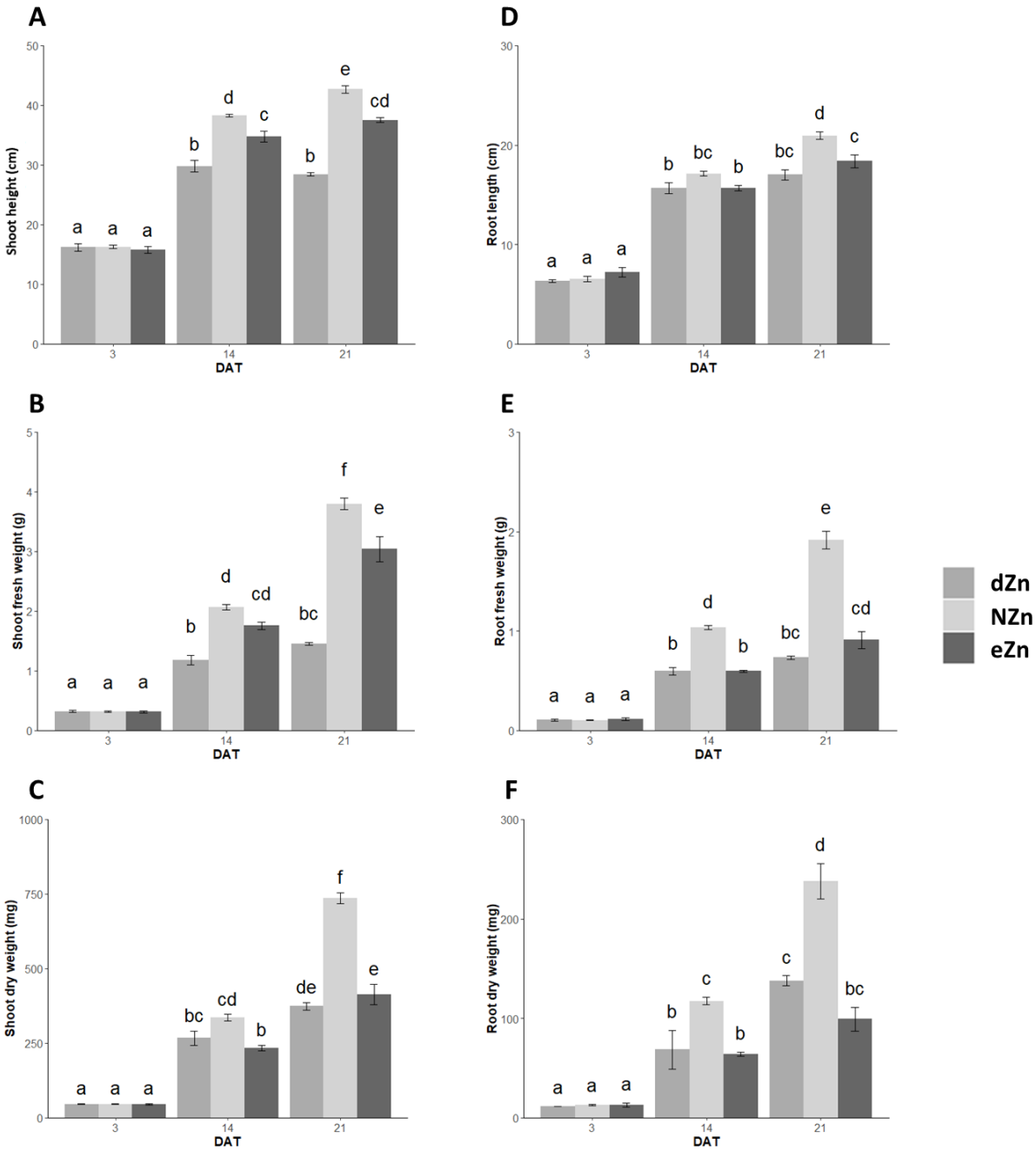

Figure 9. Physiological measurement of rice growth overtime under Zn treatments.

Quantitative measurement of (**A)** Shoot height, (**B)** root length, (**C)** shoot fresh weight, (**D)** root fresh weight, (**E)** shoot dry weight, (**F)** root dry weight was done with 10-day-old rice seedlings treated with dZn (Zn deficiency, gray), NZn (normal Zn, light gray) and eZn (excess Zn, dark gray) for 3, 14, and 21 days. Two-way ANOVA followed by Tukey post hoc statistical analysis was used for statistical analysis. Different letter denotes significant differences amongst groups with $p<0.05$. DAT = Days after treatment. The Zn concentration used in this study are: dZn = 0.002 µM $ZnSO_4$, NZn = 0.2 µM $ZnSO_4$, eZn = 300 µM $ZnSO_4$. The average value was from four replicates.

doi:10.6342/NTU202100671

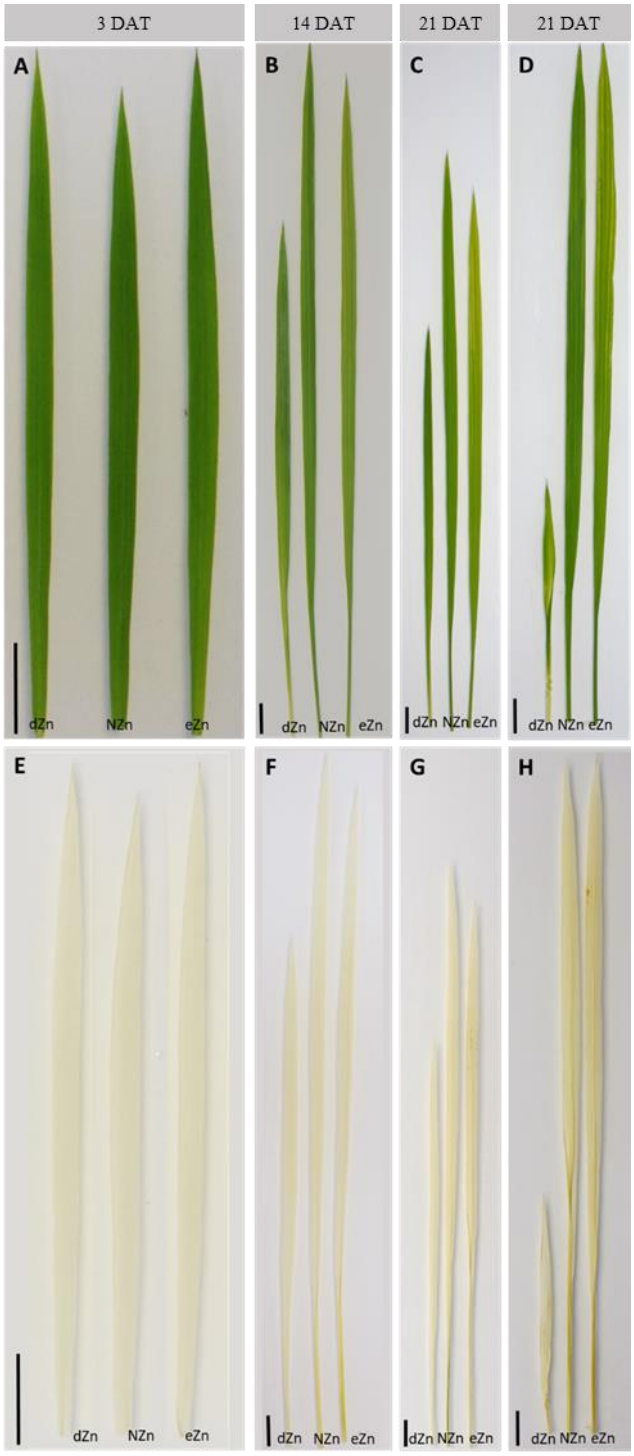

Figure 10. Leaf phenotype of rice under different Zn treatments.

Both Fresh leaves (**A-D)** and de-chlorophyll leaf (**E-H)** were shown. The 10-day-old rice seedlings were treated with dZn (Zn deficiency), NZn (normal Zn) and eZn (excess Zn) for 3, 14, and 21 days. The newly expanded leaf was chosen at each time point. **A & E:** the second leaf of 3 days after treatment (DAT). **B & F:** the fourth leaf of 14 DAT. **C & G:** the fourth leaf of 21 DAT. **D & H:** the fifth leaf of 21 DAT. The Zn concentration used in this study were: dZn = 0.002 μM $ZnSO_4$, NZn = 0.2 μM $ZnSO_4$, eZn = 300 μM $ZnSO_4$. Scale bar is 1cm.

doi:10.6342/NTU202100671

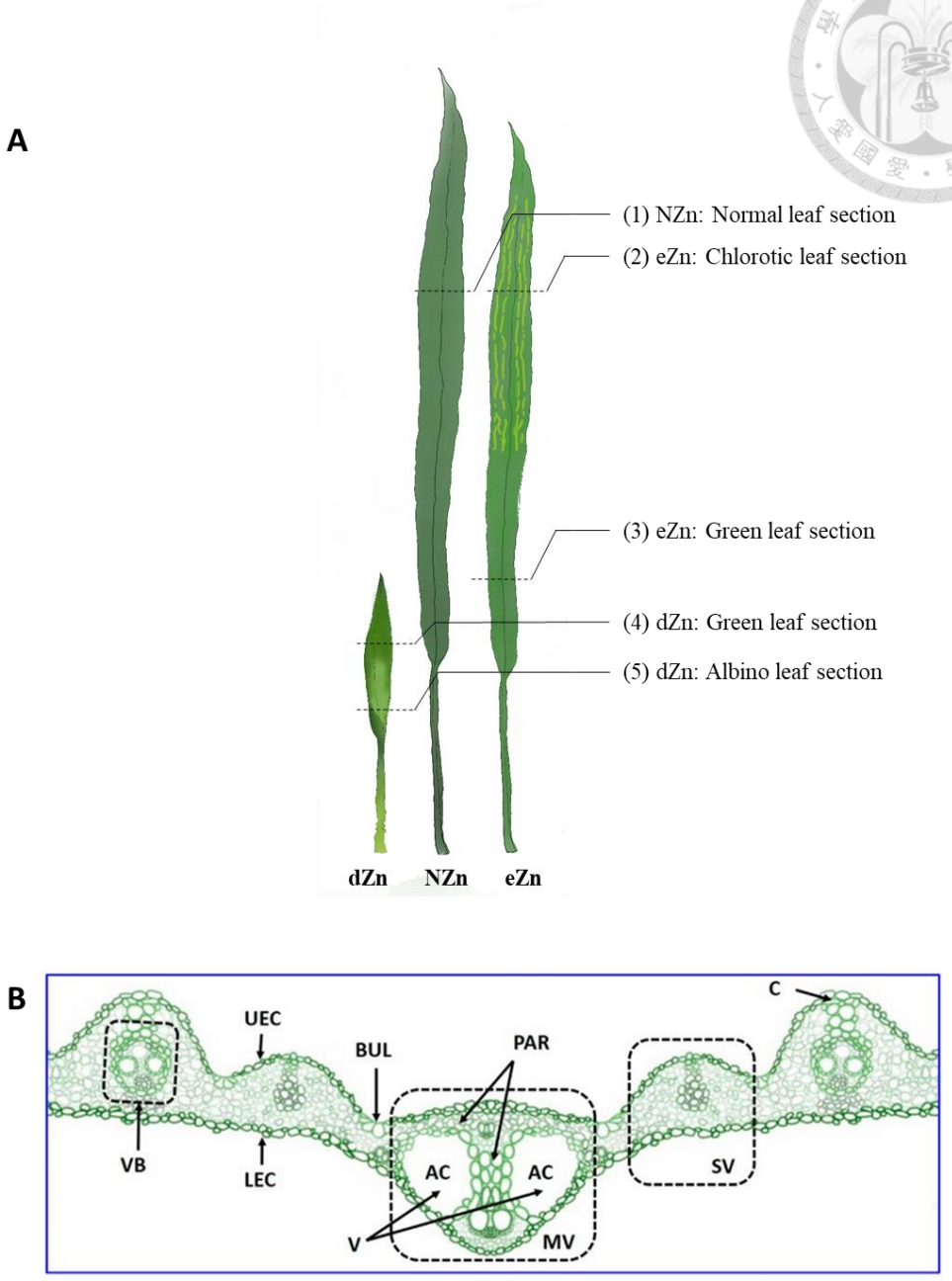

Figure 11. Illustration of microscope sections of rice leaf.

(**A**) The leaves for cellular structure and ultrastructure observation were sampled at 21 DAT. Dashed lines representing the parts of rice leaf selected for observation of fine structure. The NZn (normal Zn) represent leaves collected from normal Zn concentration (1). The inter-veinal chlorosis leaves near leaf tip (2) and green leaves on the basal part of the leaf (3) were sampled from eZn (excess Zn) treated leaves. The green leaves near leaf tip (4) and albino leaves on the basal part of the leaf (5) were sampled from dZn (Zn deficient) leaves. (**B**) Diagram showing the structure of rice leaf cross section (Kim et al., 2019). Abbreviations: **AC**, aerenchyma; **BUL**, bulliform cells; **C** , collenchyma; **L,** lower epidermis cells; **MV**, mid-vein; **PAR** , parenchyma; **SV**, small vein; **U** , upper epidermis cells; **V** , vacuum regions; **VB**, vascular bundle.

doi:10.6342/NTU202100671

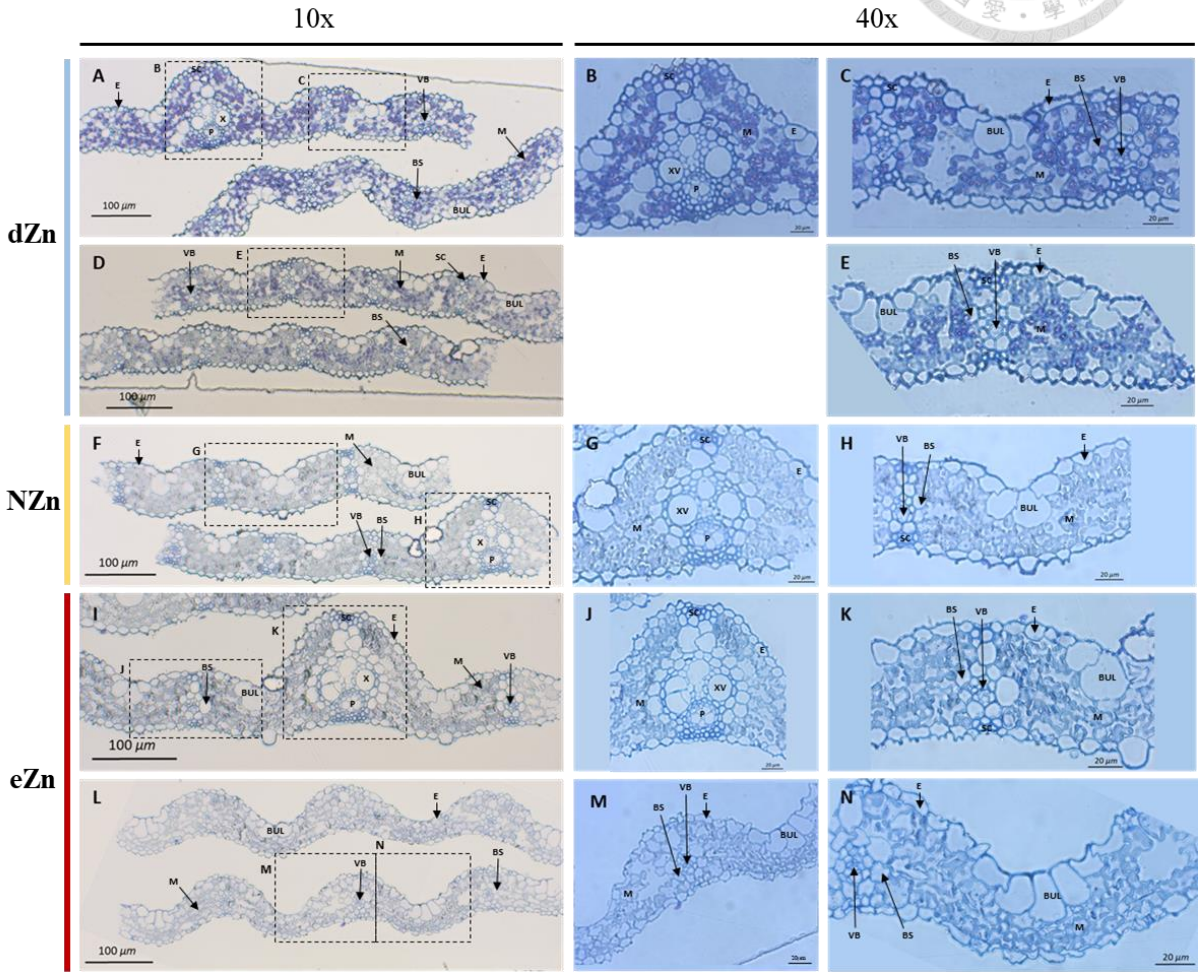

Figure 12. Optical microscope images of rice under Zn treatment at 21DAT.

The 10-day-old rice seedlings were treated with dZn (Zn deficiency, **A-E**), NZn (normal Zn, **F-H**) and eZn (excess Zn, **I-N**) for 21 days. Leaf cross section were then collected and observed under optical microscope at 10x (**A, D, F, I & L)** and 40x (**B, C, E, G, H, J, K, M, & N)** magnification. Different sections were cut according to **Figure 11A**: the albino section (**A, B & C)** and the green section (**D & E)** of dZn treated rice; the NZn treated rice leaf (**F, G & H)**; the green section (**I, J, & K)** and the chlorotic section (**L, M & N)** of eZn treated rice leaf. Abbreviations: **BS**, bundle sheath; **X,** xylem; **XV**, xylem vessel; **P**, phloem; **SC**, Sclerenchyma; **VB**, vascular bundle; **BUL**, bulliform cells; **M**, mesophyll; **E**, epidermis. Black dotted-line square represent corresponding magnified regions. The Zn concentration used in this study are: dZn = 0.002 μM $ZnSO_4$, NZn = 0.2 μM $ZnSO_4$, eZn = 300 μM $ZnSO_4$.

doi:10.6342/NTU202100671

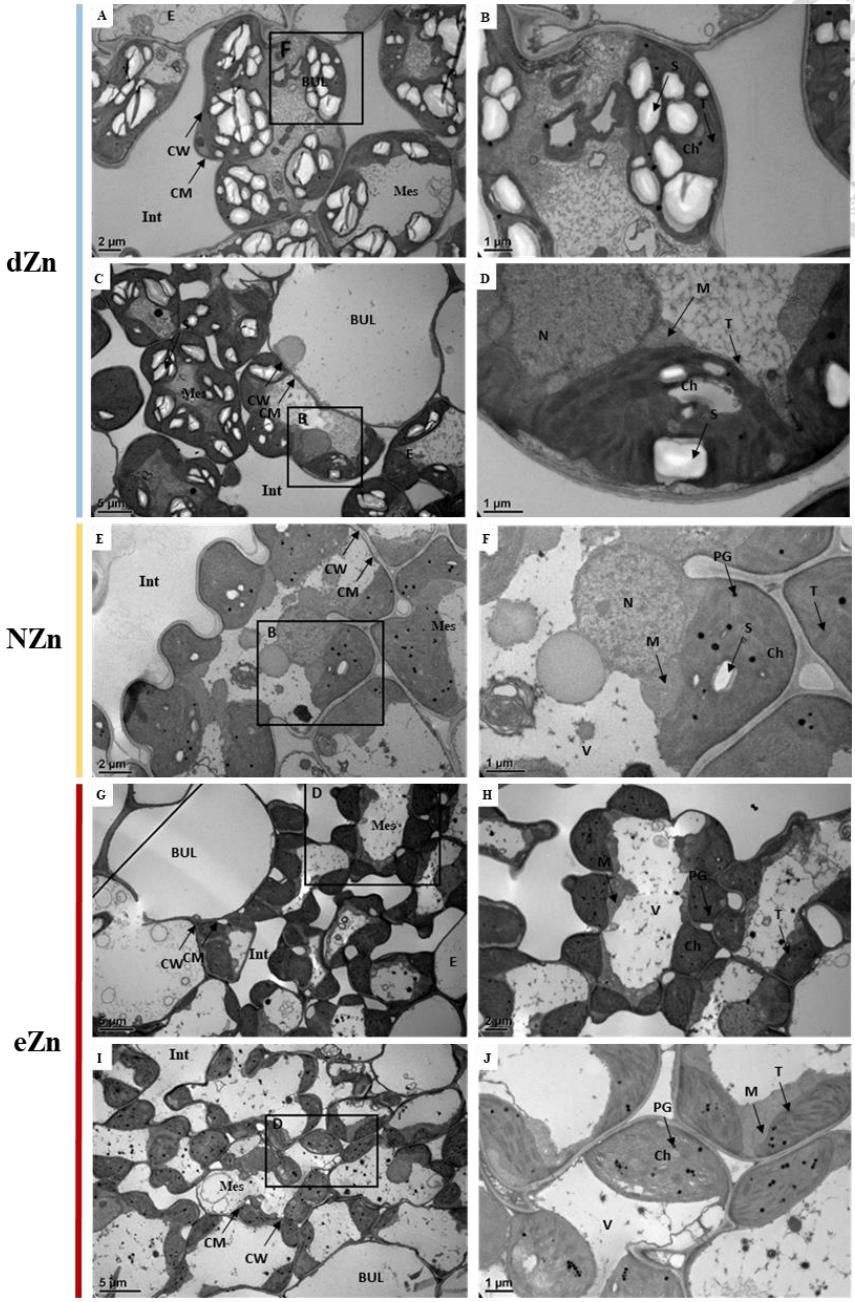

Figure 13. Transmission electron microscope images of rice leaves under Zn stress at 21DAT.

The 10-day-old rice seedlings were treated with dZn (Zn deficiency, **A**-**D**), NZn (normal Zn, **E, F**) and eZn (excess Zn, **G**-**J**) for 21 days. Different sections were observed according to **Figure 11A**: the albino section (**A&B)** and the green section (**C&D)** of dZn treated rice; the NZn treated rice leaf (**E&F)**; the green section (**G&H)** and the chlorotic section (**I&J)** of eZn treated rice leaf. Abbreviations: **CW**, cell wall; **CM**, cell membrane; **Int**, intercellular space; **BUL**, bulliform cell; **Mes**, mesophyll cell; **E**, epidermis; **Ch**, Chloroplast; **S**, starch grain; **PG**, plastoglobules; **V**, vacuole; **M**, mitochondria; **N**, nucleus; **T**; thylakoid. The Zn concentration used in this study are: dZn = 0.002 μM $ZnSO_4$, NZn = 0.2 μM $ZnSO_4$, eZn = 300 μM $ZnSO_4$.

doi:10.6342/NTU202100671

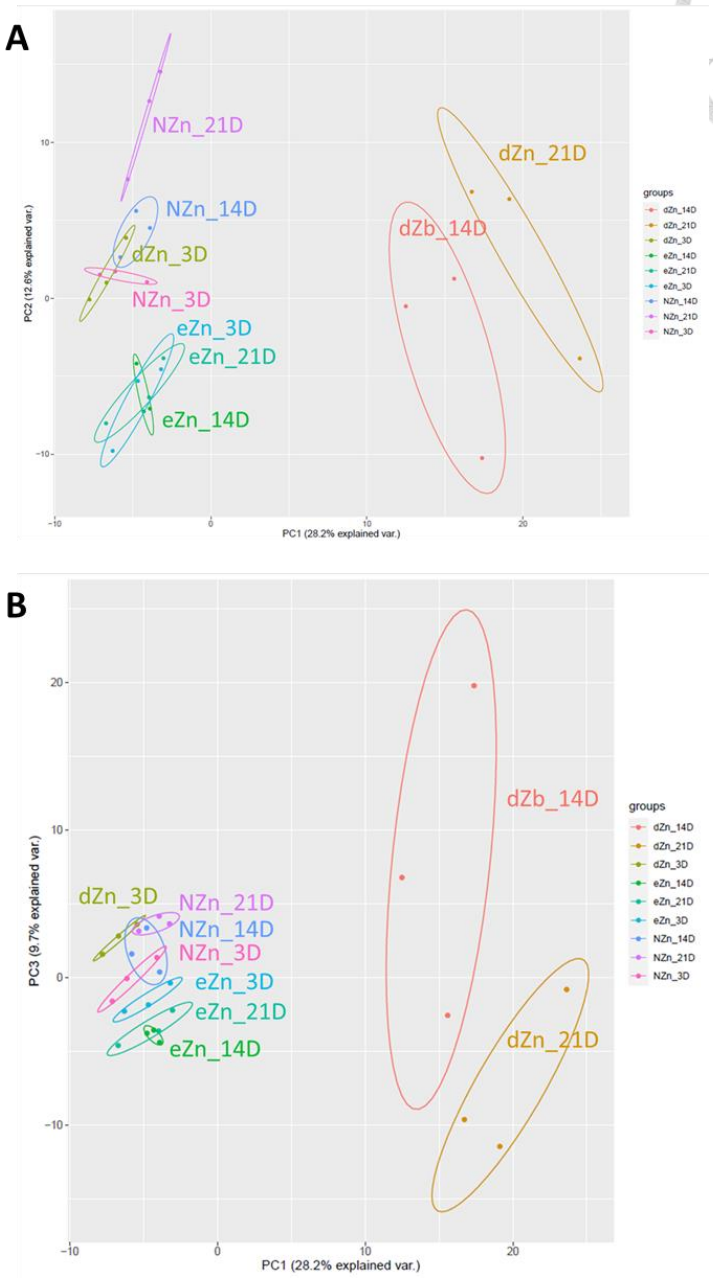

Figure 14. Principal Component Analysis (PCA) plot of rice shoot metabolites during Zn treatments.

The 10-day-old rice seedlings were treated with dZn (Zn deficiency), NZn (normal Zn) and eZn (excess Zn) for 3, 14, and 21 days (D). The metabolite peak area from GC-MS was used to draw two PCA plot: (**A)** Principal component (PC) 2 vs. PC1, and (**B)** PC3 vs. PC1. The Zn concentration used in this study are: dZn = 0.002 μM $ZnSO_4$, NZn = 0.2 μM $ZnSO_4$, eZn = 300 μM $ZnSO_4$. n is 3.

doi:10.6342/NTU202100671

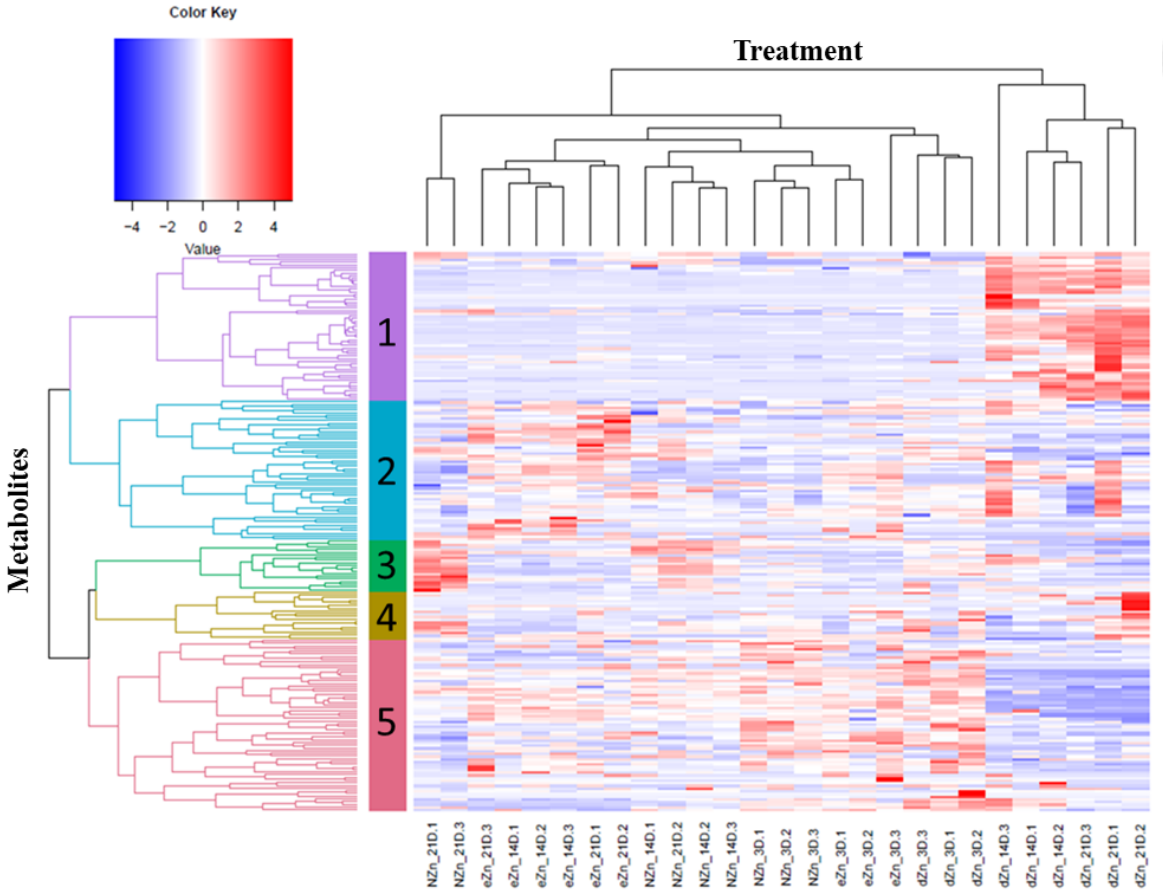

Figure 15. Proportion of rice shoot metabolites concentration during Zn treatments overtime.

The 10-day-old rice seedlings were treated with dZn (Zn deficiency), NZn (normal Zn) and eZn (excess Zn) for 3, 14, and 21 days (D). The metabolite peak area from untargeted GC-MS was used to draw the heatmap. The metabolite dendrogram is divided into 5 major clusters and increase or decrease in accumulation of metabolites is represented by the colors: red and blue respectively. The number at the end of the labels represent biological replicates. Heatmap was constructed using RStudio with z-score normalization, heatmap clustered using the Pearson's correlation coefficient and the Euclidean correlation coefficient. Heatmap constructed with z-score normalization, treatment clustering using pairwise complete and pearsons, and metabolite clustering using Euclidean and complete method in. The Zn concentration used in this study are: dZn = 0.002 μM $ZnSO_4$, NZn = 0.2 μM $ZnSO_4$, eZn = 300 μM $ZnSO_4$. n is 3.

doi:10.6342/NTU202100671

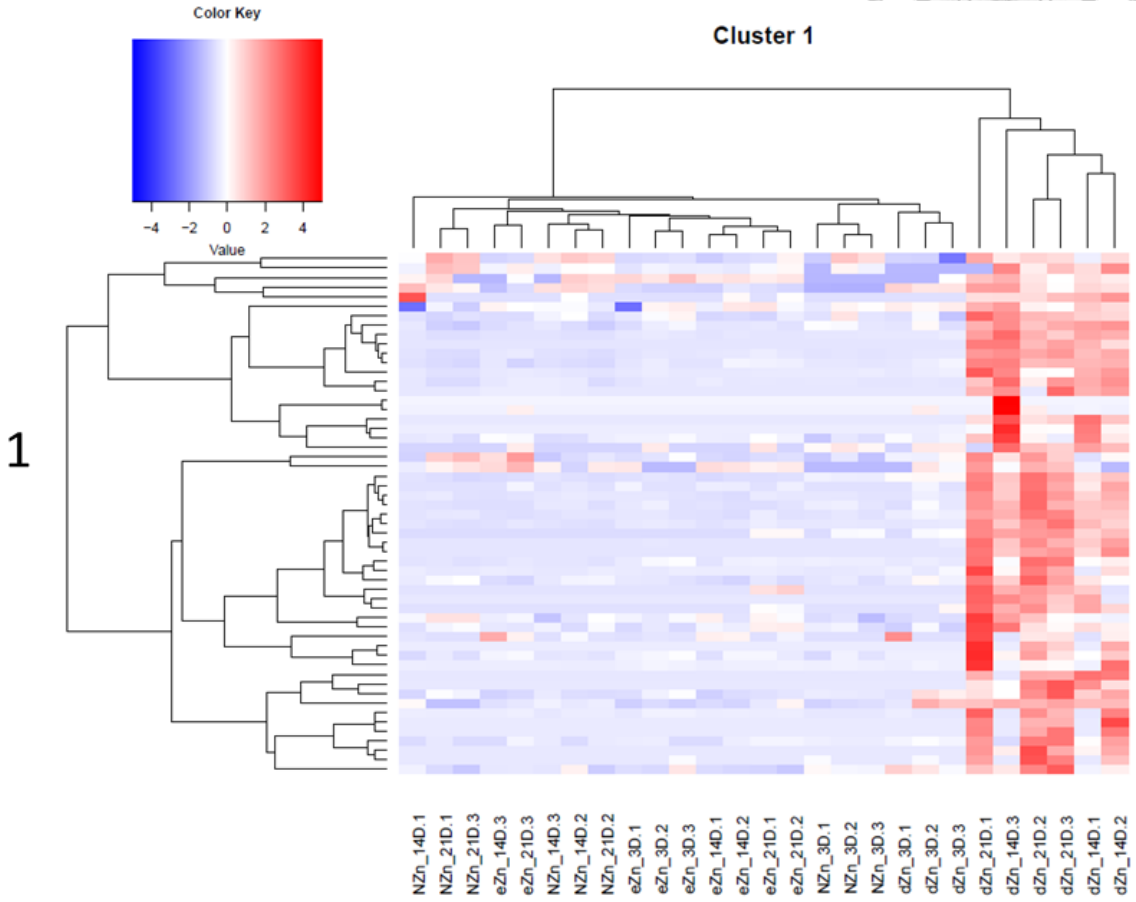

Figure 16. Metabolite accumulation of the cluster 1.

Heatmap drawn from the metabolite list of cluster 1 in **Figure 15** and is represented mostly by amino acids. The 10-day-old rice seedlings were treated with dZn (Zn deficiency), NZn (normal Zn) and eZn (excess Zn) for 3, 14, and 21 days (D). The number at the end of the labels represent biological replicates. Heatmap constructed with z-score normalization, treatment clustering using pairwise complete and pearsons, and metabolite clustering using Euclidean and complete method in. The Zn concentration used in this study are: dZn = 0.002 μM $ZnSO_4$, NZn = 0.2 μM $ZnSO_4$, eZn = 300 μM $ZnSO_4$. n is 3.

doi:10.6342/NTU202100671

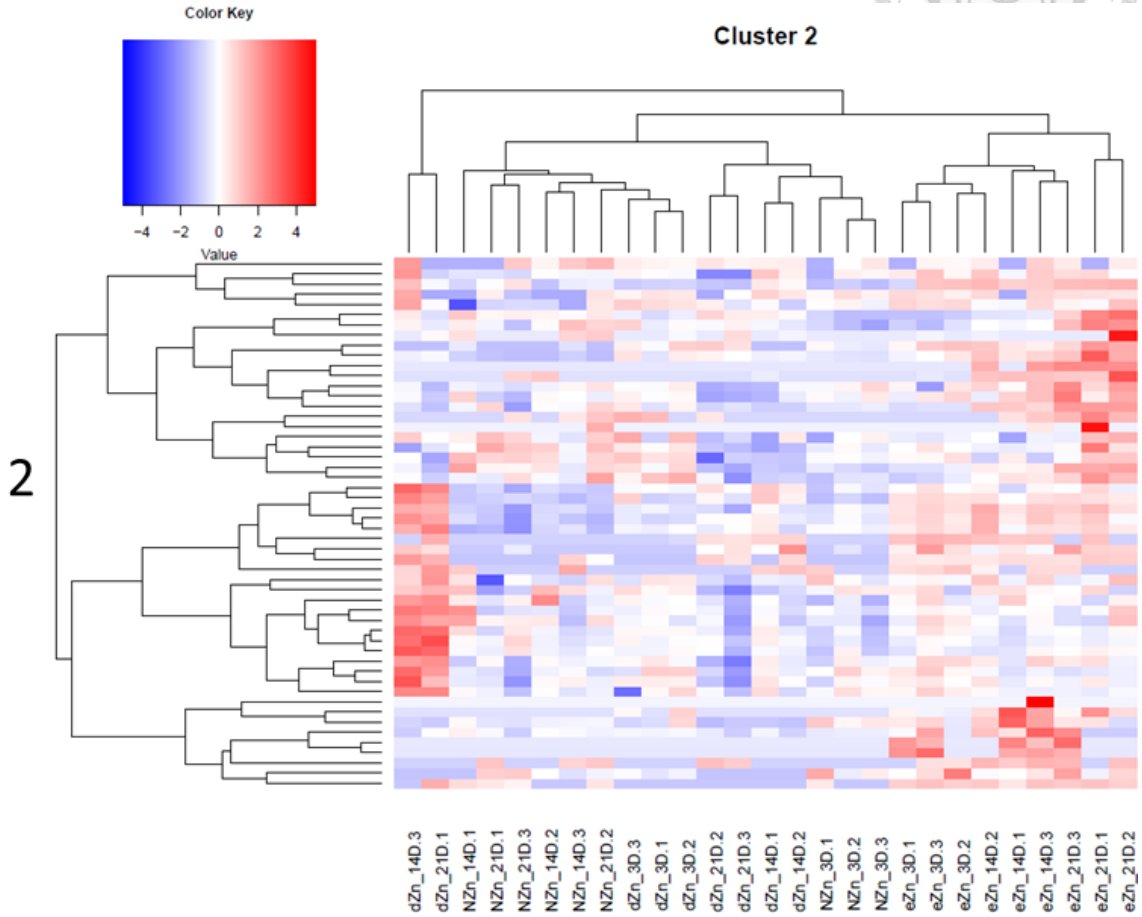

Figure 17. Metabolite accumulation of the cluster 2.

Heatmap drawn from the metabolite list of cluster 2 in **Figure 15** represented mostly by alkanes and fatty acid. The 10-day-old rice seedlings were treated with dZn (Zn deficiency), NZn (normal Zn) and eZn (excess Zn) for 3, 14, and 21 days (D). The number at the end of the labels represent biological replicates. Heatmap constructed with z-score normalization, treatment clustering using pairwise complete and pearsons, and metabolite clustering using Euclidean and complete method in. The Zn concentration used in this study are: dZn = 0.002 μM $ZnSO_4$, NZn = 0.2 μM $ZnSO_4$, eZn = 300 μM $ZnSO_4$. n is 3.

doi:10.6342/NTU202100671

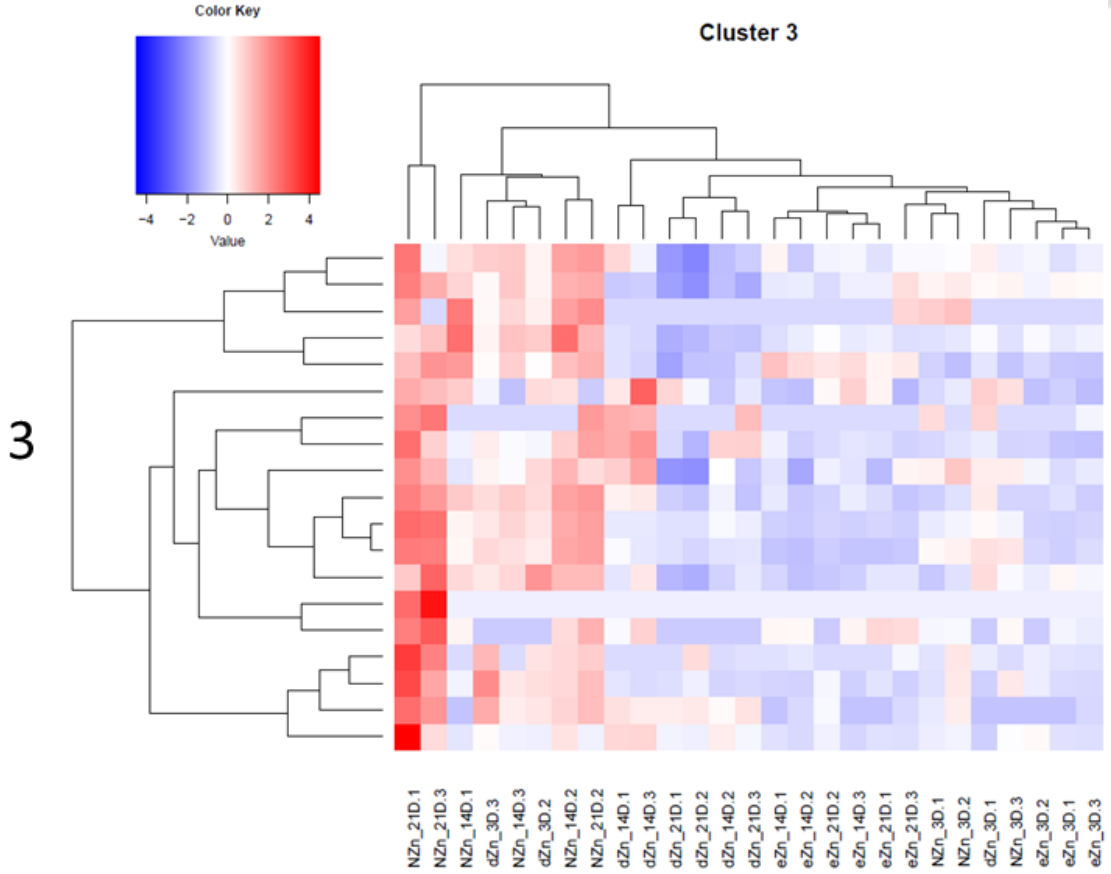

Figure 18. Metabolite accumulation of the cluster 3.

Heatmap drawn from the metabolite list of cluster 3 in **Figure 15** represented mostly by sugar and fatty acid. The 10-day-old rice seedlings were treated with dZn (Zn deficiency), NZn (normal Zn) and eZn (excess Zn) for 3, 14, and 21 days (D). The number at the end of the labels represent biological replicates. Heatmap constructed with z-score normalization, treatment clustering using pairwise complete and pearsons, and metabolite clustering using Euclidean and complete method in. The Zn concentration used in this study are: dZn = 0.002 μM $ZnSO_4$, NZn = 0.2 μM $ZnSO_4$, eZn = 300 μM $ZnSO_4$. n is 3.

doi:10.6342/NTU202100671

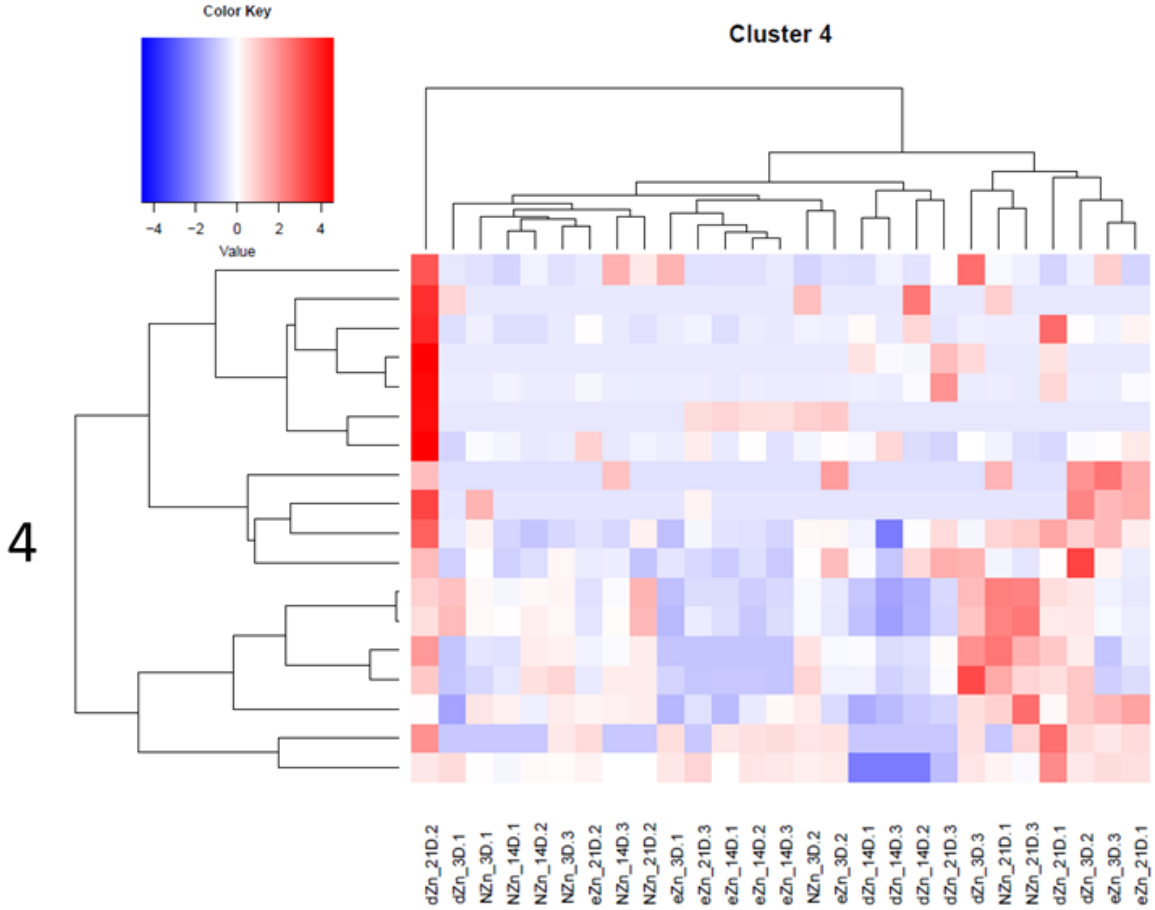

Figure 19. Metabolite accumulation of the cluster 4.

Heatmap drawn from the metabolite list of cluster 4 in **Figure 15** represented mostly by sugar. The 10-day-old rice seedlings were treated with dZn (Zn deficiency), NZn (normal Zn) and eZn (excess Zn) for 3, 14, and 21 days (D). The number at the end of the labels represent biological replicates. Heatmap constructed with z-score normalization, treatment clustering using pairwise complete and pearsons, and metabolite clustering using Euclidean and complete method in. The Zn concentration used in this study are: dZn = 0.002 μM $ZnSO_4$, NZn = 0.2 μM $ZnSO_4$, eZn = 300 μM $ZnSO_4$. n is 3.

doi:10.6342/NTU202100671

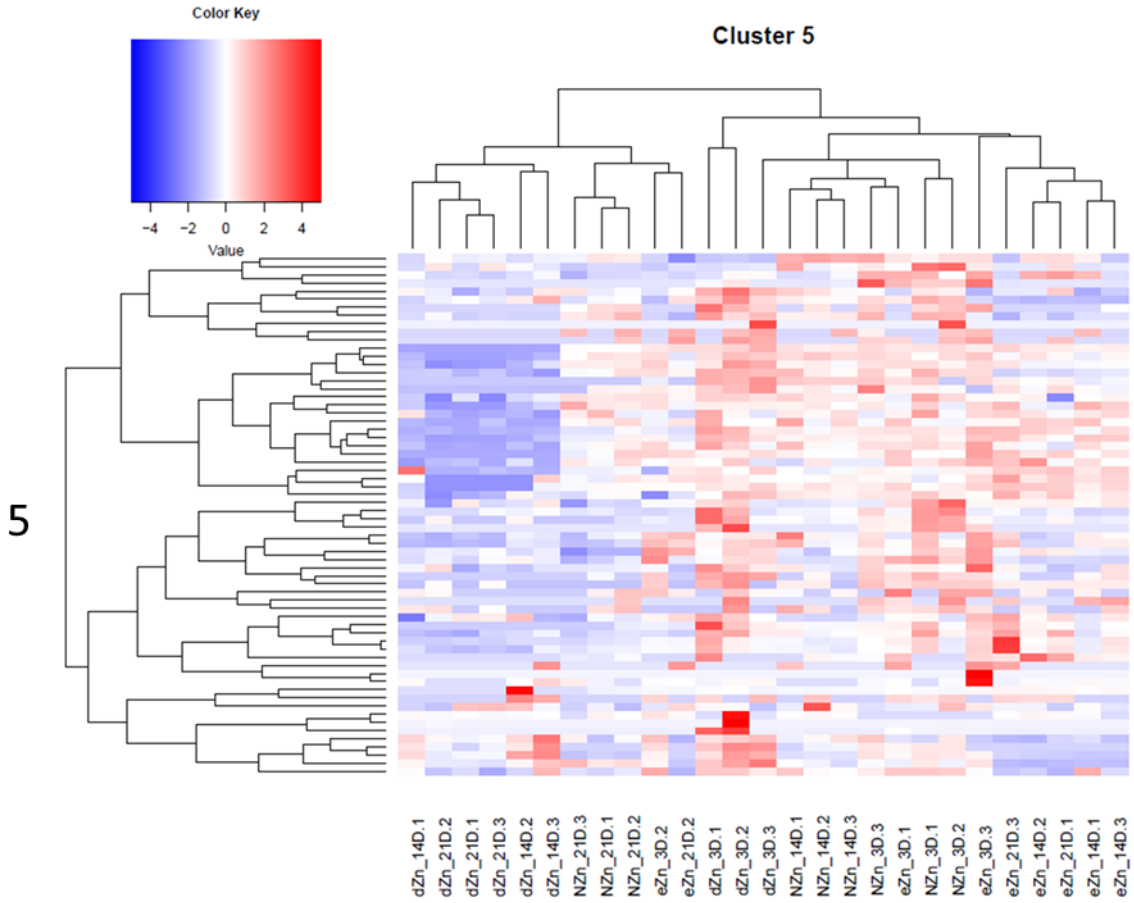

Figure 20. Metabolite accumulation of the cluster 5.

Heatmap drawn from the metabolite list of cluster 5 in **Figure 15** represented mostly by sugar and organic acid. The 10-day-old rice seedlings were treated with dZn (Zn deficiency), NZn (normal Zn) and eZn (excess Zn) for 3, 14, and 21 days (D). The number at the end of the labels represent biological replicates. Heatmap constructed with z-score normalization, treatment clustering using pairwise complete and pearsons, and metabolite clustering using Euclidean and complete method in. The Zn concentration used in this study are: dZn = 0.002 μM $ZnSO_4$, NZn = 0.2 μM $ZnSO_4$, eZn = 300 μM $ZnSO_4$. n is 3.

doi:10.6342/NTU202100671

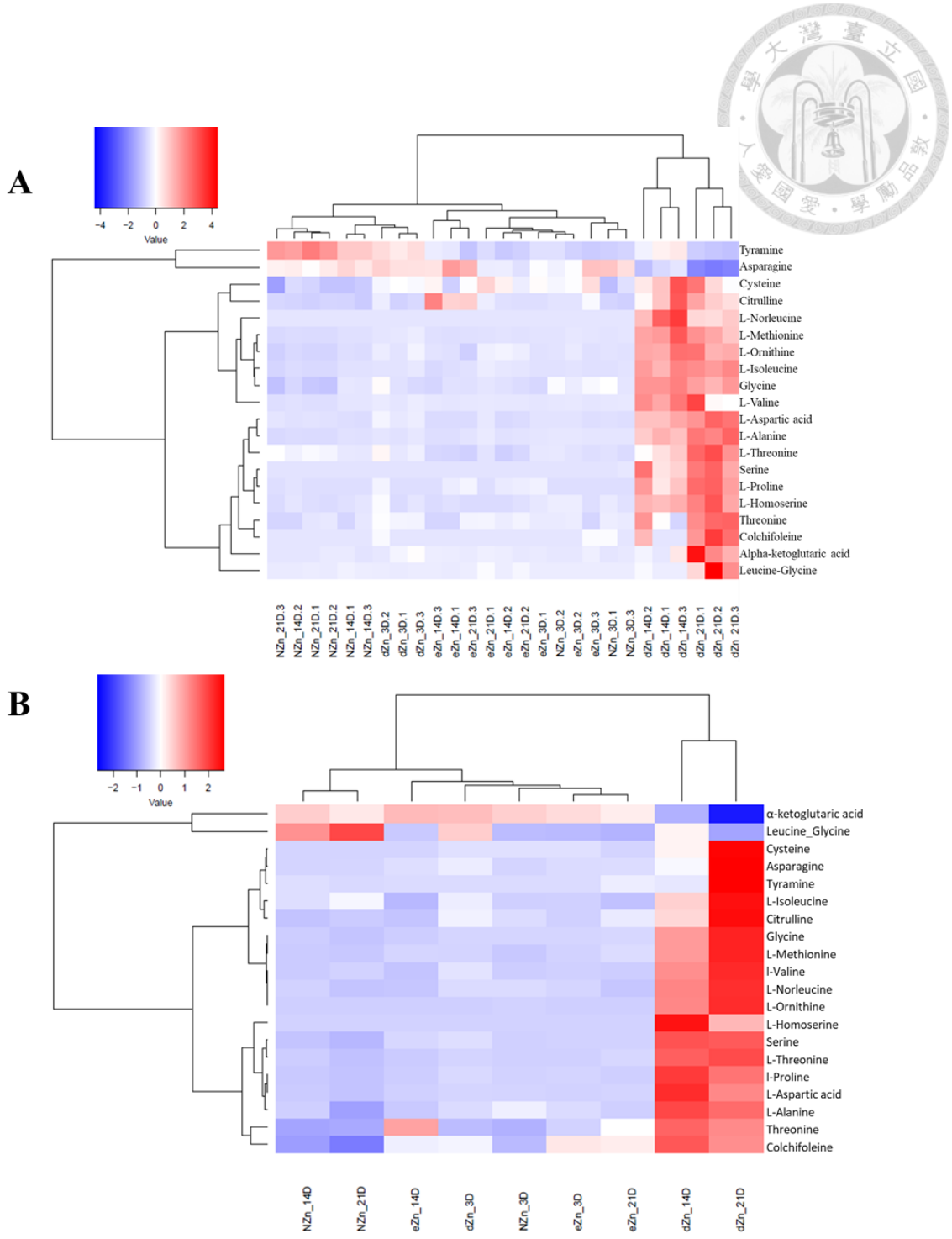

Figure 21. Heatmap of rice shoot amino acid under different Zn treatments. Heatmap drawn from the amino acid content in untargeted metabolite profile **Figure 15.** (**A**) Heatmap including all 3 replicates (**B**) and average of the 3 replicates. The 10-day-old rice seedlings were treated with dZn (Zn deficiency), NZn (normal Zn) and eZn (excess Zn) for 3, 14, and 21 days (D). The number at the end of the labels represent biological replicates. Heatmap constructed with z-score normalization, treatment clustering using pairwise complete and pearsons, and metabolite clustering using Euclidean and complete method in. The Zn concentration used in this study are: dZn = 0.002 μM $ZnSO_4$, NZn = 0.2 μM $ZnSO_4$, eZn = 300 μM $ZnSO_4$.

doi:10.6342/NTU202100671

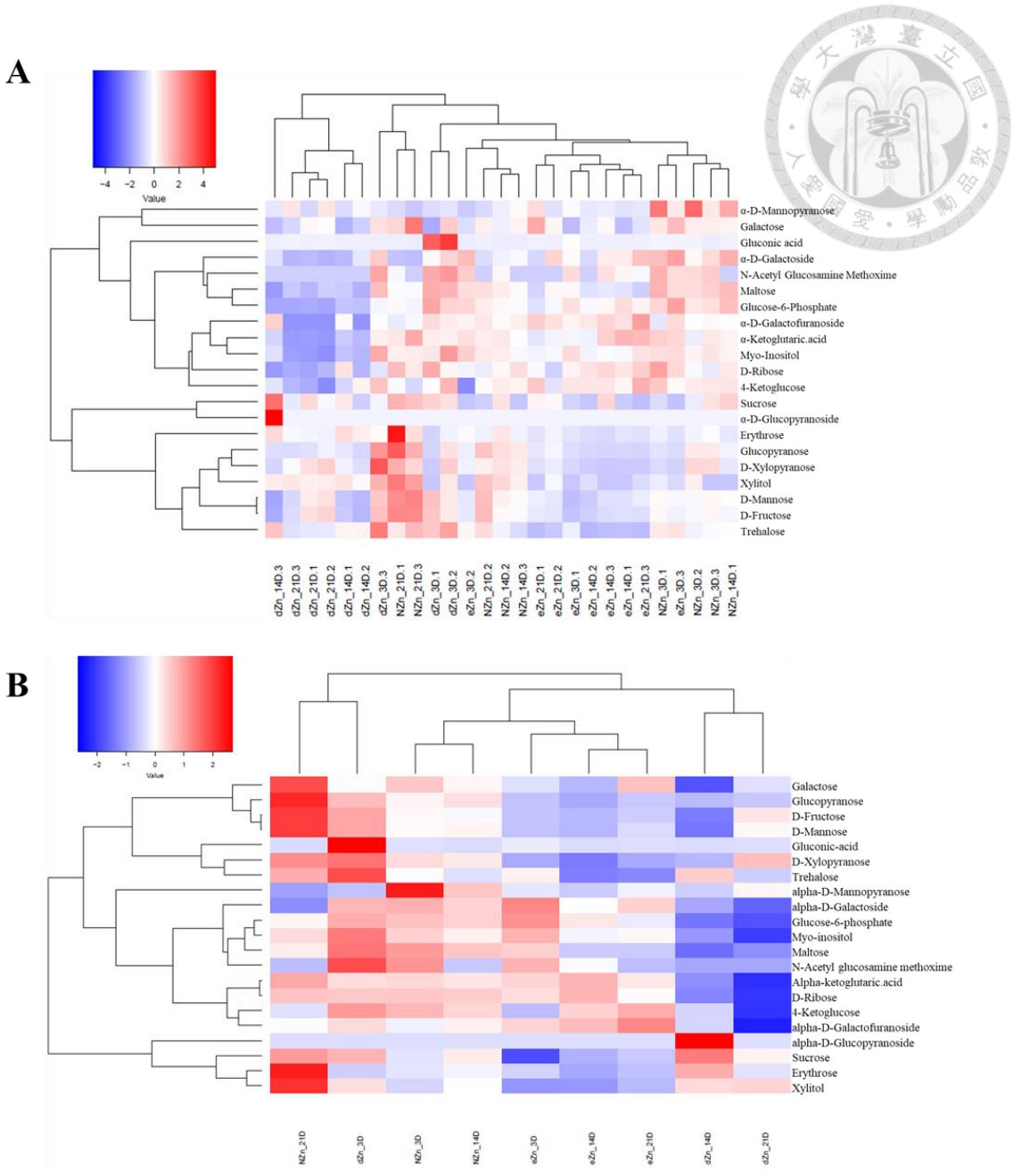

Figure 22. Heatmap of rice shoot carbohydrate under different Zn treatments.

Heatmap drawn from the carbohydrate content in untargeted metabolite profile **Figure 15.** (**A**) Heatmap including all 3 replicates (**B**) and average of the 3 replicates. The 10-day-old rice seedlings were treated with dZn (Zn deficiency), NZn (normal Zn) and eZn (excess Zn) for 3, 14, and 21 days (D). The number at the end of the labels represent biological replicates. Heatmap constructed with z-score normalization, treatment clustering using pairwise complete and pearsons, and metabolite clustering using Euclidean and complete method in. The Zn concentration used in this study are: dZn = 0.002 μM $ZnSO_4$, NZn = 0.2 μM $ZnSO_4$, eZn = 300 μM $ZnSO_4$.

doi:10.6342/NTU202100671

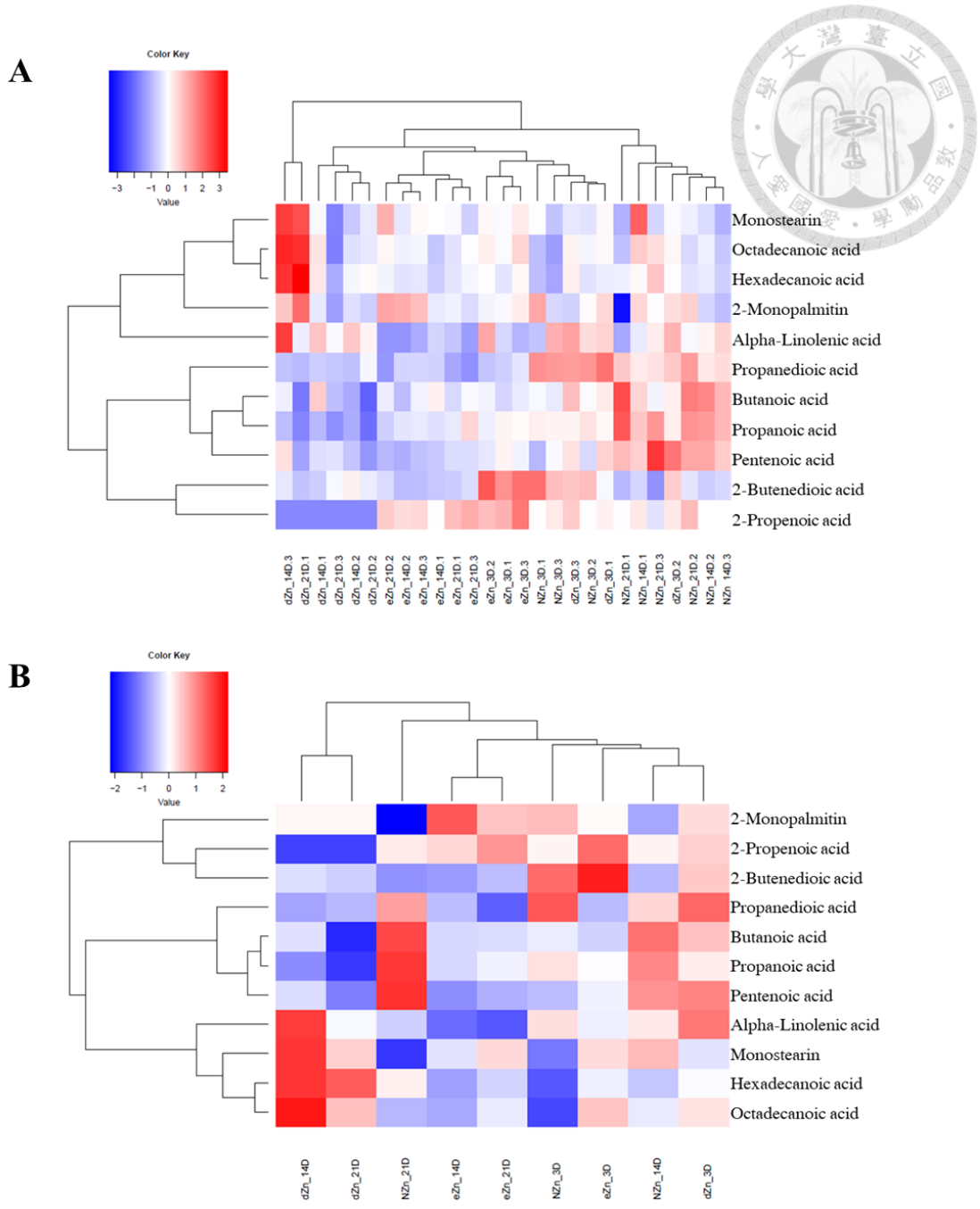

Figure 23. Heatmap of incomplete rice shoot fatty acid under different Zn treatments.

Heatmap drawn from the fatty acid content in untargeted metabolite profile Figure 15. (A) Heatmap including all 3 replicates (B) and average of the 3 replicates. The 10-day-old rice seedlings were treated with dZn (Zn deficiency), NZn (normal Zn) and eZn (excess Zn) for 3, 14, and 21 days (D). The number at the end of the labels represent biological replicates. Heatmap constructed with z-score normalization, treatment clustering using pairwise complete and pearsons, and metabolite clustering using Euclidean and complete method in. The Zn concentration used in this study are: dZn = 0.002 μM $ZnSO_4$, NZn = 0.2 μM $ZnSO_4$, eZn = 300 μM $ZnSO_4$.

doi:10.6342/NTU202100671

Figure 24: Changes of the primary metabolites pathway under Zn stress at 14 DAT.
The 10-day-old rice seedlings were treated with dZn (Zn deficiency), NZn (normal Zn) and eZn (excess Zn) for 14, and 21 days (D). Metabolites detected in rice shoots were indicated with a red color, asterisk represents significance, and the relative abundance of these metabolites were depicted using a boxplot. Two sided t-test analysis performed to find significance: pvalue < 0.05 at 0.95 confidence interval. The Zn concentration used in this study are: dZn = 0.002 µM $ZnSO_4$, NZn = 0.2 µM $ZnSO_4$, eZn = 300 µM $ZnSO_4$ and n is 3. Figure adapted from (Wang et al., 2015)

doi:10.6342/NTU202100671

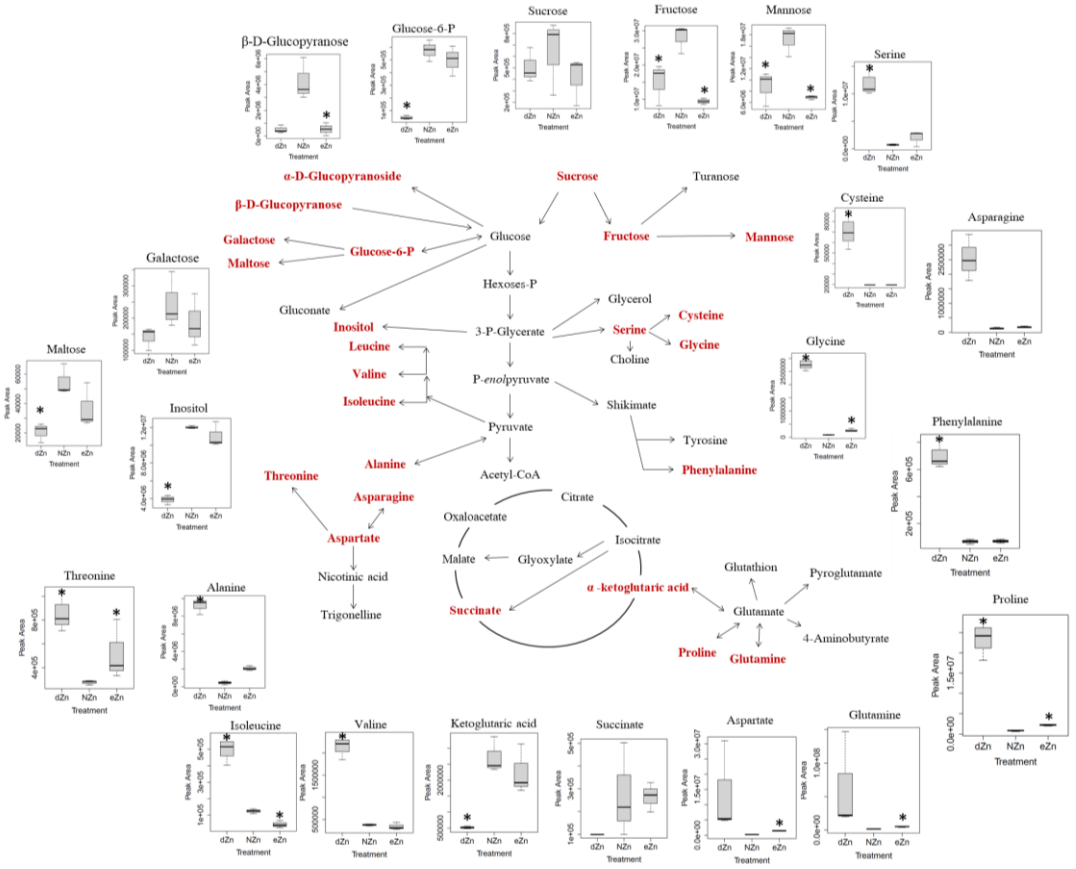

Figure 25: Changes of the primary metabolites pathway under Zn stress at 21 DAT.

The 10-day-old rice seedlings were treated with dZn (Zn deficiency), NZn (normal Zn) and eZn (excess Zn) for 3, 14, and 21 days (D). Metabolites detected in rice shoots were indicated with a red color, asterisk represents significance, and the relative abundance of these metabolites were depicted using a boxplot. Two sided t-test analysis performed to find significance: pvalue < 0.05 at 0.95 confidence interval. The Zn concentration used in this study are: dZn = 0.002 µM $ZnSO_4$, NZn = 0.2 µM $ZnSO_4$, eZn = 300 µM $ZnSO_4$ and n is 3. Figure adapted from (Wang et al., 2015).

doi:10.6342/NTU202100671

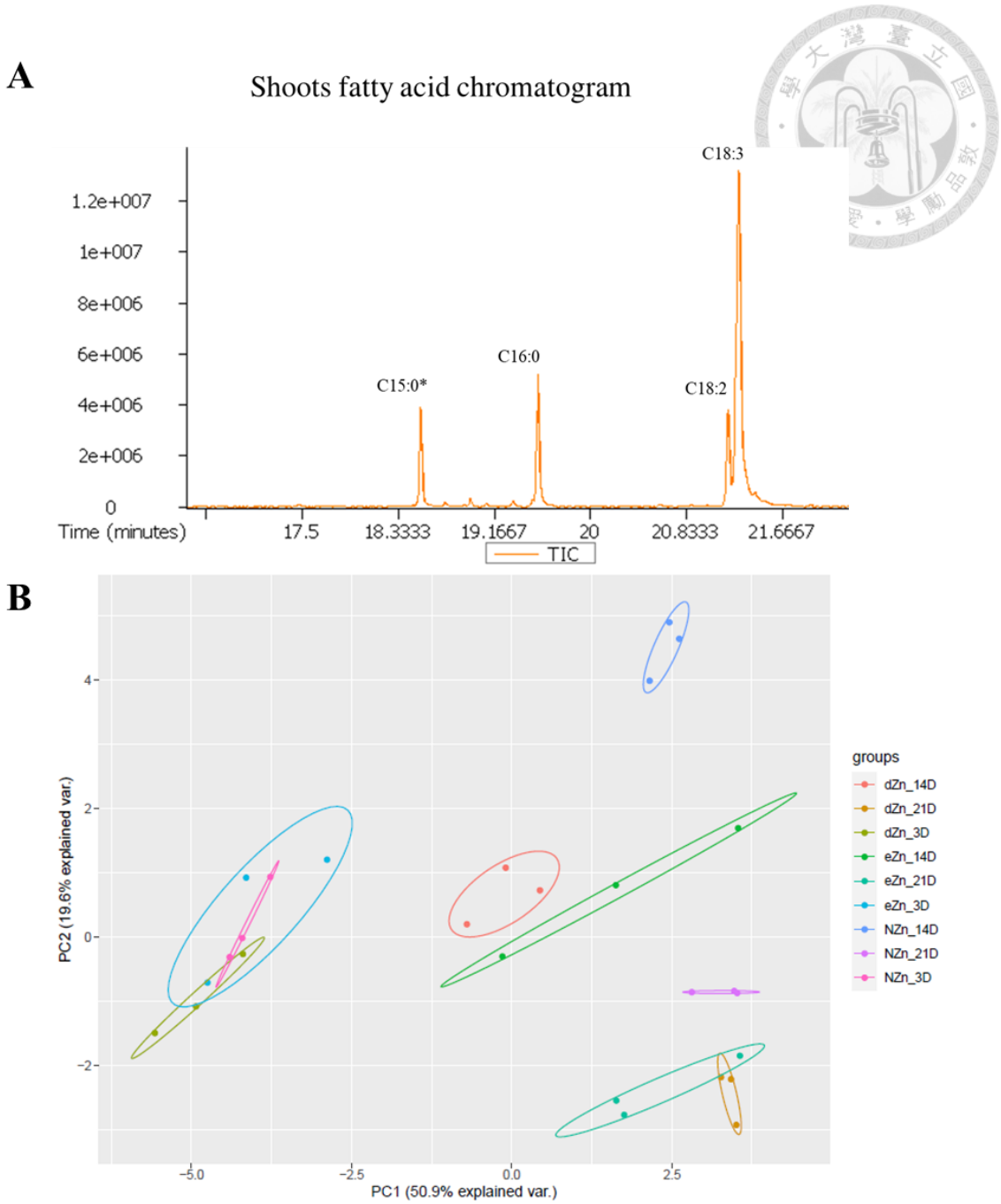

Figure 26. Fatty acid profiling of rice leaf non-polar extraction in response to Zn treatments.

The 10-day-old rice seedlings were treated with dZn (Zn deficiency), NZn (normal Zn) and eZn (excess Zn) for 3, 14, and 21 days (D). A total of four replicates were done but an outlier was removed to reduce the variation. (**A)** Total ion chromatogram (TIC) of GC-MS chromatogram with the y-axis displaying peak area and the x-axis, retention time. Major peaks are: C15:0, pentanoic acid (*internal standard); C16:0, hexadecanoic acid; C18:2, 9,12-octadecandienoic acid; C18:3, 9,12,15-octadecatrienoic acid. **(B)** PCA plot (PC1 vs. PC2) of the fatty acids identified through GC-MS. The Zn concentrations used in this study are: dZn = 0.002 μM $ZnSO_4$, NZn = 0.2 μM $ZnSO_4$, eZn = 300 μM $ZnSO_4$.

doi:10.6342/NTU202100671

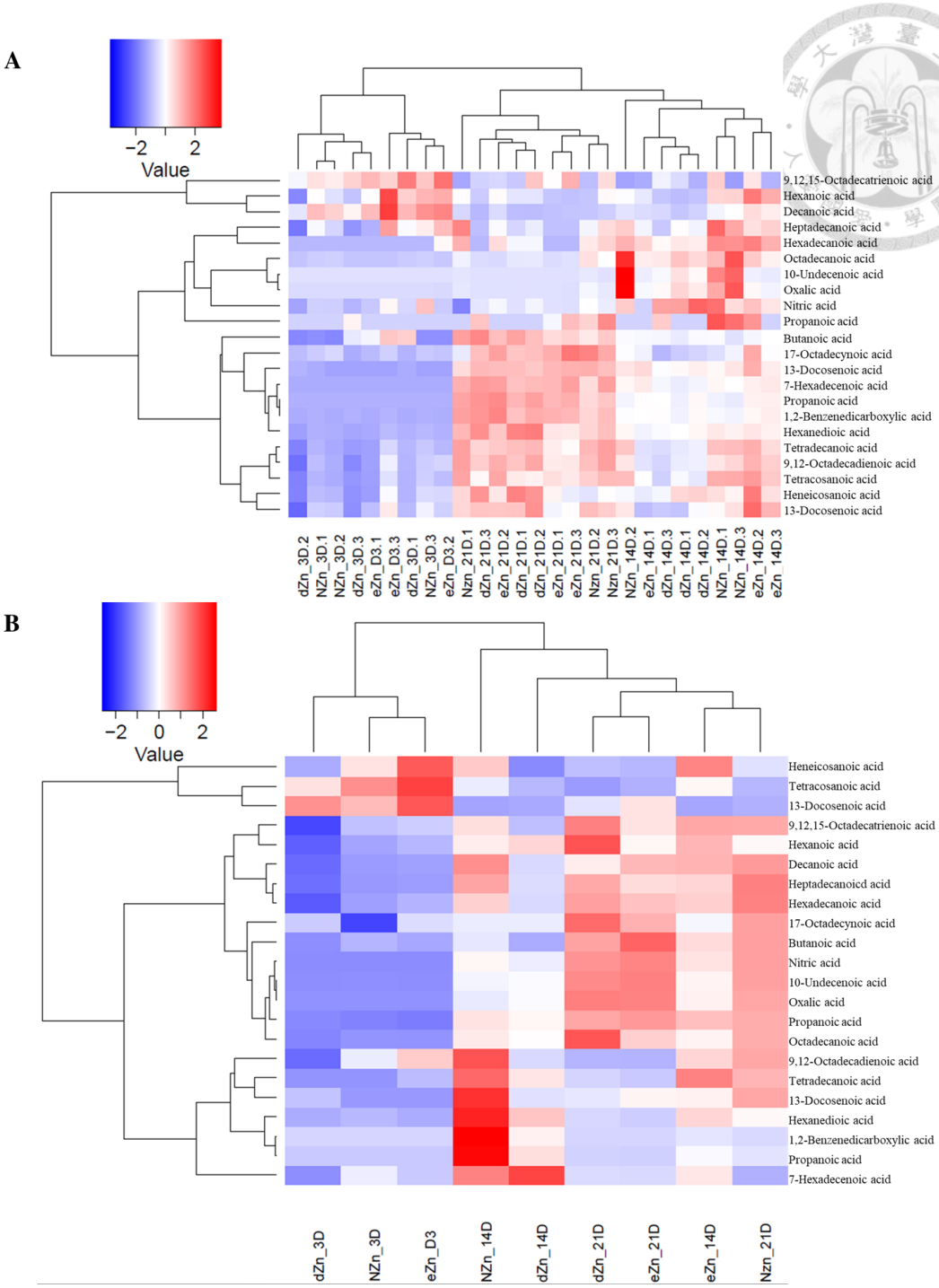

Figure 27. Heatmap of rice shoot fatty acid under different zinc treatments.
The 10-day-old rice seedlings were treated with dZn (Zn deficiency), NZn (normal Zn) and eZn (excess Zn) for 3, 14, and 21 days (D). Heatmap drawn from non-polar leaf lipid extraction: (**A**) heatmap including 3 replicates (**B**) and average of the 3 replicates. The number at the end of the labels represent biological replicates. Heatmap constructed with z-score normalization, treatment clustering using pairwise complete and pearsons, and metabolite clustering using Euclidean and complete method in. The Zn concentration used in this study are: dZn = 0.002 μM $ZnSO_4$, NZn = 0.2 μM $ZnSO_4$, eZn = 300 μM $ZnSO_4$.

doi:10.6342/NTU202100671

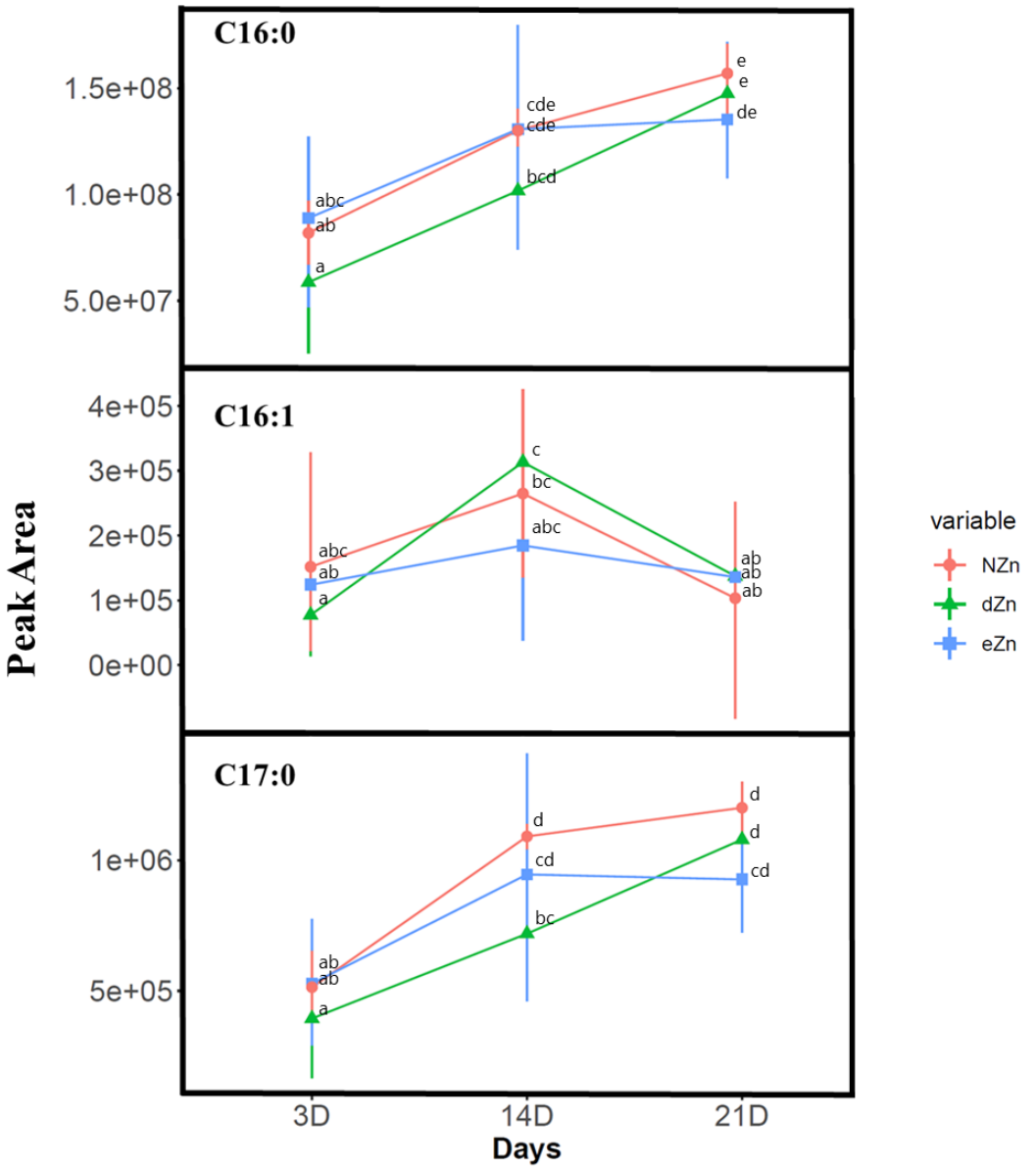

Figure 28. Fatty acid contents under Zn treatments over time.

The 10-day-old rice seedlings were treated with dZn (Zn deficiency), NZn (normal Zn) and eZn (excess Zn) for 3, 14, and 21 days. The relative quantity of hexadecanoic acid (C16:0), 7-hexadecanoic acid (C16:1), and heptadecanoic acid (C17:0) under different Zn treatments were shown over time course. Analyzed using two-way ANOVA followed by Tukey post hoc test. Different letter denotes significant differences amongst groups with p-value of less than 0.05. The Zn concentration used in this study are: dZn = 0.002 μM $ZnSO_4$, NZn = 0.2 μM $ZnSO_4$, eZn = 300 μM $ZnSO_4$. n is 3.

doi:10.6342/NTU202100671

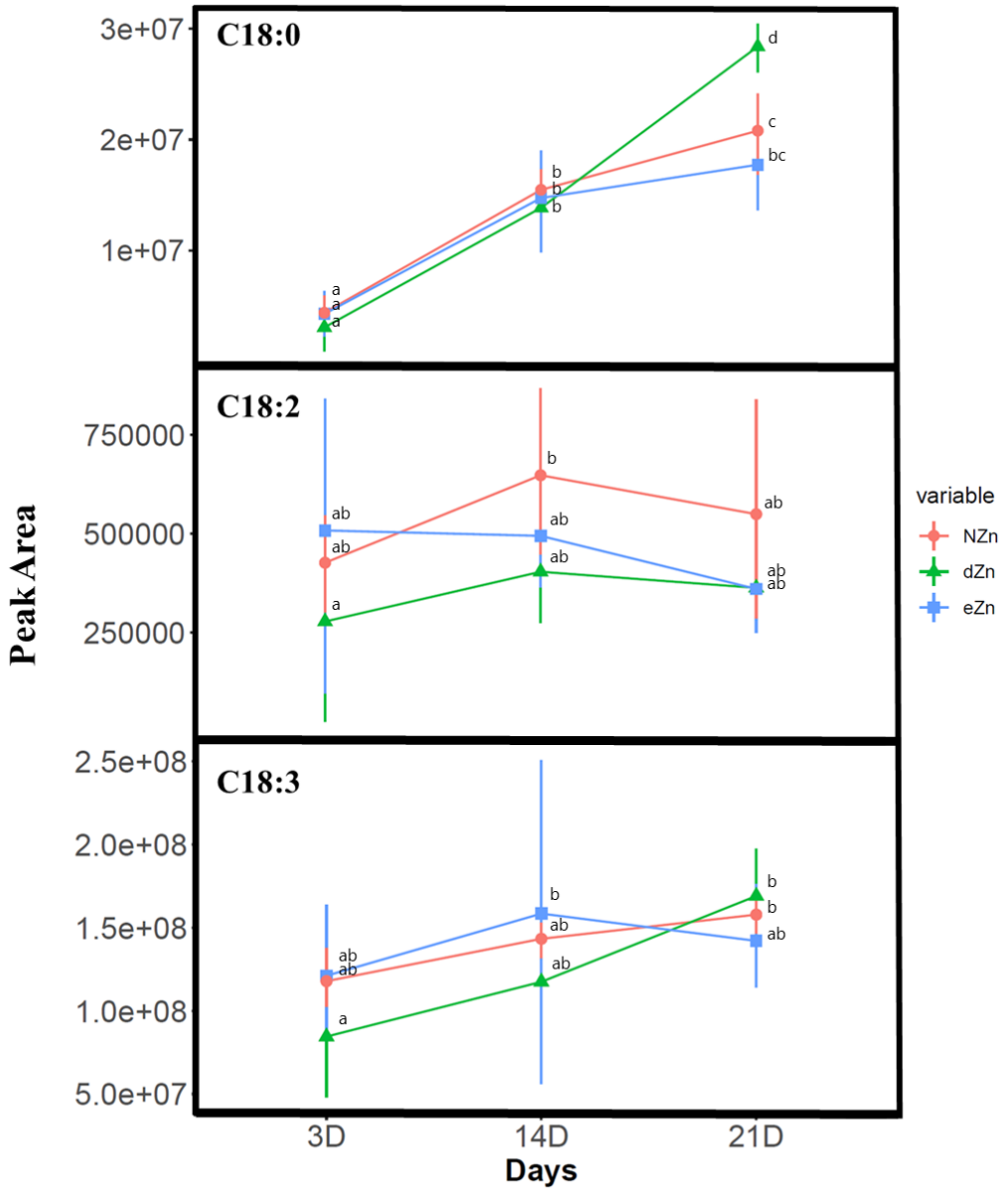

Figure 29. Fatty acid contents under Zn treatments over time.

The 10-day-old rice seedlings were treated with dZn (Zn deficiency), NZn (normal Zn) and eZn (excess Zn) for 3, 14, and 21 days. The relative quantity of octadecanoic acid (C18:0), 9,12-Octadecadienoic acid (C18:2), and 9,12,15-Octadecatrienoic acid (C18:3) under different Zn treatments were shown over time course. Analyzed using two-way ANOVA followed by Tukey post hoc test. Different letter denotes significant differences amongst groups with p-value of less than 0.05. The Zn concentration used in this study are: dZn = 0.002 μM $ZnSO_4$, NZn = 0.2 μM $ZnSO_4$, eZn = 300 μM $ZnSO_4$ and n is 3.

doi:10.6342/NTU202100671

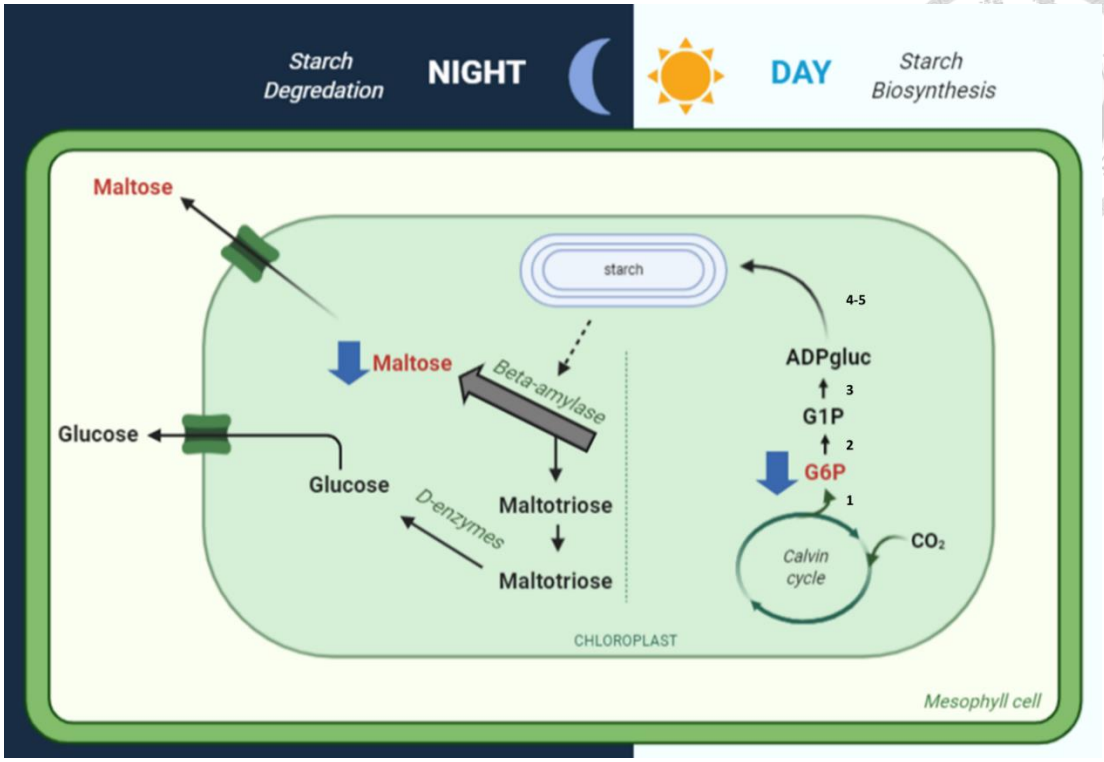

Figure 30. Model of starch accumulation under Zn deficiency based on starch synthesis and hydrolytic degradation pathway

Under Zn deficiency, the accumulation of starch in the leaf chloroplast was obvious. This may due to the increased starch synthesis or reduced starch degradation. Based on our results, we proposed possible pathways. Under Zn deficient condition, a reduced amount of glucose-6-phosephate (G6P) may explained by increasing starch synthesis; on the other hands, the hydrolytic degradation of starch was somehow to be blocked, which lead to the reduced maltose. Combined both effects, the starch granules were therefore accumulated on Zn-deficient leaves. Enzymes involved in this pathway were (1) phosphoglucose isomerase; (2) phosphoglucomutase with the intermediate of calvin cycle glucose-6-phosephate (G6P); AGPase (3) and the glucose units are then joined via Starch Synthase(4), Starch Branching Enzyme(5), and Debranching Enzyme (6) to synthesize starch. During the hydrolytic degradation pathway, transitory starch is broken down by beta-amylase and other enzymes to produce the main products maltose . Both products maltose and glucose is then exported to the cytosol to synthesize sucrose. Pathway was adapted from Sharkey et al (2006) and Geigenberger (2011) with minor modifications.

doi:10.6342/NTU202100671

Appendices

Appendix 1. List of cluster 1 metabolites.

Metabolites obtained from GCxGC-TOFMS were classified into different groups, namely unknown (U), amino acids (A), alkanes (Al), fatty acid s(F), and carbohydrates (C). The order of metabolite table generated according to the cluster 1 heatmap (**Figure 16**) and the values represent peak area. DAT represents days after Zn treatment. Zn concentration used in this study was dZn = 0.002μM $ZnSO_4$, NZn = 0.2μM $ZnSO_4$, eZn = 300μM $ZnSO_4$.

		Optimal Zn treatment (NZn)									*Zn deficient treatment (dZn)*									*Zn excess treatment (eZn)*								
Metabolite	***Groups***	***3 DAT***			***14 DAT***			***21 DAT***			***3 DAT***			***14 DAT***			***21 DAT***			***3 DAT***			***14 DAT***			***21 DAT***		
Analyte 337	U	124893.6	278811.3	248288.7	194596.091	274088.5	240941.7	316086.3	256351.5	281814.5	135399.727	133549.2	0	174925.303	249704.365	230201.437	322641.062	259848.858	248321.793	142827.3	147081.8	154804.9	126248.4	144506.2	138465.7	153622.2	215795.9	144194
Analyte 215	U	0	0	0	266397.14	41438.24	0	0	0	0	0	0	0	132524.981	178002.739	84757.78	84170.145	88144.195	123449.871	0	0	0	0	46893.04	0	0	42904.32	0
Analyte 154	U	128055.8	161978.5	153552.6	0	148756.1	148228.3	138912.9	130577	99236.57	170236.995	158735.4	169647.8	208053.859	189572.534	257307.626	232555.699	166600.654	152992.276	0	162910.6	171615.4	135530.8	176433.2	165090	180845.2	144798.3	151177
l-Alanine	A	194714.6	181441.6	114447.0	121762354	747126.6	115992.0	314742	221705.7	108516.6	103703288	218260.9	794803.3	539897.285	581160111	613913943	478061.8312	410644448	495939872	756797.2	135434.9	170768.0	106476.5	106190.6	72316.03	118030.4	92210.5	101365.0
l-Proline	A	245656.9	256931.9	287834.8	204124264	110302.4	176742.1	820892.5	965212.8	617173.5	310210925	285443.8	413155.4	266561.585	246041914	390318179	282145.9097	241685867	181892467	26764.70	315831.5	271278.5	171.4303	239928.8	179389.1	235.6417	222807.2	194675.1
Threonine	A	727453.6	813430.2	796713.8	798202.903	577246.9	720074.7	438764.5	435085.4	340501	806824.213	883335.4	103376.6	514064.609	600034.452	737419.994	685794.4.605	612924.061	688531.109	776404.5	894938.3	827817.5	912781.3	100232.2	893.861	125.1472	908586.8	105422.7
Serine	A	2001192	2006600	179423.5	1534956.76	111083.4	140145.6	859306.3	727290.2	552380.6	2034727.65	262016.5	317974.8	106337.467	1102190.6	1555439.1	152176.32.32	1014481.6	1082035.4.6	181.0656	250793.7	168247.9	168.7378	316633.5	199070.6	287.3697	279337.7	386537.3
L-Aspartic acid	A	1371932	1384802	166930.7	1105433.95	548294.5	115509.7	237566.4	285288.6	138016	1093124.24	180926.0	221250.3	171660.797	209802.26	238842.854	309890.25.91	541681.891	487044.878	120.7831	161836.7	119364.9	125.3021	126444.3	126245.4	158.8146	146113.8	148252.2
Analyte 181	U	55663.31	55265.32	38156.61	447975.49	57381.12	67776.26	0	0	0	414105.11	45763.75	42203.12	454528.365	558734.008	704051.454	358433.105	212705.693	529784.873	33595.33	54914.24	45239.8	67698.46	44660.38	46277.04	54460.27	47707.23	64262.26
***α*-D-Glucopyranoside**	C	0	0	0	0	0	0	0	0	0	0	0	0	0	0	257469.833	0	0	0	0	0	0	0	0	0	0	0	0

doi:10.6342/NTU202100671

		Optimal Zn treatment (NZn)									Zn deficient treatment (dZn)									Zn excess treatment (eZn)								
Metabolite	***Groups***	***3 DAT***			***14 DAT***			***21 DAT***			***3 DAT***			***14 DAT***			***21 DAT***			***3 DAT***			***14 DAT***			***21 DAT***		
Analyte 248	U	0	0	0	0	0	0	0	0	0	0	825671.7	0	84818.898	0	6607623.3	0	785505.645	0	0	0	0	0	0	0	0	0	726840.5
Analyte 133	U	0	0	0	0	0	0	0	0	0	0	0	40415.74	127131.963	74911.444	115424.209	189786.197	151895.233	81432.888	0	0	0	0	0	0	33550.58	23738.87	0
Analyte 413	U	97823.41	100685.66	84825.34	108599.562	101555.3	87886.77	123559.9	111818.33	123718.44	96752.998	99731.65	98550.04	109329.205	106212.078	150975.831	190655.418	136064.175	112851.35	107153.3	103038.4	110105.66	117840.55	100511.44	105175.66	115702.55	110775.88	108250.66
Analyte 43	U	687418 8	715728 2	587720 0	6102341.94	576108 1	705110 6	726242 7	755846 2	767419 6	5093745.9	746741 3	515659 6	9991344.19	8667667.69	1571 2233	18508899.7	9695585.67	8194860.39	562430 2	659697 3	570460 6	728891 2	682399 4	656741 9	873999 1	894540 6	637725 8
Analyte 222	U	0	0	0	0	0	0	0	0	0	0	0	0	0	32128.386	0	71991.443	32440.204	21029.322	0	0	0	0	0	0	0	0	0
Pentadecane	Al	124562	149453.6	134449.7	124870.591	138898.8	136848.6	141291.6	135439.9	130354.7	147653.33	147514.2	147333.1	163294.665	216774.799	173344.358	373481.314	256535.555	189013.925	148673.4	154146.8	159936	132535.8	154805.2	152159.3	153426.2	142749	156811.5
I-Glutamine	A	208 1990	262 8150	224 2376	1047 659.78	717 797.4	130 8853	691 827.1	436 024.5	371 652.1	1111 418.53	350 9453	166 2863	2892 294.55	7807 9646.2	4063 866.08	10764 2359.2	1397 1594	1138 6585.5	171 4989	423 4729	274 6086	105 5707	211 0875	955 620.5	222 8255	254 9494	141 0823
Analyte 291	U	0	0	0	0	0	0	0	0	0	0	0	0	137733.73	128938.837	0	86166.898	89843.623	87444.601	0	0	0	0	0	0	0	0	0
Analyte 379	U	221343.7	214971.6	201710.4	133769.254	164061.3	213592.9	292078.9	154118	245666.6	186479.798	440928.8	363870.5	500847.716	665826.482	298475.638	429912.895	775030.839	985910.491	161508.7	238148.1	292727.9	105942.7	153748.4	110223.4	169288	188506.9	141894.6
Analyte 482	U	41923.12	64346.88	72907.23	17056.677	98568.09	12198.72	0	11127.52	0	9247.212	35964.23	29936.43	32906.495	32774.427	36567.361	31266.846	34386.437	38624.025	3284.974	6359.404	3656.324	6433.839	4752.259	7830.859	9936.429	1817.512	9249.423
Analyte 312	U	0	0	0	0	0	0	0	0	0	0	0	0	0	27565.757	0	19204.106	12961.562	13140.69	0	0	0	0	0	0	0	0	0
Analyte 283	U	0	0	0	0	0	0	0	0	0	0	0	0	0	10987 81.47	0	1032584.36	77375 8.223	11381 24.66	0	0	0	0	0	0	0	0	0
Citrulline	A	24420.4	19811.33	20509.93	0	0	17803.69	15331.45	18573.2	0	30506.506	40173.44	30049.37	43931.1045	15295 3.418	0	161451.214	19854 2.557	20338 8.327	20031.15	21967.76	0	0	21613.39	0	30542.04	29968.94	29060.1
L-Ornithine	A	0	0	18006.01	0	0	0	0	0	0	0	0	0	0	58472 3.186	18977 51.166	71376 3.983	22837 63.14	35958 90.82	19041 70.88	0	0	0	0	0	0	0	0	0
Cysteine	A	8974.249	0	0	0	0	0	0	0	0	0	8179.475	0	0	39061.365	0	53457.209	90189.037	69320.284	0	0	9009.702	0	0	0	0	0	0

doi:10.6342/NTU202100671

Appendix 2. List of cluster 2 metabolites.

Metabolites obtained from GCxGC-TOFMS were classified into different groups, namely unknown (U), amino acids (A), alkanes (Al), fatty acid s(F), and carbohydrates (C). The order of metabolite table generated according to the cluster 2 heatmap (**Figure 17**) and the values represent peak area. DAT represents days after Zn treatment. Zn concentration used in this study was dZn = 0.002μM $ZnSO_4$, NZn = 0.2μM $ZnSO_4$, eZn = 300μM $ZnSO_4$.

		Optimal Zn treatment (NZn)							Zn deficient treatment (dZn)								Zn excess treatment (eZn)									
Metabolite	***Groups***	***3 DAT***			***14 DAT***			***21 DAT***			***3 DAT***			***14 DAT***			***21 DAT***			***3 DAT***			***14 DAT***			***21 DAT***	
Analyte 516	U	0	185467.4	243562.3	0	210573.5	3101 15.753	0	356672.8	312910.2	208205.3	202227.2	228135.5	219355.4	2290 21.188	4222 71.139	0	2456 45.616	2083 87.952	0	2012 22.216	2080 89.832	0	2240 00.333	2967 30.035	0	228872.589	232209.4
Analyte 138	U	966 0.672	322 36.67	307 01.03	2242 4.233	291 92.56	2676 5.281	222 01.8	263 74.29	191 34.46	290 43.66	273 66.44	312 33.49	421 82.4	3236 1.071	5357 0.117	1817 4.437	0	0	3346 1.973	3062 4.889	4300 5.157	2656 8.036	4222 9.699	4105 4.294	3809 9.594	28868.79	36799.8
Hexacosane	Al	178 69.27	240 25.21	178 99.54	2688 5.226	197 83.94	3507 4.8875	410 77.38	363 82.25	527 80.47	251 09.85	263 61.11	229 78.51	500 30.36	4423 8.475	6500 7.177	3919 5.35	2095 6.077	1894 2.522	2707 0.2065	6442 2.354	6348 1.6845	5856 4.9215	6761 2.0645	6029 0.6685	6719 9.382	69423.733	656 09.89
Analyte 55	U	536 11.85	707 51.95	582 65.3	0	0	0	593 58.1	670 65.44	152 39.98	661 58.48	636 99.64	560 40.08	772 99.73	6475 6.939	1012 10.819	0	0	5013 3.761	7288 5.286	5984 9.617	6904 9.667	0	7268 6.416	7586 1.786	6759 2.925	65428.899	690 58.18
Analyte 483	U	553 18.03	583 40.95	502 69.66	0	427 38.36	2801 0.65	419 15.91	617 06.14	433 78.62	656 97.8	632 24.56	702 86.76	536 90.99	3872 6.147	8332 0.921	5580 9.989	5955 9.704	4625 0.12	6824 3.152	6721 1.432	6508 9.703	5199 5.888	5347 3.246	6647 2.284	5300 9.673	74367.846	579 20.24
Analyte 509	U	397 65.22	232 96.66	249 31.82	1035 73.569	756 79.81	6576 3.274	729 24.11	816 79.44	773 09.26	419 75.66	556 69.84	565 19.16	800 67.82	7076 8.716	8119 2.211	4607 9.68	9542 1.579	7872 9.302	2653 5.611	3272 3.428	2638 8.323	5006 0.154	4955 5.139	5428 7.976	1463 56.13	161511.73	963 70.58
D-Glucuronic acid	C	869 32.37	435 18.52	0	1814 34.899	158 860.2	2581 58.3	137 011.6	220 367.2	503 85.73	120 685.6	157 860.4	229 784.2	137 784.8	1141 40.501	1727 12.773	1201 79.984	1437 54.716	1744 54.684	7587 1.647	1052 44.818	3846 0.425	1384 91.869	1514 42.265	1534 03.94	3612 65.871	332198.902	262 645.6
Analyte 503	U	0	0	0	5350 2.737	0	6563 6.88	0	745 77.35	0	0	140 61.19	0	0	1034 8.116	0	2660 9.108	0	5804 1.861	0	0	1151 5.133	0	8072.916	0	0	259934.809	0
Analyte 207	U	287 30.18	183 65.44	154 88.17	1706 0.372	0	1317 5.503	0	0	0	242 40.77	447 14.69	315 92.88	0	0	0	0	4697 1.694	3755 4.942	2919 7.63	5097 1.456	4663 9.357	3560 1.337	4809 9.78	3174 7.054	6810 3.053	59678.824	421 27.32
Analyte 350	U	0	0	0	0	0	0	0	0	0	0	0	0	0	0	0	0	0	0	0	0	0	0	1820 36.559	2161 38.167	2444 82.836	242886.655	250 549.7

doi:10.6342/NTU202100671

Metabolite	Groups	Optimal Zn treatment (NZn)									Zn deficient treatment (dZn)									Zn excess treatment (eZn)								
		3 DAT			*14 DAT*			*21 DAT*			*3 DAT*			*14 DAT*			*21 DAT*			*3 DAT*			*14 DAT*			*21 DAT*		
Nonane	Al	0	0	0	0	84528.55	0	0	0	73031.3	0	0	0	11962.87	0	0	0	0	0	0	0	8646.096	92878.978	89595.068	90718.824	81566.934	201030.776	83554.04
Analyte 168	U	0	0	0	0	0	50035.024	0	75793.38	54813.78	85120.24	0	92881.23	0	0	0	0	50815.925	0	0	0	0	54259.94	0	73592.227	128236.263	87023.788	87450.29
Analyte 213	U	35188.48	47497.39	34331.04	44870.719	68067.83	40787.8	86697.88	76412.63	71836.8	47126.22	57736.33	55801.17	0	13182.233	0	31921.589	18522.345	13097.159	44953.314	45405.314	58381.154	34923.095	38174.624	40357.928	109632.492	59628.985	47377.93
2-Deoxy-galactopyranose	C	203383.5	206178	193250	285596.199	248036	195504.068	256495.3	257926.5	264168.4	239084.9	250107	273700.7	144785.2	141591.82	210241.444	104141.508	31590.5405	153748.551	213724.018	243042.293	216624.349	228706.843	154553.761	146931.541	269674.981	272413.52	203210.5
3,5-dioxooctanedioic acid	C	102236.7	126075.6	127638.4	137126.2	140994.6	131334.549	130672.2	208623.4	167691.3	184784.6	200178.4	151439.4	111615.2	117134.192	143196.577	112294.387	138763.75	69354.6654	110077.79	131421.946	116700.62	164029.285	146548.17	160124.901	216950.487	190381.659	173940.3
Colchifoleine	A	97037.52	121447.6	111875.1	99409.169	109359.9	103077.705	106477.1	99242.86	83463.57	125289.3	121051.5	122474.5	150518.4	134648.515	198968.43	183737.047	140870.881	124217.875	126136.079	124404.815	139702.671	104747.124	130848.042	129535.729	144427.031	117796.935	124082.1
Heneicosane	Al	74336.24	92676.74	76924.1	83201.5385	89170.63	73503.5925	89572.06	85524.97	94872.45	88931.41	95403.59	154020.3	160773.9	131948.953	207193.71	187719.991	128286.274	100937.236	141968.475	142544.081	149573.101	122299.066	144754.198	143311.554	143596.25	135834.329	147992.7
Tetradecane	Al	201671.9	241246	216363.6	191352.735	198964.1	203331.512	183249.3	179403.2	134929	225797.6	206678.9	215877.4	241502.5	207546.974	318817.72	310735.004	199478.761	149544.566	263450.538	269128.445	280517.949	263039.066	319804.547	291805.117	305770.208	267580.864	283827.6
Analyte 129	U	25335.91	25422.47	24030.61	16720.005	21151.11	22636.473	17578.77	18228.36	13383.95	23843.13	25524.58	24571.09	28038.23	21063.748	34441.669	39821.913	23281.822	25873.712	27570.403	28590.969	30149.618	24936.393	34564.478	29296.141	30719.648	27991.007	28960.72
Analyte 268	U	0	0	0	0	0	0	0	0	0	0	10322.46	0	116313.2	116639.414	0	166405.97	102902.529	96510.556	138156.648	153308.263	165071.674	128292.999	142210.592	132870.023	140427.932	0	0
Benzoic acid	O	0	22024.56	0	0	0	0	0	0	27967.12	0	0	0	43355.91	142153.407	92968.402	73915.055	45407.575	71602.229	59105.858	73994.721	132812.55	67290.476	34649.456	39882.92	85291.415	83058.607	127457.4
Analyte 493	U	0	0	0	0	0	15754965.2	0	9086873	0	0	0	0	0	14672501.3	24194902.5	20514424.1	15906774.5	12980713.6	12617844.4	12682213.5	11950203.1	13961981.1	12402895.9	13927638.5	16846207.2	16242658.9	13336736
Eicosane	Al	62925.4	0	0	65328.421	0	87723.26	0	0	0	0	0	0	60215.33	71887.323	59271.005	98939.167	0	0	53089.424	68195.223	57379.278	0	40048.165	54530.072	0	0	54429.21
2-Monopalmitin	F	108404.6	80866.32	66424.85	92481.708	65818.26	58091.664	0	95456.33	78840.45	92373.53	90258.07	64761.45	72431.62	69904.525	98475.933	129042.403	63675.013	48079.497	78133.699	75915.575	85372.6	72834.592	106685.72	100878.123	75293.463	109622.414	68439.97
Analyte 459	U	53252.64	65518.19	51739.81	74452.972	96287.74	58357.96	63264.18	65085.26	72731.52	68317.17	69591.02	72260.16	69441.03	60018.455	92600.815	96035.304	63310.967	51252.693	70887.352	64172.097	78976.325	81107.508	66349.585	69569.013	59962.636	72650.983	71071.87
monostearin	F	8263808	7745212	7087726	11448281.4	7580017	6759742.4	6741715	7992248	7481237	8445934	8236943	7829116	8148295	7247264.79	12165456.3	11823458	7880358.5	5807246.83	8240905.73	8430171.17	8689642.23	8294414.83	7821856.31	8402819.74	8182572.19	9850023.26	7355808
Analyte 515	U	4237710	4222668	3339570	5811639.09	4867945	3676110.21	4698691	5055440	4805465	4532732	4151639	4430256	4629436	3778402.3	6120588.69	5798004.52	4443425.2	3134312.38	4321757.67	4827821.04	5146648.92	4148741.15	4532178.37	4644709.14	3984279.82	5398684.21	4107753

doi:10.6342/NTU202100671

Metabolite	Groups	Optimal Zn treatment (NZn)									Zn deficient treatment (dZn)									Zn excess treatment (eZn)								
		3 DAT			14 DAT			21 DAT			3 DAT			14 DAT			21 DAT			3 DAT			14 DAT			21 DAT		
Octadecanoic acid	*F*	*4621338*	*5235112*	*4291537*	*5865229.39*	*5157851*	*4727864.64*	*4661312*	*4923176*	*5670296*	*5397027*	*5410735*	*5422881*	*5617670*	*4998757.97*	*7620695.02*	*7523306.29*	*5079850.39*	*3973683.52*	*5273587.96*	*5475515.31*	*5774233.93*	*4714562.92*	*5179088.5*	*5230158.75*	*5028075.55*	*5415315.57*	*5306158*
Hexadecanoic acid	F	4594641	4965382	4358043	5303943.75	5033401	4771164.6	5091599	4967359	5818062	5071247	5218057	5385091	5470564	5148589.72	7281528.76	7777102.66	5269997.46	4427660.99	4980947.16	5264122.38	5306957.48	4743139.64	4961464.9	5007962.93	4977332.03	5129828.39	5156816
Analyte 189	U	76919.83	92751.69	84230.62	75428.277	89352.69	84941.502	89685.72	86605.77	68549.48	94230.4	86592.35	89596.49	92498.14	83380.958	112756.383	116193.359	69682.653	55727.627	86406.484	97788.779	99182.001	82060.752	93230.917	100085.707	96432.506	84685.268	93147.51
Dodecane	Al	227894.1	262514.7	236787	213641.034	216648.6	224393.596	202334.5	198217.4	164477	265539	263277.2	205814.5	237540.1	214082.321	338580.096	302438.887	197892.853	150414.001	244941.61	234477.672	267543.004	202778.036	222763.448	218582.955	208904.038	215292.037	202264.8
Heptane	Al	143208.2	172268.7	164597.1	155747.712	169263.2	173767.394	152627.7	158115.2	109821.1	176598.9	174457.6	175123.9	180442.2	165206.883	256138.377	201036.417	135868.62	107593.861	174549.162	167077.903	179021.503	155539.834	180617.661	170213.358	177082.334	158317.719	159294.5
Tridecane	Al	98523.57	115529.8	105320.8	104211.198	102251.5	90570.3605	96216.03	96124.45	75454.9	104717.2	119045.4	40391.85	116911.3	85497.6375	151144.167	152494.152	98609.7875	74889.379	105070.386	108998.478	121392.037	96260.2555	104476.498	94477.413	93352.256	99069.8895	96304.52
Analyte 256	U	0	0	0	0	0	0	0	0	0	0	0	0	0	0	0	0	0	0	0	0	0	0	0	117357.797	0	0	0
Analyte 401	U	0	0	0	0	0	0	0	0	0	0	134611.1	66319.42	0	0	0	0	0	0	75027.81	22617.218	34246.703	361503.051	112489.23	220021.905	251133.952	114820.002	68524.17
Ethanedioic acid	Al	2732510	1865798	2154938	1805869.99	1458466	1513727.85	1225755	1529110	1155199	1033400	2457422	881171.9	690103	572792.875	921637.603	723109.657	428184.148	704204.02	2110817.71	1282568.67	2526386.93	4689139.1	2664358.26	3471569.84	2224391.56	1058040.82	2213734
Analyte 136	U	54720.62	63342.34	64137.84	121406.74	100585.7	84680.873	82950.51	71316.77	0	74646.93	81419.1	80039.13	74799.54	10966.62	0	93328.957	55273.106	0	84634.173	50342.789	268904.538	150598.787	214140.955	392335.277	0	0	312252
Analyte 9	U	0	0	0	0	0	0	0	0	0	0	0	0	0	0	0	0	0	0	128391.899	0	100385.273	147735.918	0	88099.276	0	0	175411.7
Analyte 260	U	0	0	0	0	0	58888.711	69098.04	66679.95	0	0	0	0	0	0	0	0	72533.331	63192.65	0	49692.848	50987.547	64322.821	78292.206	80472.403	0	71371.826	77896.97
Oxamic acid	O	150404.5	41020.48	78521.16	0	60507.85	28018.727	110903.8	49231.38	114588.9	33388.17	48892.18	57744.77	0	0	0	0	0	0	62786.055	197496.002	97656.102	61229.645	57866.264	88080.056	47460.618	104755.316	158185
Analyte 160	U	45759.44	0	0	53432.561	0	0	47415.12	48273.64	39855.77	0	0	0	0	0	0	80884.407	0	0	61712.614	61436.027	69910.209	47219.063	64921.225	68807.95	68503.66	60480.942	63938.11

doi:10.6342/NTU202100671

Appendix 3. List of cluster 3 metabolites.

Metabolites obtained from GCxGC-TOFMS were classified into different groups, namely unknown (U), amino acids (A), alkanes (Al), fatty acid s(F), and carbohydrates (C). The order of metabolite table generated according to the cluster 2 heatmap (**Figure 18**) and the values represent peak area. DAT represents days after Zn treatment. Zn concentration used in this study were dZn = 0.002µM $ZnSO_4$, NZn = 0.2µM $ZnSO_4$, eZn = 300µM $ZnSO_4$.

		Optimal Zn treatment (NZn)								Zn deficient treatment (dZn)								Zn excess treatment (eZn)							
Metabolite	**Groups**	**3 DAT**			**14 DAT**			**21 DAT**		**3 DAT**			**14 DAT**			**21 DAT**		**3 DAT**			**14 DAT**			**21 DAT**	
Butanoic acid	A	4197458	4259561	39492678	5062405	64385269	55504719	74919955	66388617	41367328	46784976	46044906	54689224	52419339	28126309	40528309	1943463	1530716	31842435	3577080	4103580	3962881	4548231	3122822	4113970	3643759	4023850	4211993
Propanoic acid	A	419278.6	443392	411707.822	500490.4	592264.435	533471.161	730204.002	608204.525	599056.44	401903.764	419482.89	406623.762	243582.769	219134.821	252311.685	136498.4	90830.51	157266.253	408299	353215.8	394272.2	326306.2	334612.4	343982.7	344981.8	292478.2	471805.2
2-octene	Al	227255	256838.1	0	441301.4	348527.118	198966.777	345641.155	396878.686	0	0	138792.682	115959.22	0	0	0	0	0	0	0	0	0	0	0	0	0	0	204322.6
Prostagladin	F	136024.5	83509.43	948144.14	540818.3	436187.485	390031.916	435279.584	476334.904	560045.11	187913.414	262599.047	268616.153	176614.357	950355.991	140173.176	0	90069.14	164157.383	105587.8	153092.5	101287.8	429422.6	357729.7	356123.2	291273.6	330280.5	314848.1
Sucrose	C	325572.7	399112.2	632793.109	725907.6	624915.598	213141.197	869822.715	263108.648	789477.063	710607.268	648571.777	444238.732	599646.673	252806.876	120370.8	675926.8	456151.2	387451.509	281426.4	215174.5	194863.4	234702.6	207910.2	697038.8	545295.9	525898.5	172768.2
Analyte 334	U	217420.6	0	0	0	0	0	458717.215	417832.054	529321.05	233389.435	0	0	358114.71	0	335741.39	0	0	315781.609	0	0	76379.17	0	0	0	0	0	0
Citric acid	O	717672.4	804478.4	6934867.65	914455.3	13914053.8	10013466.9	2152145.4	1751207.85	13869899.8	8696436.54	9511337.96	11671282	1674656.67	13686596.8	1851154.76	727984.8	442894.3	13891679.8	570456.9	697403.0	546856.5	897785.8	660594.0	827109.9	780937.9	745345.6	669875.0

doi:10.6342/NTU202100671

		Optimal Zn treatment (NZn)									Zn deficient treatment (dZn)								Zn excess treatment (eZn)							
Metabolite	**Groups**	**3 DAT**			**14 DAT**			**21 DAT**			**3 DAT**			**14 DAT**			**21 DAT**		**3 DAT**			**14 DAT**			**21 DAT**	
Analyte 338	U	5101.515	36696.49	0	0	42919.172	0	136964.616	50947.085	95232.151	9416.68	36944.027	63866.693	0	0	0	0	41512.05	4026.144	50306.084	11177.64	33105.748	30855.571	68466.178	0	0	0	16087.51
Glucopyranose	C	466746.4	188158.4	1870486.83	946428.9	2256702.55	1915535.71	6100603.04	3025919	3626224.35	3427 3.653 5	2118606.45	4340948.66	563513.17	118401.359	3025 89.537	404426.7	862327.8	2655 65.577	293836.5	819806.5	257647.7	114808.5	101688	42701.8	537808.4	103636.5	44201.4
Xylitol	C	503335.8	970044.2	0	0	1284450.07	955483.586	2553987.56	1545735.34	2040049.3	0	1056714.07	1789017.5	1130145.58	8209 13.921	9842 82.71	960415.9	101622 2	1080238.48	871 1.59 1	0	260274.3	715 7.07 2	293026	0	117 18.62	665005.9	280374.2
Erythrose	C	783884.2	881351.7	1094061.76	623171.1	1649957.73	842095.87	6040040.26	8426 01.00 7	1798651.02	2019 92.62 5	8360 03.78 9	1199120.51	1862990.6	1488627.39	1919221.34	901462	822195.6	9704 17.86	553989.9	123352 5	505551.6	565938.1	404074.8	323731.2	536979.7	850095.6	485107.6
Tetronic acid	O	511601.9	616430.7	5179 05.69 8	413329.8	6578 26.43 8	4693 26.16	7552 31.91	5606 37.74 7	6545 81.48 1	5209 14.37 4	5689 59.03 8	5042 22.9	5982 26.78 1	4774 43.72 9	7034 85.78 8	214144.6	200750.2	3427 19.45 5	385848.7	451135.4	425754.5	410208	258812.8	409688	305194.7	438378	502102.3
Leu-Gly	A	489 87.5 8	684 02.8 1	5466 3.638	163910	2099 40.83 9	1631 49.56 9	2487 97.22 7	2207 10.15 6	2194 88.48 2	1273 00.19 7	1444 66.71 8	1423 16.46 4	1184 42.55	8853 7.519	1282 81.60 9	483 33.3 4	396 50.6 9	3389 9.592	681 82.9 1	544 36.6 8	456 21.3 6	775 43.9 2	434 22.2 7	817 73.8 9	650 82.0 3	518 15.8 8	390 82.7 2
Quinic acid	O	930228 1	990907 2	1122 9823. 8	944309 5	1762 3386. 8	1181 6427. 8	2229 3314. 2	1831 9437. 2	2190 2153. 5	1177 2972. 2	1046 5615. 1	1250 1855. 3	8254 778.1 1	5729 402.1 3	6080 535.8 5	532 547 1	418 735 2	5893 840.7 3	355 394 7	432 765 1	489 949 1	240 740 7	193 459 1	246 219 9	245 606 5	337 935 6	295 327 9
Pentenoic acid	F	773051	905 117. 8	1031 781.8 8	124 296 4	1401 390.5 2	1257 497.9 9	1324 987.7 9	1402 719.4 5	1843 553.6 2	1227 224.6 5	1599 200.6 7	1167 948.5 6	9257 48.86 5	8266 73.35 5	1176 450.5	689 065. 4	645 040. 6	9446 34.33 1	109 984 3	959 093. 4	100 860 7	843 771. 1	737 146. 1	810 753. 3	920 389. 6	778 438. 4	920 196. 8

doi:10.6342/NTU202100671

Appendix 4. List of cluster 4 metabolites.

Metabolites obtained from GCxGC-TOFMS were classified into different groups, namely unknown (U), amino acids (A), alkanes (Al), fatty acid s(F), and carbohydrates (C). The order of metabolite table generated according to the cluster 4 heatmap (**Figure 19**) and the values represent peak area. DAT represents days after Zn treatment. Zn concentration used in this study was dZn = 0.002μM $ZnSO_4$, NZn = 0.2μM $ZnSO_4$, eZn = 300μM $ZnSO_4$.

		Optimal Zn treatment (NZn)										Zn deficient treatment (dZn)										Zn excess treatment (eZn)					
Metabolite	**Groups**	**3 DAT**			**14 DAT**			**21 DAT**				**3 DAT**			**14 DAT**			**21 DAT**			**3 DAT**			**14 DAT**			**21 DAT**	
Analyte 489	U	83840.9	0	74718.6	0	162415	680982	205372	370711	159070	111208	154850	1058572	63484.7	85279.7	169679	0	1192979	248647	666781	69929.8	510698	83843.6	76457	131468	0	131541	70267.9
Analyte 115	U	0	18824.4	0	0	0	0	15353.4	0	0	13821.9	0	0	0	34550.8	0	0	50118.8	0	0	0	0	0	0	0	0	0	0
Tryptophan	A	67738.3	74247.8	49375.5	0	0	44740.6	61236.1	15941.9	60685.8	0	134206	68964.4	145465	275623	48177.5	698570	955846	27669.9	53024.1	69039.3	80432.3	0	51779.4	40400.3	169004	134952	80213.3
Tyramine	A	34481.4	26797.6	26825.5	119238	20053.2	50999.2	39159.2	19885.7	0	16002.4	49496.5	30346.8	65992.3	249897	64920.4	906012	40887900	19814112	31429.5	40461.3	28226.8	0	56841.8	25634.2	265434	192803	64253.4
Analyte 120	U	0	85309.2	0	0	0	0	0	0	0	0	0	0	0	0	0	0	326723	0	0	93380.5	0	79348.5	68699.9	67768.7	0	0	71805.6
Analyte 75	U	0	0	0	0	0	35596.3	40267.6	0	0	0	53939.1	0	0	0	0	0	37346.5	0	0	49905.4	65703.6	0	0	0	43689.7	0	0
Analyte 455	U	66690.5	65128.2	42926.9	42264.1	34083.8	42822.7	80943.9	68051.6	86087.1	51996.2	83628.3	57228	54979.1	61104.9	0	103800	135515	78449	31989.3	65393.4	94569.8	48862	47816.3	42292.8	70780.4	48717.2	57792.1
Analyte 387	U	434030	439492	477030	181358	249718	337722	372306	98538.3	290764	176709	1466256	844717	414317	638744	119097	445197	808413	871658	295085	803006	496296	147543	254245	139958	330242	327359	220550
D-fructose	C	709619 9	612086 2	725755 9	603950 1	701520 9	634978 8	1.5E+07	1.2E+07	1.5E+07	1.1E+07	8222294	1.1E+07	2820698	1430771	495428	8795292	9775213	4082735	2308487	5044611	5618685	4332821	3245307	4078083	5143325	4682292	4260156
d-Mannose	C	897247 9	795271 2	915112 1	861885 8	968145 1	882296 7	1.8E+07	1.4E+07	1.9E+07	1.4E+07	1E+07	1.3E+07	3614165	2620163	961741	1E+07	1.1E+07	5325065	3017433	6607507	7953992	5974252	4110490	5866862	7142080	6475985	7011080
D-Xylopyranose	C	184861	930842	916246	319247	827611	719433	1325869	697164	934696	25843.5	1037950	2205398	420845	218752	132770	843583	1023163	503242	141189	406933	94172	29714.9	40578.6	5848.87	224624	356186	26670.9
Galactose	C	189103	181942	179852	173211	134176	172374	213045	177978	344273	38786.3	226948	197491	480619	88863.8	66335.9	164814	157422	99418.2	61091.2	109370	248721	65974.5	128131	163966	275200	167398	116264
Analyte 302	U	0	96604.4	92080.6	0	0	0	0	0	116078	0	106844	102469	0	0	0	236183	197128	0	103186	97239.1	94139.1	92979.2	101733	106000	109227	108823	0

doi:10.6342/NTU202100671

Appendix 5. List of cluster 5 metabolites.

Metabolites obtained from GCxGC-TOFMS were classified into different groups, namely unknown (U), amino acids (A), alkanes (Al), fatty acid s(F), and carbohydrates (C). The order of metabolite table generated according to the cluster 5 heatmap (**Figure 20**) and the values represent peak area. DAT represents days after Zn treatment. Zn concentration used in this study were dZn = 0.002μM $ZnSO_4$, NZn = 0.2μM $ZnSO_4$, eZn = 300μM $ZnSO_4$.

		Optimal Zn treatment (NZn)									Zn deficient treatment (dZn)									Zn excess treatment (eZn)								
Metabolite	**Groups**	**3 DAT**			**14 DAT**			**21 DAT**			**3 DAT**			**14 DAT**			**21 DAT**			**3 DAT**			**14 DAT**			**21 DAT**		
Decane	Al	62703.6	74124.6	101005	96634.6	103192	96973.3	70917.2	66397.6	52690	30072.7	32817.6	27240.1	37570.9	40824.5	50936.8	49539.4	58678.2	51692.9	70438.4	36861.6	74778.4	64426.1	73652.6	30901.1	75382	0	28305.3
alpha-D-Mannopyranose	C	7267837	7789390	3244628	5525916	1908923	2579347	1164415	1095099	489092	1215431	1498748	1709298	1226507	2226812	1563889	1000972	3371140	3344326	2332114	597111	3204623	1462057	1613432	1779714	3655583	1382235	1583903
Undecane	Al	46939.4	24665.8	48234.1	13107.1	13637.2	21910.9	11266	12129.5	0	14438	25170.1	25339.5	23495.4	14159.7	21788.4	12972.7	11551.5	8052.28	48996.5	13956.2	51761.4	44821.7	48472.9	13844.8	54128	10639	11608.2
Analyte 488	U	372895	351385	320917	423905	383064	339162	284857	315705	382045	485939	608789	469343	345885	218270	368965	152663	290363	259532	240999	269733	174379	154457	282305	223910	425674	330854	283556
Propanedioic acid	O	187011	182096	180857	115183	116441	127505	142658	176609	122766	210110	140883	176231	60111	50295.1	51531.1	45468.7	92969	54196.2	62001.2	53168.5	79441.4	64604.2	65787.9	67059.7	29762	16378.4	12718.9
Analyte 285	U	0	691700	400674	0	0	83418.2	0	88034.8	779100	0	770377	964828	0	0	0	0	0	0	0	0	77886.2	79476.4	0	0	0	89818.2	0
Analyte 176	U	0	25297.3	202100	0	0	0	0	22414.7	0	0	32832.3	29287.2	0	0	0	0	0	0	18557.5	0	31149.8	0	0	0	23788.4	32343.6	0
Myo-inositol	C	1.3E+07	1.2E+07	1.3E+07	1.2E+07	1.2E+07	1E+07	1.2E+07	1.2E+07	1.2E+07	1.2E+07	1.8E+07	1.6E+07	6742276	5892755	8748223	3941712	3306748	4345088	1.3E+07	1.4E+07	1.3E+07	1E+07	1E+07	1.1E+07	1E+07	1E+07	1.3E+07
Maltose	C	87963.5	68345.4	73521.2	84115.8	58689.8	52054.3	49266.8	66945.3	48436.6	91048.2	87163.9	82958.3	24219.5	11302.8	0	13429.4	26022.4	22948.6	53272.1	67118	67133.7	36405.9	34352.5	38728.5	29097.1	54157.8	26957.6
Analyte 195	U	145157	115416	366676	144906	168724	106631	147718	140554	0	207701	252649	329261	0	0	0	0	0	0	144781	163531	0	129680	111873	97588.2	192987	137292	181920

doi:10.6342/NTU202100671

		Optimal Zn treatment (NZn)									Zn deficient treatment (dZn)								Zn excess treatment (eZn)							
Metabolite	**Groups**	**3 DAT**			**14 DAT**			**21 DAT**			**3 DAT**			**14 DAT**		**21 DAT**			**3 DAT**			**14 DAT**			**21 DAT**	
Heptadecane	Al	97786.4	120099	63534	43578.5	99111	63268	73790.6	108754	97929.2	78919.6	121551	564753	0	56027.9	12321.6	29922.4	25195.2	9500.04	120585	77303.9	141801	105370	164330	80714.3	74882.5	87423.9	128656
alpha-D-Galactofuranoside	C	250381	321573	338893	323181	334509	366693	264330	394972	304036	429487	372876	316766	318434	0	468042	0	0	0	359447	358719	433681	412266	396213	449625	473624	410664	606375
Analyte 128	U	91471.6	103495	103350	96603.6	112978	98768.1	92572.6	90161.4	82901.1	109167	104150	126355	51501	0	78512.5	0	0	0	122035	91803.1	125202	101081	133864	120754	127791	90482.3	138286
4-Ketoglucose	C	75272.4	60050	62062.4	63430.6	59070.4	56749.4	49808.9	52762.2	35084.4	52711.4	84108.9	78089.4	33634.6	55941.6	40468.8	13806.2	0	20013.9	62757.8	0	53407.3	55474.4	62513.4	63453	76409.3	39727.9	86607.6
Butane	Al	87683.3	113516	36241.7	31723.1	34092.6	38482.2	29290.5	26498.7	0	61053	67392.5	35661.8	40626.5	33179.2	55553.4	55161.6	0	28559.6	60516	44201.2	49488.2	47722.1	50866.2	56410.9	52924	43037.7	51559.7
Arabinonic acid	O	163164	147115	76402.2	58005.4	40317.8	53494.7	0	27797.5	0	215212	150841	533292	0	66527.3	0	0	67874	0	68831.7	40463.4	63874.8	33271.4	36093.4	39651.4	65578.7	29208.7	37355.2
alpha-D-Galactoside	C	543512	336976	442613	590220	261283	294931	100985	188165	80527.9	328542	468334	496911	635492	233392	201471	71671	370695	488796	326103	556745	647235	378002	174257	379642	166205	458031	535851
2-Butenedioic acid	O	115357	875125	875899	48495.1	45862	49643.1	38454.6	54283.9	23994.6	60966.7	81826	84197.2	45588.6	68736.5	54921.6	42088.5	56771.5	61546.7	103511	124438	115697	43479.2	39110.9	40117.5	44930.8	50948.9	51345.9
Analyte 330	U	201061	200536	221557	142001	142159	0	0	0	0	238757	304121	0	0	0	0	0	116768	118301	167160	199487	200319	143160	135975	141402	145646	0	140358
Analyte 39	U	0	11447	7369.24	0	0	0	0	7129.94	0	0	12445.7	0	0	0	0	0	0	0	5176.26	0	0	8708.66	0	9989.02	0	0	6926.93
Analyte 383	U	123925	489335	639098	610461	479486	47046	0	315693	0	241414	114357	701446	0	0	0	0	0	0	666877	381001	104341	284569	653175	529498	565637	274433	130452
Glyceraldehyde	C	303733	117658	177772	159313	115365	124953	92928	105534	57135.9	422662	223535	158009	396512	753171	778787	561932	305700.8	404366	222358	158739	302039	123845	181960	262520	229821	153465	751864
Succinic acid	O	0	293313	270133	0	0	0	219086	0	502507	227959	392619	393257	376087	342131	751724	0	0	0	347363	308394	268641	414931	297852	298149	272757	326909	198743
Analyte 355	U	640041	830918	0	0	912636	0	0	0	0	730349	0	990387	0	148437	114173	0	0	0	742596	769109	0	0	717343	0	691829	0	758094
Analyte 101	U	0	0	0	0	0	0	0	0	0	0	63.698	0	0	0	0	0	0.92	0	0	0	0	0	0	0	0	0	0
Gluconic acid	C	300427	226990	0	138794	0	0	37448.9	38721.3	0	9799340	1.2E+07	672801	635877	909554	287279	242954	108646	193494	1003540	0	320397	645688	807036	545782	168102	710689	514945
Alpha-Linolenic acid	F	467616	938961	116765	663335	821208	997297	330049	748100	865692	998058	114831	123809	106429	104193	174685	683658	828066	744300	57205	121582	398718	556425	238618	344957	480576	232192	276337
Ala-Gly	A	1955128	1839581	2014251	708228	840823	791236	423984	241196	947199	199842	3480078	3094874	2182014	3287420	3868102	1206571	959015	1215979	1513582	1672713	1612684	273741	389311	264609	335941	489214	526356
Trehalose	C	194671	140823	155978	163830	143993	106497	197117	216223	267803	246003	303376	360784	177409	178426	251154	127065	129750	116406	140014	174407	203742	673078	527845	648011	623756	815957	591417
Analyte 434	U	189552	144278	119418	153072	128296	129197	136255	140605	154718	150915	136417	634758	751132	952988	868916	139521	0	0	954412	139521	115351	109819	122098	121463	0	118239	115018
Alpha-ketoglutaric acid	A	140938	907339	122809	111826	122987	105203	122840	116865	168182	117406	114455	116362	645739	507903	710559	280506	241437	254602	972548	127991	133669	160624	933333	140131	840823	961484	156496
d-Ribose	C	937558	493659	426255	608803	548935	665219	822796	444743	609297	885479	554633	404298	637846	195796	6790.73	107936	191988	151546	572466	470339	690236	624559	639617	694451	501119	316899	730719
Acetic acid	O	300782	272305	294491	293177	224329	281228	170332	225901	173822	454344	394348	380260	574119	628139	718692	510363	785686	785741	306179	199996	396463	220419	352597	318266	315259	161711	380508
Analyte 82	U	163834	134957	148251	137782	145088	137155	105782	143948	101985	207432	199711	159818	418038	263341	589136	167022	120344	148143	144021	139042	192537	189778	154467	186151	123461	979246	197569
Glucose-6-phosphate	C	780687	678348	734104	916562	594570	531228	581087	657151	488528	106950 7	799717	504671	214552	190457	464046	633574	334693	393342	731143	795300	109237 0	749941	518980	591603	372784	511798	608295

doi:10.6342/NTU202100671